Universidade do Minho
Escola de Engenharia

Diana Raquel dos Santos Morais

Development and characterization of an injectable bone substitute based on a hydrogel and glass-reinforced hydroxyapatite (GR-HA) granules

Setembro de 2012

Universidade do Minho
Escola de Engenharia

Diana Raquel dos Santos Morais

Development and characterization of an injectable bone substitute based on a hydrogel and glass-reinforced hydroxyapatite (GR-HA) granules

Tese de Mestrado em Engenharia Biomédica
Ramo de Biomateriais, Reabilitação e Biomecânica

Trabalho efectuado sob a orientação do
Professor Luís Augusto Sousa Marques Rocha
Professora Cláudia Manuela da Cunha Ferreira Botelho
Doutora Marta Alexandra Ribeiro dos Santos

Setembro de 2012

Universidade do Minho, ___/___/_____
Assinatura: _____

Acknowledgements

Esta dissertação representa para mim o fim de uma etapa de 5 anos extremamente importante na minha vida, em que enriqueci muito o meu conhecimento intelectual e pessoal. No entanto, nunca teria chegado ao fim sem o apoio de várias pessoas que merecem todo o meu reconhecimento e gratidão.

Pelo trabalho que realizei durante este ano, gostaria de agradecer todo o apoio e ensinamento aos meus orientadores, Professor Luís Rocha, Professora Cláudia Botelho e Doutora Marta Santos. Professora Cláudia, obrigada pela disponibilidade e paciência com as minhas perguntas infinitas, pela confiança no meu trabalho e pelo incentivo diário de fazer melhor. Agradeço também à Professora Ascensão Lopes pela disponibilidade constante em me esclarecer algumas dúvidas e pelas sugestões e ensinamentos para conseguir um trabalho melhor.

Agradeço ao Miguel Rodrigues pela transmissão de conhecimento, pela paciência com as minhas dúvidas constantes e por incentivar sempre o meu espírito crítico. Agradeço também aos meus colegas de gabinete pelo apoio e boa disposição, ao João Coelho, Cátia Fidalgo e Vânia Rodrigues. Agradeço ainda à D. Amélia por toda a ajuda no laboratório e pela alegria que me transmitia todos os dias.

Agradeço à minha amiga Sofia Alves, que sempre foi uma grande companheira, esteve sempre comigo nos momentos mais difíceis. Agradeço também ao João Póvoas, pela confiança que depositou em mim e pelo carinho, que me motivava dia após dia para continuar a lutar e a acreditar. Agradeço ainda a todos os meus amigos que não refiro aqui, mas que sabem a sua importância no caminho que percorri.

Por último, tenho que agradecer à minha principal fonte de inspiração: a minha família. Obrigado pai e mãe, pelo carinho, por todo o apoio nas minhas escolhas, por confiarem sempre em mim e nas minhas capacidades, por serem um exemplo e pelos princípios que sempre me transmitiram e me ajudaram a ser mais forte e perseverante. Obrigada avó pelo carinho e palavra de conforto que sempre tiveste para mim. Obrigada mana pelas tuas gargalhadas, pelos teus abraços, pela tua perspectiva da vida, pelas tuas palavras ingénuas, mas tão genuínas, o que me ajudou sempre a continuar a lutar e não desistir do caminho que eu quero traçar. Esta tese é dedicada a ti…

Abstract

Bone defects caused by a disorder or injury, affect millions of patients worldwide, limiting their life quality. Thus, in the last few years, scientists have developed synthetic bone substitutes to treat those defects. Injectable bone substitutes (*IBS*s), which represent a minimally invasive surgical approach, are very promising systems for specific clinical applications.

Therefore, this work aimed to develop a biocompatible, biodegradable and bioactive polymeric vehicle to associate with the bone substitute glass-reinforced hydroxyapatite (GR-HA) granules, allowing their injection directly to the wound site, and also improving the substitute osteoconductive properties.

Firstly, three different alginate-based hydrogels were produced, one composed just by an alginate matrix cross-linked with Ca^{2+} ions (*Alg*), and other two resulted from the combination of chitosan or hyaluronic acid with that alginate matrix (*Alg/Ch* and *Alg/HA*). These vehicles, as well as the respective *IBS*s (GR-HA granules plus hydrogel) were fully characterized from the physical-chemical point of view. Weight change studies revealed the swelling and degradation rate of the developed materials. The rheology tests showed that the hydrogels have a non-Newtonian viscoelastic behavior, and the injectability tests revealed that low extrusion forces are required to inject the three *IBS*s. Thus, all the developed hydrogels can be successfully used as vehicles for the bone substitute.

Furthermore, the hydrogels were also characterized from the biological point of view to evaluate their biocompatibility. The measured metabolic activity of osteoblastic cells was higher on the *Alg/HA_IBS* than on the other two *IBS*s and GR-HA granules alone. Scanning electron microscopy (SEM) analysis demonstrated different cell morphologies on the surface of each *IBS*. A spreader cell shape was observed on the *Alg/HA_IBS* surface, proving the improvement of the substitute bioactive ability by association of the hydrogel *Alg/HA*. This hydrogel was even subcutaneously implanted in rats revealing a slight irritating tissue response. Considering the physical-chemical and biological results, the hydrogel *Alg/HA* was considered as the best vehicle among the three. Additionally, significant antimicrobial properties were granted to the hydrogel *Alg/HA* by incorporation of Ce(III) ions, without compromising the improvement of the osteoblastic cells metabolic activity.

Resumo

Os defeitos ósseos provocados por doença ou lesão afectam milhões de pacientes em todo o mundo, limitando a sua qualidade de vida. Assim, os cientistas têm desenvolvido, nos últimos anos, substitutos ósseos sintéticos para tratar esses defeitos. Os substitutos ósseos injectáveis (*IBS*s), que permitem uma abordagem de tratamento minimamente invasiva, são muito promissores para aplicações clínicas específicas.

Assim, neste trabalho, pretendeu-se desenvolver um veículo polimérico, biocompatível, biodegradável e bioactivo para associar com grânulos do substituto ósseo: hidroxiapatite reforçada com vidro (GR-HA). Essa associação permite a aplicação directa dos grânulos no local lesado, bem como melhorar as propriedades osteocondutivas do substituto ósseo.

Desta forma, foram desenvolvidos três hidrogéis baseados em alginato, um composto por uma matriz de alginato reticulada com iões Ca^{2+} (*Alg*), e outros dois que resultaram da combinação de quitosano ou ácido hialurónico com a matriz de alginato (*Alg/Ch* e *Alg/HA*). Estes veículos, assim como os respectivos *IBS*s (grânulos de GR-HA mais hidrogel), foram caracterizados do ponto de vista físico-químico. Os estudos de variação de massa revelaram a taxa de aumento de volume e de degradação dos materiais desenvolvidos. Os testes de reologia demonstraram que os hidrogéis têm um comportamento não-Newtoniano e viscoelástico. Os testes de injectabilidade revelaram baixas forças de extrusão para injectar os três *IBS*s. Assim, todos os materiais desenvolvidos são potenciais veículos para o substituto ósseo GR-HA.

Além disso, os hidrogéis foram também caracterizados biologicamente para avaliar a sua biocompatibilidade. A actividade metabólica das células osteoblásticas registada para o *Alg/HA_IBS* foi superior à dos outros dois *IBS*s e dos grânulos de GR-HA. Na superfície do *Alg/HA_IBS* as células apresentaram uma morfologia mais esticada do que nos outros *IBS*s, provando que a associação do hidrogel *Alg/HA* ao substituto ósseo melhora a sua bioactividade. O hidrogel *Alg/HA* foi implantado subcutaneamente em ratos, ocorrendo uma resposta dos tecidos ligeiramente irritante. Considerando os resultados físico-químicos e biológicos, o hidrogel *Alg/HA* foi considerado como o melhor veículo entre os três desenvolvidos. Adicionalmente, conferiu-se a este hidrogel propriedades antimicrobianas por incorporação de iões Ce(III), sem comprometer a melhoria da actividade metabólica dos osteoblastos.

Table of contents

List of Abbreviations

Alg	Hydrogel of alginate
Alg/Ch	Hydrogel of alginate and chitosan
Alg/Ch_IBS	Injectable bone substitute with the hydrogel of alginate and chitosan
Alg/HA	Hydrogel of alginate and hyaluronic acid
Alg/HA_IBS	Injectable bone substitute with the hydrogel of alginate and hyaluronic acid
Alg_IBS	Injectable bone substitute with the hydrogel of alginate
ASTM	American Society for Testing and Materials
BCP	Biphasic Calcium Phosphate
BMP	Bone Morphogenetic Protein
BMP's	Morphogenetic Proteins
CFU	Colony-Forming Units
CMC	Carboxymethyl Cellulose
DBM	Demineralized Bone Matrix
DD	Deacetylation Degree
ECM	Extracellular Matrix
FTIR-ATR	Fourier Transform Infrared-Attenuated Total Reflectance
G	α-L-Guluronic Acid
GR-HA	Glass-Reinforced Hydroxyapatite
HA	Hyaluronic Acid
HAP	Hydroxyapatite
HCl	Hydrochloride
HMDS	Hexamethyldisilazanes
***IBS*s**	Injectable Bone Substitute
ISO	International Organization for Standardization
KHP	Potassium Hydrogen Phthalate
M	β-D-Mannuronic Acid
MTT	3-[4,5-Dimethyl-Thiazol-2-yl]-2,5-Diphenyltetrazolium
PBS	Phosphate Buffered Saline
PEG	Poly(Ethylene Glycol)

PEO	Poly(Ethylene Oxide)
PNIPAAm	Poly(N-isopropylacrylamide)
PPO	Poly(Propylene oxide)
RGD	Arginine-Glycine-Aspartic Acid
SEM	Scanning Electron Microscopy
TCP	Tricalcium Phosphate
USA	United States of America

List of Figures

Chapter 1

General introduction

Chapter 2

Synthesis and physical-chemical characterization of biodegradable alginate based hydrogels as vehicles for glass-reinforced hydroxyapatite (GR-HA) granules

Chapter 3

Biological evaluation of biocompatible alginate based hydrogels as vehicles for glass-reinforced hydroxyapatite (GR-HA) granules

Chapter 4

Implantation of one developed injectable bone substitute

List of Tables

Chapter 1

General introduction

1.1. Bone

1.1.1. Bone tissue

The skeletal system plays several functions in the body, it provides physical support, vital internal organs and structures protection, body movement, blood cells production and mineral storage, thus having an important action in the ionic gradient balance and in the organic homeostasis regulation.[1-3] This system is composed of bones, cartilages and ligaments, which together form a strong and flexible framework that confers structure to the body.[2]

Bone is the main calcified tissue present in the skeletal system of vertebrates, it is a connective tissue formed by the process named osteogenesis.[4]

There are four general categories of bones, according to their shape and function, short bones, long bones, flat bones, and irregular bones (figure 1.1).

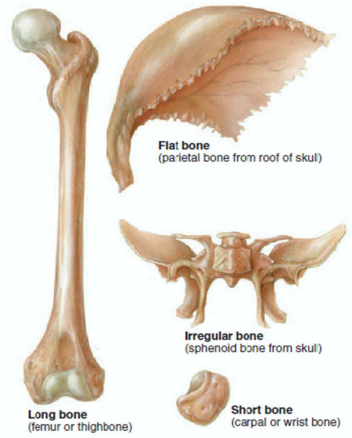

Figure 1.1: The four bone categories.[adapted from [1]]

Long bones have four main components, the diaphysis, the epiphysis, the metaphyses and the epiphyseal plate (figure 1.2). The diaphysis is mainly composed of **compact bone** and this component encloses a space named the medullary cavity, where there is bone marrow. The epiphysis (above the epiphyseal plate) and the metaphyses (below the

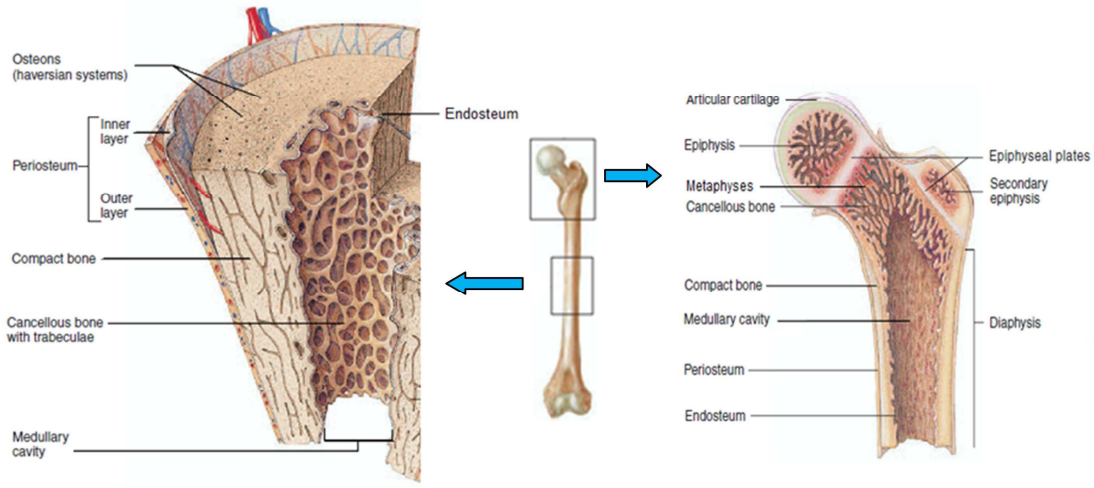

Figure 1.2: Structure of the long bones.[adapted from [1]]

epiphyseal plate) are mainly composed of **cancellous bone**, but the outer surface is a layer of compact bone. Between the epiphysis and diaphysis there is the epiphyseal, or growth, plate, which is hyaline cartilage.[1-3]

Flat bones, normally, have no diaphyses or epiphyses, they consist in a cancellous bone layer between two compact bone layers (figure 1.3). Short and irregular bones are not elongated and they have a compact bone surface surrounding a cancellous bone center.[1, 2]

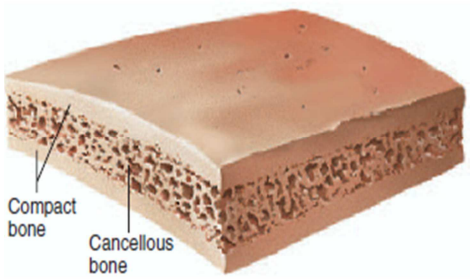

Figure 1.3: Structure of a flat bone.[adapted from [1]]

The outer surface of the compact bone is covered by a connective tissue membrane, called the periosteum (figure 1.2)**.** This membrane is composed by an outer collagen *fibrous layer*, which contains blood vessels and nerves, and an inner single *layer* of bone cells, namely osteoblasts, osteoclasts, and osteochondral progenitor cells. There is also another connective tissue membrane just composed by a thin single layer of bone cells (including osteoblasts, osteoclasts, and osteochondral progenitor cells), called endosteum (figure 1.2)**.** This membrane covers the internal surfaces of the bone cavities, like the medullary cavity in the diaphysis and the cavities in cancellous and compact bone.[1, 2]

The bone tissue consists of extracellular bone matrix with bone cells, but according to its macroscopic features, it can be distinguished in two different types: the compact bone, which represents 80% of bone tissue, and the cancellous bone, which represents 20% of bone tissue.[3, 5] The compact bone is mostly comprised of bone matrix, but with few small cavities. On the other hand, the cancellous bone tissue is mostly composed by small cavities surrounded by bone matrix.[1, 2]

The compact bone tissue has blood vessels and the bone lamellae are mainly oriented around them. The vessels parallel to the long axis of the bone are in central (or haversian) canals, which have blood vessels, nerves and loose connective tissue, and are lined with endosteum. The central canals are surrounded by circular layers of bone matrix, named concentric lamellae, which have osteocytes between them (figure 1.4). The system composed by a central canal, the concentric lamellae and osteocytes, is called of osteon or haversian system (figure 1.4). Moreover, in the outer surface of

the compact bone there are flat plates extended around the bone, which are named of circumferential lamellae, and between the osteons, exist also the interstitial lamellae (older bone in the bone remodeling process).[1-3]

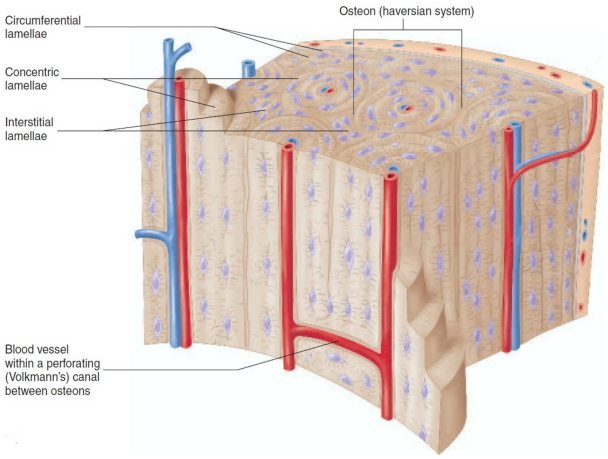

Figure 1.4: Structure of the compact bone.[adapted from [1]]

The cancellous bone (or spongy bone) tissue consists in a network composed by slender interconnecting rods or plates of bone called trabeculae (figure 1.5).[1-3] In the trabeculae there are pores, that are filled with bone marrow and blood vessels. The majority of trabeculae are thin, varying between 50-400 µm, and are composed by some lamellae, with osteocytes between them (figure 1.5). Besides that, the surface of the trabeculae is coated with a single layer that mostly contains osteoblasts, and few osteoclasts (figure 1.5).[1, 2]

It should be referred, that the trabeculae are not randomly arranged, they are oriented along the bone's lines of stress. So, if for some reason, the direction of weight-bearing stress is changed, the trabeculae orientation changes to realign with the new lines of stress.[1, 2]

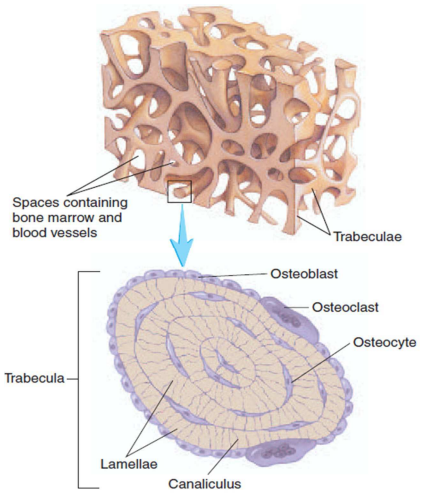

Figure 1.5: Structure of the cancellous bone.[adapted from [1]]

1.1.1.1. Bone cells

In bone tissue different cell types can be distinguished according to its origin and function, standing out the osteoblasts, osteoclasts and osteocytes.

a) *Osteochondral progenitor cells or osteogenic cells*

The connective tissue is embryologically developed from mesenchymal cells and some of them become stem cells. This cell type is characterized for being able of giving rise to more differentiated cells types.[1, 2]

In this case, osteogenic cells are stem cells that can become to osteoblasts (bone cells) or chondroblasts (cartilage cells). These bony cells lie, for instance, in the inner layer of the periosteum, and in the endosteum, and, through their mitosis and differentiation, they are the only source of new osteoblasts, since these ones are nonmitotic cells.[1, 2, 6]

The mitosis and differentiation of the osteogenic cells are accelerated by cases of stress and fractures, which consequently cause a rapid osteoblasts number increase.[2]

b) *Osteoblasts*

Osteoblasts are responsible for bone formation, by a process named ossification, or osteogenesis, they produce the organic material of the bony matrix and they also participate in the mineralization of the bone tissue.[1, 2]

These cells have an extensive endoplasmic reticulum and numerous ribosomes, they are arranged in rows in the endosteum and inner layer of periosteum, and they are connected by gap junctions throughout the cell processes. Osteoblasts synthesize collagen and proteoglycans, which are incorporated into vesicles by the Golgi apparatus and then released to the extracellular medium by exocytosis. Besides that, inside these cells there are other vesicles which incorporate calcium ions (Ca^{2+}), phosphate ions (PO_4^{3-}), and various enzymes (for example, the alkaline phosphatase). These components are also released from the intracellular medium to the extracellular medium by exocytosis to form hydroxyapatite crystals, occurring by this way the mineralization of the bony matrix.[1, 2, 6]

c) *Osteocytes*

An osteocyte is a mature bone cell, more exactly, it is a terminally differentiated osteoblast that has became surrounded by the bone matrix that it has produced. In spite of becoming less active than the most osteoblasts, they function within networks and are able to produce components which are needed to maintain the bone structure and metabolism.[2, 5, 6]

By this way, osteocytes do not have a significant action in formation or resorption bone event. However, when they detect strain in a bone, they pass the information to osteoblasts at the surface, that will provide bone formation where it is needed and inform osteoclasts to reabsorb bone in another place.[1, 2, 6]

The osteocyte cells bodies are positioned in tiny cavities in the bony matrix named lacunae, and its extensive processes are in slender channels called canaliculi (figure 1.6). These channels allow the contact between the processes of neighboring osteocytes, which are connected by gap junctions. Through these gap junctions osteoblasts exchange nutrients, gases and chemical signals, and transport wastes to the closest blood vessel for disposal.[7, 8]

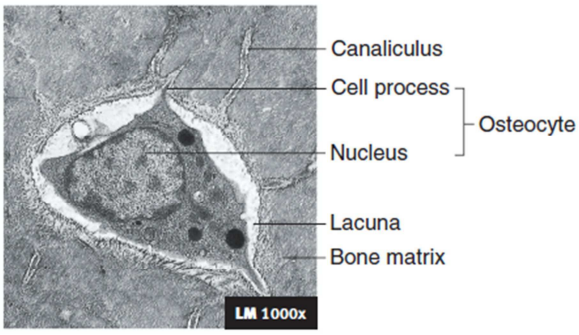

Figure 1.6: Photomicrograph of an osteocyte in a lacuna. [adapted from [3]]

d) *Osteoclasts*

Osteoclasts are large and multinucleated cells (3 or 4 nuclei, and sometimes up to 50), responsible for bone resorption, and most of them are derived from bone marrow monocyte-macrophage precursor cells.[2, 3, 9]

The plasma membrane of osteoclasts forms many deep infoldings in the contact zone with the bone matrix, called a ruffled border (figure 1.7).[3, 6, 9] Across this border hydrogen ions are expelled to the

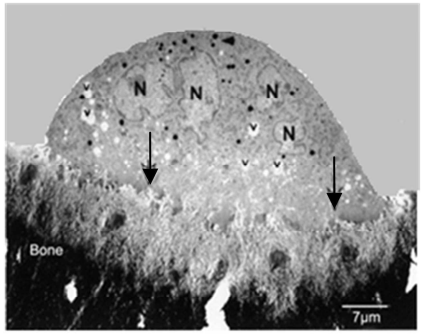

Figure 1.7: Transmission electron micrograph of a human osteoclast. Black arrows: ruffled border; N: nucleus.[adapted from [9]]

extracellular medium, causing an environment acidification, giving rise to the bone matrix decalcification.[8, 9] Moreover, the protein components of the matrix are digested by enzymes also released by the osteoclasts. After the breakdown of the matrix components, some of the resultant products of it are then reabsorbed by these cells through the endocytosis process.[1, 6]

Osteoclasts action is improved when they contact directly with mineralized bone matrix. This event is enhanced by the osteoblasts, once they produce enzymes which breakdown the unmineralized organic matrix layer that usually covers the bone, enabling the direct contact of osteoclasts with the mineralized bone part.[1, 6]

1.1.1.2. Bone matrix

The bone matrix is about 35% organic and 65% inorganic matter, by weight. The organic material mainly consists in 90% of type I collagen fibers and various protein-carbohydrate complexes such as glycosaminoglycans, proteoglycans, glycoproteins and growth factors. The inorganic material is approximately 85% of hydroxyapatite (HAP), a crystallized calcium phosphate salt [$Ca_{10}(PO_4)_6(OH)_2$], 10% of calcium carbonate ($CaCO_3$), and smaller amounts of magnesium, sodium, potassium, fluoride, sulfate, carbonate, and hydroxide ions.[1, 2, 5]

The bone functional characteristics are defined by the collagen and the mineral components. The mineral components give the matrix compression strength, whereas the collagen fibers determine the elasticity and toughness of the tissue. Thus, if the mineral components are removed from the bone, it becomes extremely flexible, but, if the collagen does not exist, the bone becomes overly brittle. So, the bone physical features are ensured by the complementary relation between the organic and mineral part.[1, 2, 5]

1.1.2. Bone physiology

1.1.2.1. Bone formation

The process by which occurs the bone formation is named of ossification or osteogenesis. During fetal development, there are two types of ossification, the intramembranous, in which the process occurs in connective tissue, and the endochondral, in which the process occurs in cartilage.[1, 2, 6]

- **Intramembranous ossification:**

In this process are produced, for instance, the flat bones of the skull and most of the clavicle. Around the fifth week of evolution, the embryonic mesenchyme forms a membrane of connective tissue with collagen fibers, and about the eighth week, some of the mesenchymal cells in the membrane become osteogenic cells, which are then differentiated in osteoblasts.[1, 2, 6]

After this, osteoblasts start to produce an organic matrix, and the formation of thin trabeculae occurs. Meanwhile, the trabeculae become larger and longer, because osteoblasts continue to produce more and more bone, calcium phosphate is deposited in the matrix and some osteoblasts stay trapped in the lacunae, becoming osteocytes. Then the formation of cancellous bone occurs, by the junction of the trabeculae. The trabeculae at the surface of the developing bone continue to calcify in order to fill the empty spaces and produce compact bone. Besides that, the cells at the new bone tissue surface specialize to form the periosteum.[1, 2, 6]

- **Endochondral ossification:**

The endochondral formation occurs from the cartilage and begins about the eighth week of fetal development. This process is responsible for the production of, for example, the vertebrae, pelvic bones and bones of the limbs.[1, 2, 6]

In this process, mesenchymal cells are differentiated into chondroblasts, which produce a hyaline cartilage structure with a similar shape to the future bone. Chondroblasts become chondrocytes as they stay surrounded by cartilage matrix produced by them. The hyaline cartilage model is wrapped by perichondrium (fibrous connective tissue membrane), and some of its cells become osteoblasts. These bone cells start to produce compact bone on the cartilaginous structure surface, creating a bone collar. At this time, the surrounding fibrous membrane is considered as periosteum. Besides that, by this time, the chondrocytes inside the cartilage structure hypertrophy, and the cartilage matrix is calcified by deposition of calcium carbonate. In this calcified medium, the death of chondrocytes eventually occurs, appearing lacunae in the matrix.[1, 2, 6]

Then, the blood vessels and osteoblasts from periosteum invade the calcified cartilage, forming a primary ossification center. Osteoblasts form bone on the calcified cartilage surface, producing cancellous bone. After this, osteoclasts reabsorb bone

existent in the central part of the diaphysis, forming the medullary cavity. Besides the primary center, there are also the secondary ossification centers located in the epiphyses. The process of bone formation in these centers is the same of the primary, but, in this case, the medullary cavity formation does not exist.[1, 3]

1.1.2.2. Bone growth

Mature bone growth occurs by the appositional mechanism, which consists in the formation of new bone on the surface of older bone or cartilage.[1, 2]

In the appositional growth, osteoblasts produce and deposit new bone in layers parallel to the surface of the existent bone. During the deposition of new bone tissue at the outer bone surface, osteoclasts remove bone from the inner surface, increasing the marrow cavity size. These two processes, the bone formation and removal, function in a balanced way between them. If one of them is intensified relatively to the other, several bone abnormalities occur.[1, 2]

The longitudinal and radial bone growth happens in the childhood and adolescence. The width of long bones, as the size or thickness of other bones, increases through the appositional method. The length of long bones increases through the growth at the epiphyseal plate by new cartilage formation, and the appositional bone growth on the surface of the new cartilage.[1-3]

1.1.2.3. Bone remodeling and repair

- **Bone remodeling**

The bone remodeling process is responsible for replace old bone for new bone to maintain the bone strength and the mineral homeostasis. The remodeling starts before the birth and is maintained until the death to prevent accumulation of bone microdamage. The system responsible for this phenomenon is composed by osteoclasts and osteoblasts, which reabsorb old bone and form new bone, respectively. In women the remodeling process increases in perimenopausal and early postmenopausal period, but with further aging it is slowed besides continuing at a higher rate than in premenopausal period. In aging men, the remodeling process is thought to exhibit a mild increase.[1-3]

The remodeling is present in bone growth, bone repair, changes in bone shape, bone adjustment to stress, and calcium ion regulation. The remodeling points can be

randomly developed, but they also exist in specific sites which need to be repaired. The process is composed by four sequential phases, activation, resorption, reversal, and formation: [1, 3]

1) Activation: this phase mainly consists in recruitment and activation of mononuclear monocyte-macrophage osteoclast precursors from the circulation, which will give raise to the osteoclasts;[1, 3]

2) Resorption: this lasts about two to four weeks in the process, and it consists in the resorption of old bone by the osteoclasts. These cells digest the organic matrix forming resorption pits, named as Howship's lacunae, on the cancellous bone surface and in the Haversian canals of the compact bone;[1, 3]

3) Reversal: during this phase bone resorption transits to bone formation. The chemical signals between the end of bone resorption and the beginning of bone formation are as yet unknown, but some signal candidates has already been proposed, for instance, bone morphogenetic proteins and bone matrix-derived factors. Besides that, it has also been proposed that this phase can be mediated by the strain gradient in the lacunae. Thus, osteoclasts are activated when there is a reduced strain, and osteoblasts are activated when there is an increased strain;[1, 3]

4) Formation: the formation phase lasts about four to six months, and it consists in the production of new organic matrix by the osteoblasts to substitute the old bone that have been removed.[1, 3]

- **Bone repair**

The bone tissue has the ability to repair after damage to it. The bone repair process can be described in four main steps:

1) Hematoma formation (figure 1.8-1)**:** in case of a bone fracture a hematoma (localized blood mass, released from blood vessels, limited in an organ or space) is formed, caused by the damage of the bone blood vessels and the periosteum. The damage of blood vessels in the central canals causes inappropriate blood sustainability of osteocytes, which induces the death of the bone tissue next to the fracture local. Furthermore, the tissues around the bone usually suffer inflammation and swelling.[1, 6]

2) Callus formation (figure 1.8-2)**:** in this phase at the fracture local a callus is formed, which is a tissue mass that connects the bone broken ends. The internal callus,

exists between the bone ends and in the medullary cavity (in case of a long bone. Some days after the fracture macrophages eliminate cell debris, osteoclasts reabsorb dead bone tissue, and fibroblasts (constituent cells of connective tissue) produce a collagen fibrous network. Besides that, the osteoblasts and chondroblasts produce woven bone and cartilage respectively. The external callus is a collar around the fracture site. This collar is formed by the osteoblasts and chondroblasts, which produce woven bone and cartilage respectively. The external callus allows the stabilization of the bone broken ends.[1, 6]

3) Callus ossification (figure 1.8-3)**:** in this phase the cartilage present in the external callus is converted in woven, cancellous bone by endochondral ossification. In the internal callus, the cartilage and fibers are also substituted by woven, cancellous bone. This callus ossification becomes the broken bone even more stable.[1, 6]

4) Remodeling of bone (figure 1.8-4)**:** in the last phase of the process the woven bone in the internal callus and the death bone next to the fracture local are substituted by compact bone. In this new bone, the osteons from the broken ends are extended across the fracture zone, in order to link the two parts. This repair stage is long and can last more than a year.[1, 6]

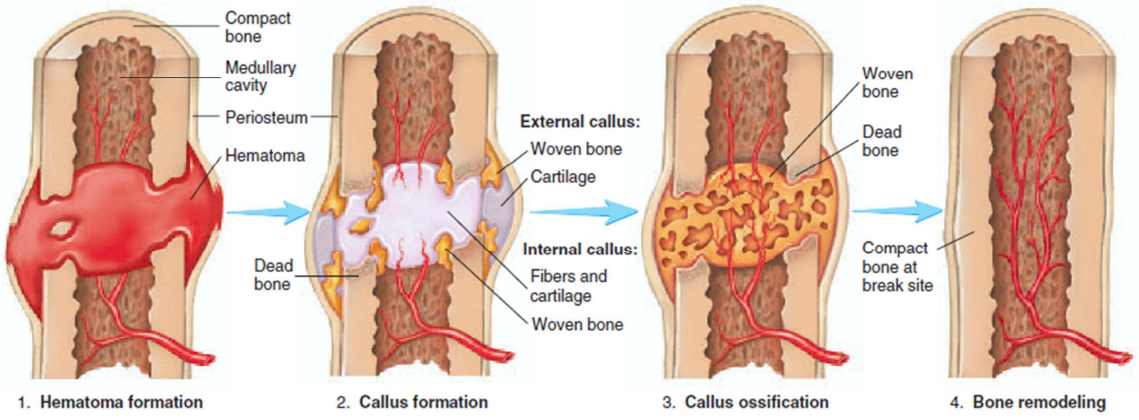

Figure 1.8: Phases of the bone repair process.[adapted from [1]]

1.1.2.4. Bone disorders

The natural bone tissue physiolology can be influenced by several types of bone disorders, as presented in figure 1.9.[1, 2, 10] These disorders can interfere with the bone growth process giving rise to bones with abnormal dimensions or very brittle, being susceptible to fracture easily. Other bone disorders can interfere with the bone remodeling process, namely, causing a bone resorption rate higher than its formation rate. This difference may cause small or large bone defects, or even its fracture.[1, 2, 10, 11]

Moreover, bone defects or fractures can occur due to injuries caused by external factors, such as falls, in which bone is exposed to an excessive stress.[1, 2]

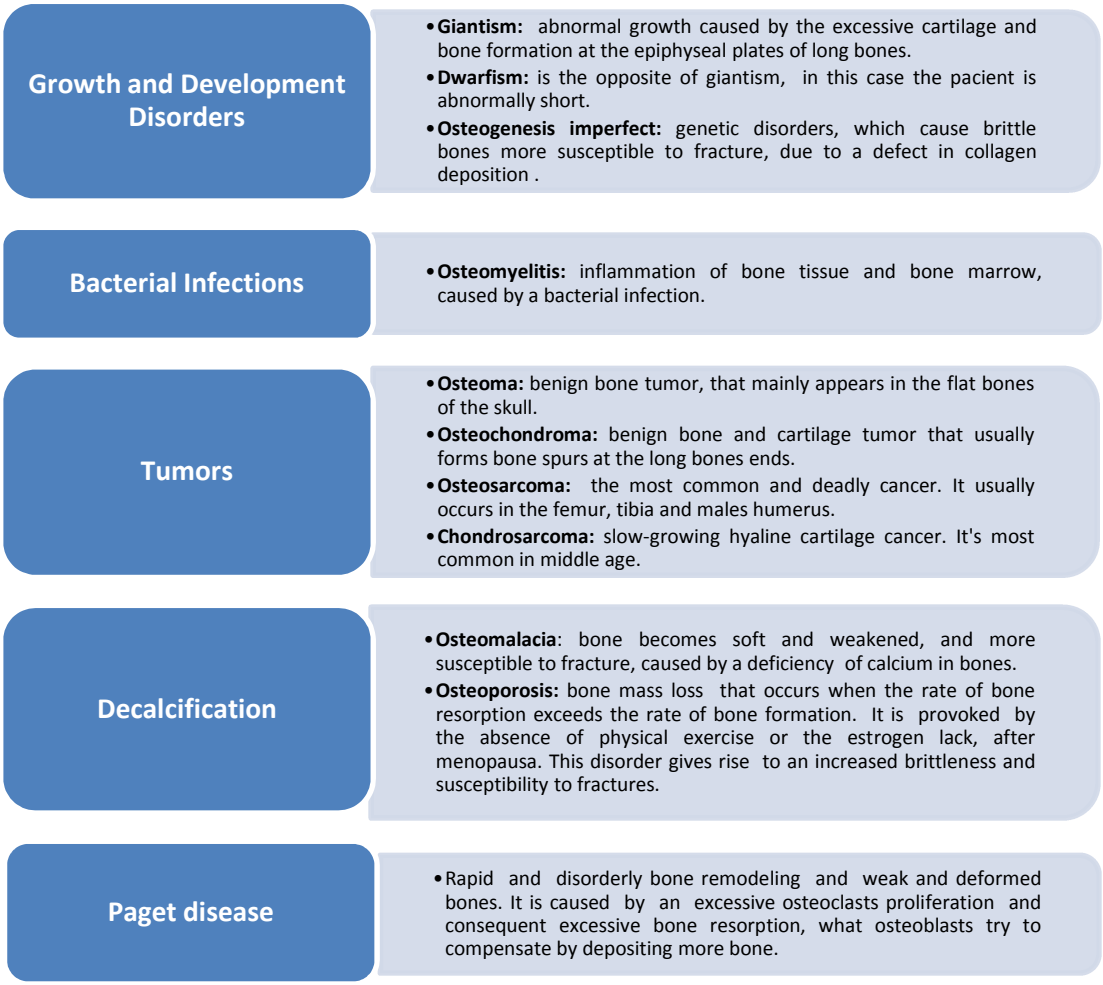

Figure 1.9: Different bone disorders.[1,2,10]

1.2. Biomaterials

The development of biomaterials has presented a big impact on the treatment of injuries and diseases. Biomaterials may be of synthetic or natural origin. Briefly, a biomaterial can be defined as a material used in contact with biological systems to replace a part or a function of the body, without harming the living organism and its components.[12-15] These materials must meet several criteria, such as biocompatibility, which is defined as "the ability of a material to perform with an appropriate host response in a specific application".[12, 13, 16] Thus, a biomaterial must simultaneously be non-toxic and satisfy the requirement of functionality for what it was designed.[16]

Biomaterials can be classified according to two different parameters, bulk and surface properties. The characterization based on bulk properties is based on the atomic composition and the respective inter-atomic bonding, according to these biomaterials can be metals, ceramics, polymers and composites. The characterization based on surface properties based describes the interaction type that happens at the material interface with the biological environment:

Bioinert: materials that retain their physical and chemical properties when implanted, presenting a minimal or even none interaction with the surrounding tissues. Examples: titanium and alumina.[15, 17, 18]

Bioactive: materials that chemically bond and interact with the surrounding tissues at the interface, presenting the ability to initiate a biological response, namely cell adhesion, proliferation, or even in some cases differentiation of some progenitor cells. Examples: synthetic HAP.[13, 15, 18]

Biotolerated: materials that are moderately accepted by the host organism when implanted, being normally involved by a fibrous capsule. Example: stainless steel.[18]

Bioresorbable: materials that, after implantation, are degraded over time and simultaneously and gradually replaced by regenerating endogenous tissue. The degradation resultant products are absorbed and released through metabolic processes. Example: tricalcium phosphate (TCP) and hyaluronic acid (HA).[15, 17, 18]

1.2.1. Synthetic bone substitutes

In order to treat bone defects, different approaches can be used: grafts either from the patient (autograft), from a donor (allograft) or from another animal specie (xenografts); demineralized bone matrix (DBM) extracted from the allografts; or synthetic bone substitutes that have been developed in the last few decades.[19-24]

Three essential elements are convenient for an ideal bone regeneration, osteogenesis, osteoinduction, and osteoconduction, resulting in an osteointegration of the graft or substitute in the host bone.[21, 22] Thus, autografts are the most used option, because they present the three essencial elements and no immune response after implantation. However, their availability is limited and they can cause chronic pain.[19-22] Allografts and xenografts present only osteoinductive and osteoconductive properties, and have risks of bacterial contamination, viral transmission, and immunogenicity.[19-21, 23] Synthetic bone substitutes, such as HAP and bioglasses, are bioactive and bioresorbable biomaterials that just present osteoconductive properties. However, they eliminate the risk of disease transmission, their availability is unlimited and possible to produce in different forms and porosity levels.[19-22] Moreover, these synthetic substitutes can be combined with biologic agents, which grant them osteoinductive and osteogenic properties.[19, 21, 23]

Synthetic substitutes options:

- **Ceramics**

HAP and TCP

The most used ceramics are synthetic HAP and β-crystalline form of TCP (β-TCP, $Ca_3(PO_4)_2$). These calcium-phosphate-based ceramics allow bone cells attachment, proliferation and migration. β-TCP and HAP present chemical similarity to the bone mineralized phase, that provides their osteoconductive potential and good biocompatibility. Although, TCP is resorbed more quickly by the osteoclasts and mechanically less stable than HAP.[20-23]

Bioactive glasses

The main components of the bioactive glasses are sodium oxide (Na_2O), calcium oxide (CaO), phosphorus pentoxide (P_2O_5) and silicon dioxide (SiO_2). However, there are different bioglasses depending on the percentage of each one of those

components in the glass. When bioglasses are exposed to physiologic aqueous solutions, a mechanically strong bond between the glass and the bone is established due to the synthesis of apatite crystals similar to that of bone, promoting the osteointegration. Thus, these materials are thought to be not only osteoconductive, but also osteoinductive. Moreover, these materials present greater mechanical strength when compared to calcium phosphate preparations.[21, 22, 25]

Therefore, in order to improve the biological and mechanical properties of HAP, bioactive glasses have been associated to it, giving rise to a material named glass-reinforced hydroxyapatite (GR-HA).[26, 27]

- **Hybrid materials**

These materials can be obtained from the combination of a ceramic matrix, which supply a structural underlay, with osteogenic cells (which can be obtained from bone marrow) and/or osteoinductive factors (namely morphogenetic proteins (BMP's)). These elements confer to the substitute osteogenic and osteoinductive properties, providing a better and quicker bone repair process.[20, 21, 23]

1.2.2. Hydrogels

Hydrogels are cross-linked three-dimensional polymeric structures, which swell in aqueous solutions.[12, 16, 28] These structures can be produced with natural polymers (such as alginate, collagen, agar and chitosan) or synthetic polymers (such as poly(ethylene glycol) (PEG), poly(N-isopropylacrylamide) (PNIPAAm), poly(ethylene oxide) (PEO) and poly(propylene oxide) (PPO)). [16, 28-33]

These cross-linked structures can contain covalent bonds between monomers, physical cross-links of entanglements, hydrogen bonds or van der Waals interactions between chains or even ionic interactions. Besides that, they can be homopolymeric hydrogels: when the network is composed by just one hydrophilic monomer type; copolymeric/multipolymeric hydrogels: when are composed by two/or more distinct monomers, being at least one of them hydrophilic to ensure the swelling property; interpenetrating polymeric hydrogels: when are composed by two intermeshed networks.[12, 28]

In recent years, hydrogels have been studied for several biomedical and pharmaceutical applications. Due to their properties they can be potentially used as

drug delivery injectable systems and as injectable scaffolds in tissue engineering. They present an inherent ability to mimic the ECM structural and compositional properties, allowing cell adhesion and proliferation and promoting the diffusion of hydrophilic nutrients and cell metabolites.[12, 16, 28, 29, 34]

1.2.2.1. Alginate

"Alginates" is the designation given to a natural family of biodegradable, biocompatible, hydrophilic (in normal physiological conditions) and non-toxic polysaccharides extracted from some marine algae and some microorganisms. [28, 35-38] This family includes alginic acid and its salts, such as sodium alginate. The alginic acid was discovered by the British chemist Stanford in 1880, and it exists in all species of the brown seaweed (*Phaeophycae*), constituting up to 40% of the dry matter, and in a few species of red algae (*Corallinacae*). [36, 39-41]

- **Chemical structure**

Alginates are linear block co-polymers composed of two different monomers, β-D-mannuronic acid (M) and α-L-guluronic acid (G), which are linked by (1-4) glycosidic bonds (figure 1.10-a). These two components are associated in a certain order, in a block-structure pattern, which can be homopolymeric, if the block is only constituted by just one monomer type (M or G) or heteropolymeric, if the block is simultaneously constituted by the two monomers alternated (figure 1.10-b). The blocks composition and their sequence in a certain alginate depends of the source of which it was extracted, however, some investigations have revealed that the most common structure comprises homopolymeric M blocks and homopolymeric G blocks interspersed by heteropolymeric MG blocks.[16, 39-41]

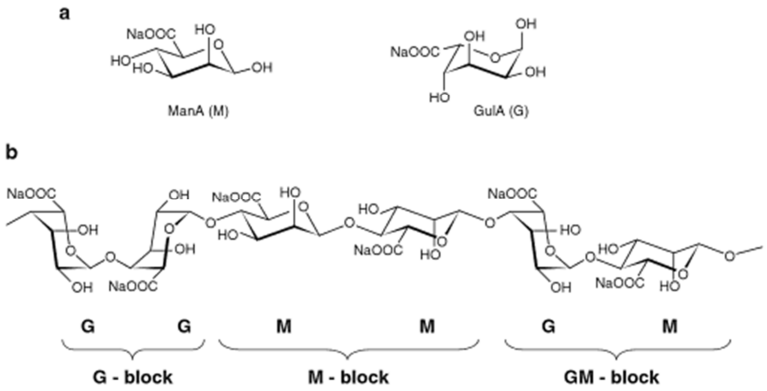

Figure 1.10: (a): Chemical structure of alginate monomers; (b): Example of a monomers sequence of alginate.[adapted from [36]]

The two monomers present distinct conformations (M presents $^4C_1$ chair conformation and G presents $^1C_4$ boat conformation) to allow the bulky carboxyl group being in the energetically best equatorial position.[36, 39] Thus, due to the different monomers conformations, the polysaccharide one will be influenced by the orientation of the glycosidic bonds, that depends of the monomers sequence in the polymer. Between two M monomers exist a diequatorial glycosidic linkage, between two G monomers exist a diaxial, in a MG sequence exist an equatorial-axial and in a GM sequence exist an axial-equatorial. So, a region composed of a M sequence (M-M-M-M) reveals a flat ribbon structure, whilst a region composed of a G sequence (G-G-G-G) reveals a buckle structure (figure 1.10-b), and besides that, it was reported that the stiffness of the chain blocks decreases in the order GG>MM>MG.[36, 39]

- **Alginate hydrogels**

The main property of alginate that potentiates its use in different areas, it is its ability to bind some divalent cations, such as Ca^{2+}, Ba^{2+}, Sr^{2+}, Cu^{2+} and Pb^{2+} in the carboxylic groups providing the gelation of the alginate solution.[36, 39, 41, 42]

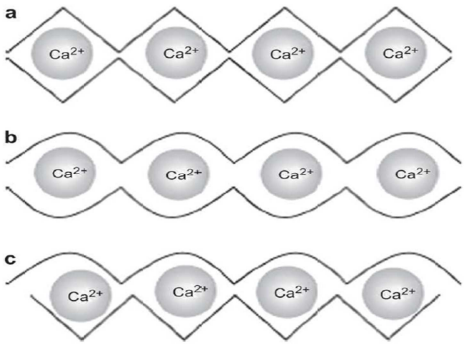

Figure 1.11: Accommodation of the calcium ions, between two alginate chains, in the different glycosidic linkages: (a) GG/GG interaction; (b) MG/MG interaction; (c) GG/MG interaction.[adapted from [42]]

Both of the constituent monomers of an alginate salt possess a carboxylic moiety, which at a pH value above its pKa (about about 3.38 and 3.65 for M and G residues,

respectively), are negatively charged, transforming the material in a polyanion, named alginate.[35, 36, 43, 44] Thus, in these conditions, the ions responsible for the gelation can bind to the carboxylic groups, happening the cross-linking of the polymeric chains. This reaction is very rapid and irreversible.[36, 41]

The two constituent monomers of alginate reveal just one difference between them, their conformation, whic results in a selective ion-binding phenomenon. It has been reported that the divalent ions have a higher tendency to bind to guluronate blocks of the polymer chains. This fact is owed to the geometrical requirements of the cavity originated by the diaxial linkage between the G monomers, that allows a higher degree of accommodation of the divalent ions than the other glycosidic linkages types (figure 1.11). Each cross-linking ion interacts with two consecutive G monomers of a polymeric chain and with two consecutive G monomers of an adjacent polymeric chain. This phenomenon establish junctions between the chains, what is named of the egg-box model of crosslinking (figure 1.12), forming a gel structure.[16, 36, 39-42]

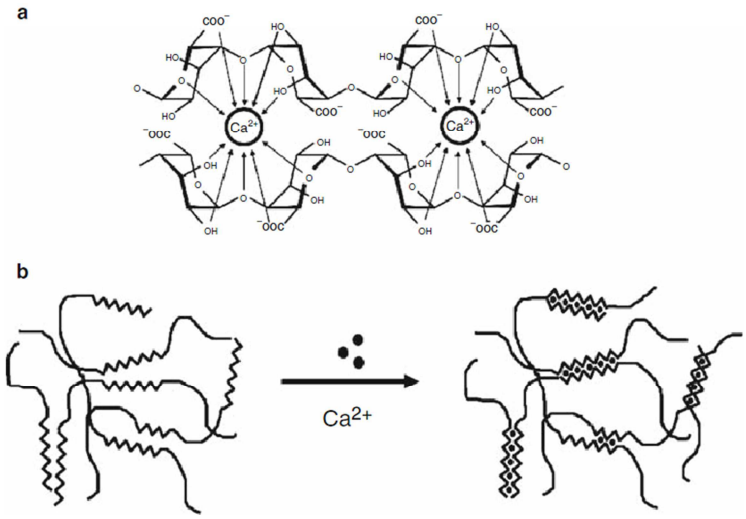

Figure 1.12: The egg-box model of cross-linking: (a): binding of the divalent cations in the G monomers of two polymeric chains; (b): formation of junction zones between polymeric chains.[adapted from [36]]

Therefore, the properties of the gel are dependent of the ratio between M and G monomers (M:G ratio). If the proportion of the G monomer is higher, it will be obtained a strong brittle gel. On the other hand, if the proportion of the M monomer is higher, the formed gel will be weaker, but more flexible, because there are less junction zones between the polymer chains.[16, 36, 40]

Besides that, it is possible to produce a hydrogel of alginate with another associated polymer, in order to better some alginate properties or even to obtain, in the gel, some inexistent features in the alginate. As alginate is a polyelectrolyte, more specifically a polyanion, it can be ionically associated with a polycation existent in the same solution through hydrogen bonding or electrostatic interactions, forming a polyelectrolyte complex. Although, to achieve this complex formation it is necessary to control the solution pH to ensure that the two polymers are on the charged state. So, the solution pH has to be above the pKa of the polyanionic polymer, and below the pKa of the polycationic polymer to obtain two polyelectrolytes oppositely charged.[35, 40, 42, 45]

- **Physical-chemical Properties**

Molecular-weight and Viscosity

Alginates are considered polydisperse relatively to the molecular weight. This fact can be justified by two aspects: alginate is not gene-encoded, their production is enzymatically controlled; the extraction process provokes a significant depolymerisation of the polymer chains. Thus, due to the polydispersity in the polymerization degree of each sample, the molecular weight of an alginate is an average of the different existent molecular weights.[36, 41]

The viscosity observed in alginate solutions depends mostly of the temperature, alginate molecular weight, solution concentration and pH value. With an alginate molecular weight increase it is verified a viscosity increase of the solution, to an increase in the concentration happens the same.[36, 40, 41] When an alginate solution is exposed to a temperature increase its viscosity decreases, what is owed to a depolymerization of the polymeric chains.[36, 41] With a pH decrease, the viscosity slightly increases and it is maximum when the pH value of the solution is below the pKa of the alginate, because the carboxylic groups along the chains become protonated forming hydrogen bonds.[40]

Rheological properties

About the rheological properties of alginates hydrogels, several studies have proved that these materials present a non-Newtonian behavior, which means that the shear rate and the shear stress are not directly proportional, so the viscosity depends of the shear rate (apparent viscosity, η).[46-49] More exactly, they present a shear thinning behavior, the viscosity decreases when the shear rate increases. Besides that, they are classified as presenting a viscoelastic behavior. A viscoelastic fluid simultaneously presents typical properties of a fluid (viscous) and a solid (elastic). The elasticity of a viscoelastic fluid, which is subjected to a not hydrostatic stress state, is revealed by its capacity of partially invert the deformation process after the removal of the stress, resembling to the elastic response of a solid.[36, 41, 46-49]

- **Biocompatibility**

In vitro and in vivo alginate biocompatibility has been widely studied. Although, it is considered as a biocompatible material, some researchers still disagree regarding the impact of the material in the organism. It has already been reported that alginates with high content of M monomer were immunogenic and induce cytokine production about 10 times more than alginates with high G monomer content. On the other hand, in some other studies alginate implants with a high M percentage were used, and it was observed an insignificant or even none immunoresponse.[40, 50, 51]

- **Biodegradation**

Alginate, like the other biodegradable polymers, when exposed to the body fluids and tissues can be degraded by chemical oxidation. When a material is implanted into the body, happens a normal and minimal inflammatory response to the foreign material. In this response inflammatory cells, mainly leukocytes and macrophages, produce highly reactive oxygen species (for example, superoxide O_2^- and hydrogen peroxide H_2O_2), which can cause the cleavage of the polymeric chains through their oxidative effect.[52]

Besides that, alginate can also be degraded by non-enzymatic hydrolysis, which consists in the cleavage of the chemical bonds in the polymer structure by the attack of water, resulting in the formation of oligomers and monomers. In addition, the hydrolysis process can also be catalyzed by the enzyme alginase, which catalyzes the

cleavage of the (1-4)-glycosidic bond by a β-elimination reaction, breaking down the polymeric chains. [36, 39, 40, 52] Nevertheless, this enzyme does not exist in mammals. However, alginate hydrogels that were ionically crosslinked can be dissolved in vivo through the cross-linking ions release into the surrounding media. This phenomenon is owed to an exchange process with monovalent cations present in the media, mainly Na^+ ions. This happens when alginate gels are exposed for some time (several hours) to a physiological concentration of Na^+. By this way, for medical applications, the average molecular weight of alginate must be a concern, it must be as low as possible, in order to respect the renal clearance threshold to ensure a complete removal of the substance from the organism.[36, 39, 40, 53]

- **Biomedical Applications**

Due to the biocompatibility, non-toxicity, biodegradability and relatively low cost of alginates, they have been studied to be used in several biomedical applications.[39, 40, 42, 54]

In the case of bone tissue engineering, to promote bone regeneration, alginate hydrogels have shown potential to be used as a structure to encapsulate and release osteoinductive factors and bone forming cells inside the body.[29, 40, 53] Furthermore, alginate hydrogels have also been used as a vehicle of inorganic materials, such as HAP, allowing its injectability.[34, 50, 55, 56] Thus, the synthetic bone substitutes can be introduced into the bone defect in a minimally invasive way and allow to fill the whole bone defect, even the most irregular one.[34, 40, 56]

However, an alginate matrix can reveal some disadvantages in biomedical applications, namely, a reduced cell adhesion and unstable and weak mechanical properties.[37, 40, 42, 53, 54] Although, to improve the low cell adhesion, alginate hydrogels have the advantage of being easily chemically modified with adhesion ligands (such as Arginine-Glycine-Aspartic acid residues (RGD)), and associated with another polyelectrolyte that presents a better cell adhesion, such as chitosan.[16, 29, 37, 40, 54, 57] Similarly, the mechanical properties can also be improved through the association of alginate with another polymer that presents better properties.[37, 40, 54, 57]

1.2.2.2. Chitosan

Chitosan is a natural and hydrophilic copolymer, and it is composed by two monomeric units, D-glucosamine and N-acetyl-D-glucosamine linked by β(1–4)-glycosidic bond, as presented in figure 1.13-B.[16, 58-60] This linear polysaccharide has been widely studied for medical applications, due to many properties that it presents, such as, biocompatibility, biodegradability, non-toxicity, antimicrobial activity, non-carcinogenicity, notable affinity to proteins, promotion of cell adhesion, as well as proliferation and differentiation.[53, 58-61] The cell adhesion is mainly promoted by the fact of chitosan having a positive charged surface, which allows this phenomenon to occur on the surface of the implanted biomedical material, due to the negatively charged cell surface.[57, 61]

This polymer is obtained from the chitin (figure 1.13-A), which is extracted from exoskeleton of crustaceans, like crabs and shrimps, and even from cell walls of several fungi.[16, 35, 59] Chitosan results from the alkaline deacetylation of the chitin, which means, the removal of some acetyl groups. Thus, the ratio between the two monosaccharides depends of the deacetylation degree (DD), what determines the percentage of amino groups in the polymeric chain. [16, 59]

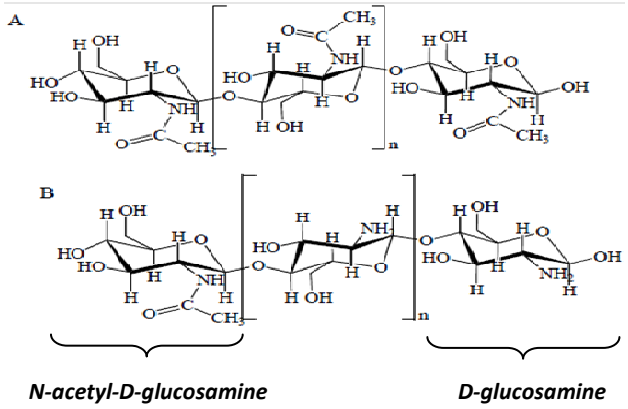

Figure 1.13: Chemical structure of: A. chitin; B. chitosan.[adpted from [61]]

At neutral or basic pH conditions, chitosan contains free amino groups, being insoluble in water. But in weekly acidic solutions, with a pH lower than its pKa (which varies between 6.2 and 7), the amino groups of the D-glucosamine monomers along the molecular chains are protonated, making chitosan soluble in water. In these conditions, chitosan is in the polycationic form and it can ionically complex with

polyanions, for instance, the alginate, resulting in a polyelectrolyte complex formation.[35, 45, 53, 61]

Chitosan insolubility at neutral pH is a limitation in some medical applications, because most biological applications for chemical substances need the material to be processible and functional at that pH value. The chitosan solubility is mainly influenced by its molecular weight and degree of deacetylation. Consequently, some techniques have been developed to lower the molecular weight of chitosan. This phenomenon is achieved by the hydrolysis of the polymeric chains, in order to produce chitosan salts which are soluble in water. To achieve the depolymerization of the chains there are chemical, physical and enzymatic techniques, for instance, the chemical process can be done by acidic hydrolysis promoted by HCl, resulting in the salt chitosan HCl.[59, 61]

In vivo, chitosan, like alginate, can be degraded by chemical and enzymatic oxidation, non-enzymatic hydrolysis and enzyme-catalyzed hydrolysis. This last process can be oriented by different proteases, such as, lysozyme, papain, chitosanase and pepsin. The lysozyme, which is present in all mammalian tissues, seems to be the main protease involved in chitosan degradation by catalyzing the acetylated residues hydrolysis. Thus, the degradation rate of the polymer is inversely dependent of the DD, for a higher DD it is observed a lower rate of enzymatic degradation.[53, 61, 62] The products of its biodegradation are non-toxic oligosaccharides of variable length, that can be incorporated to glycosaminoglycans and glycoproteins, to metabolic pathways or be excreted by the organism.[52, 53, 61]

1.2.2.3. Hyaluronic Acid (HA)

HA is a natural, hydrophilic and non-sulfated glycosaminoglycan. This polymer is a linear polysaccharide, in which, the repeating unity is a disaccharide composed by two monomers, D-glucuronic acid and *N*-acetyl-D-glucosamine, linked through alternating β(1-3) and β(1-4)-glycosidic bonds, figure 1.14.[63-66] HA has been very investigated to be used as a biomaterial in various medical applications, due to its biocompatibility, biodegradability, and nonimmunogenicity.[60, 64, 65]

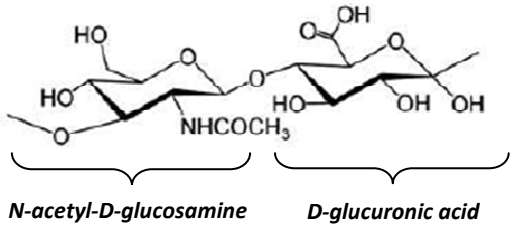

Figure 1.14: Chemical structure of the two monosaccharides of hyaluronic acid.[adpted from [68]]

HA is the main component existent in the ECM of living tissues, namely in the connective, epithelial and neural.[60, 64, 65, 67] This polymer, due to its structural and biological properties, has the ability to mediate the cell signaling and behavior, and the matrix organization. HA is able to interact with some cell surface receptors, being involved in the tissue hydrodynamics, cell migration and proliferation.[60, 64, 65]

This natural polymer HA is water-soluble and it forms highly viscous solutions with specific viscoelastic properties.[53] At a pH value above its pKa of approximately 3, HA is in the polyanionic form due to the deprotonation of the carboxylic groups existent in the D-glucuronic acid monomers, being usually called as hyaluronate or hyaluronan.[60, 66] When the polymer is in this form it can also establish, as alginate and chitosan, ionic interactions with oppositely charged polyelectrolytes.[45, 60]

In the case of bone, HA has been discovered, in high concentrations, in the early fracture callus, in the osteoprogenitor cells cytoplasm, and in lacunae, in the growth plate, surrounding chondrocytes.[63] Besides that, it was shown that high molecular weight HA can inhibit osteoclasts differentiation and can be involved in the migration of mesenchymal stem cells. Therefore, HA is a material with a big potential to be used in bone tissue engineering to treat bone defects or fractures, stimulating the bone repair process.[67]

In vivo conditions, the enzyme-catalyzed hydrolysis of HA is oriented by hyaluronidases. These enzymes catalyze the hydrolysis of the β-N-acetyl-D-glucosaminidic linkages in the polymer chains, resulting in the formation of mono and disaccharides, which then are converted into ammonia, carbon dioxide and water via the Krebs cycle. Moreover, HA can also be degraded by chemical and enzymatic oxidation and non-enzymatic hydrolysis. [52, 53, 68, 69]

1.3. Injectable synthetic bone substitutes

In order to improve the clinical potential of the synthetic bone substitutes, scientists have developed injectable bone substitutes systems able to mould to the shape of the bone defect.[24, 46, 50, 70] This minimally invasive surgical approach can decrease the surgery time, reduce the damages caused by large muscle retraction, reduce the size of scars and the post-operative pain, which provides a more rapid and economic recovery of the patient.[70, 71] Additionally, these systems are even more beneficial in clinical situations that present difficulties in the access to the bone defect, namely in the augmentation of osteoporotic fractures, in some applications in the spine and in the treatment of maxillofacial defects.[70, 71]

Therefore, to produce the injectable systems, the association of synthetic bone substitutes with hydrogels has been proposed, and several products based on this concept are already available in the market. Some examples are presented in table 1.[24, 72]

Table 1: Examples of injectable bone substitutes.[adapted from [24,72]].

Product	Composition	Company
MBCP Gels ®	Biphasic calcium phosphate (BCP) granules (60% HAP, 40% β-TCP; 0.08-0.2mm) and 2% HPMC.	Biomatlante (France)
Pepgen P-15®	HAP (0.25-0.42mm), P-15 peptide and aqueous sodium hyaluronate solution.	Dentsply (USA)
Healos® Fx	HAP (20-30%) and collagen.	DePuy Spine (USA)
Integra Mozaik™	β-TCP (80%) and type 1 collagen (20%).	Integra LifeSciences (USA)
Ceros® TCP Putty/ cyclOS® Putty	β-TCP granules (0.125-0.71mm; 94%) and recombinant sodium hyaluronate(6%).	Mathys Ltd (Switzerland)
Mastergraft®	BCP (85% HA, 15% β-TCP) and bovine collagen.	Medtronic (USA)
NovaBone®	Bioglass and synthetic binder.	NovaBone (USA)
Calstrux™	β-TCP granules and carboxymethyl cellulose (CMC).	Stryker Biotech (USA)
Therigraft™	β-TCP granules and polymer.	Therics (USA)
Collagraft	BCP granules (65% HA, 35% β-TCP; 0.5-1.0 mm), bovine collagen, and bone marrow aspirate.	Zimmer (USA)

1.4. Implant-associated infections

The risk of infection is present in every surgical process, namely when a biomaterial is implanted into the body, such as a synthetic bone substitute in orthopaedic and maxillofacial surgery. The occurrence of infection can negatively affect the regenerative ability to the implanted material, increasing the patient recovery time and associated costs.[73, 74] In orthopedic surgery the main bacteria responsible for infections are: *Staphylococcus aureus*, *Staphylococcus epidermidis* and *Pseudomonas aeruginosa*, as presented in figure 1.15.[73, 75]

The infections incidence has decreased by using antibiotics and hygienic protocols. However, these protocols are not efficient enough and the recurrent using of antibiotics can lead to antibiotic-resistant bacteria, not being affected by their action.[73, 76] Thus, ideally, a bone substitute should not only perform its supposed regeneration function, but also have the ability to prevent infection by microorganisms colonization.

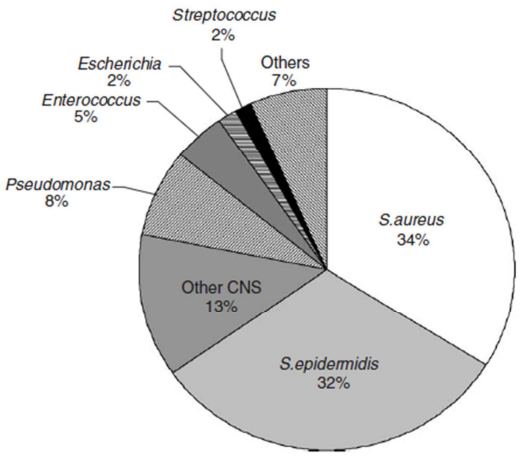

Figure 1.15: The main pathogenic species among orthopedic implant associated infections.[adapted from[73]]

Therefore, alternative methods to avoid the infection phenomenon have been tried, such as, the incorporation in the biomaterials of effective ions against bacteria growth. The most studied and used ion is Ag^+, which has already revealed an efficient antimicrobial activity against several microorganisms. However, when this ion is used in high concentrations it can be toxic to mammals.[74] More recently, it has been investigated the antimicrobial ability of some lanthanides, such as Ce(III). This ion has revealed an efficient bacteriostatic and bactericidal ability against several microorganisms. Moreover, it has been reported as non-toxic to mammals even at high concentrations.[77, 78]

1.5. Motivation and objectives

A few millions of patients worldwide, per year, need a bone graft or synthetic bone substitute to repair a bone defect resulting from an injury or a disorder. For instance, in USA, more than 500.000 bone grafting procedures are happening to treat bone defects, annually. The associated costs from the provided medical care by this country, in orthopaedic defects, are estimated to be around $849 billion/year.

In last few years, several synthetic injectable bone substitutes have been developed due to the advantages already discussed regarding to its easy application in certain clinical conditions. Moreover, one of the most attractive features of injectable bone substitutes, it is the possibility to grant additional properties to the bone substitute through the associated hydrogel. The hydrogel chemical structure and morphology can improve the cell adhesion on the substitute; it can have incorporated osteogenic cells, osteoinductive factors or even therapeutic agents. So, the hydrogel association to the substitute can promote a better integration of the implant with the host tissue, which can improve the overall treatment outcome.

Therefore, the main objective of this master dissertation was to develop a hydrogel to associate with GR-HA granules, allowing their easy injection and application in a bone defect. The developed injectable system is intended to be used in orthopaedic and maxillofacial bone defects.

Furthermore, the hydrogel should be biocompatible and biodegradable, being the desired degradation time of about 2 or 3 days. The vehicle should also enhance the osteoconductive properties of the bone substitute, improving the bone regeneration process. As an additional property, the vehicle should also present an antimicrobial activity against the main microorganisms involved in bone infections.

The developed material should be properly characterized in a physical-chemical and biological (*in vitro* and *in vivo*) point of view.

1.6. References

1. Seeley R.R., Stephens T.D., and Tate P., eds. *Anatomy and Physiology*. 6 ed. 2004, The McGraw-Hill Companies: USA. 610.
2. Saladin K.S., ed. *Anatomy & Physiology: The Unity of Form and Function*. 3 ed. 2004, The McGraw−Hill Companies: USA. 1156.
3. Clarke B., *Normal bone anatomy and physiology.* Clinical Journal of the American Society of Nephrology, 2008. **3**: p. 131-139.
4. Meyer U. and Wiesmann H.P., eds. *Bone and Cartilage Engineering*. 2006, Springer: Germany. 264.
5. Kozielski M., Buchwald T., Szybowicz M., Blaszczak Z., Piotrowski A., and Ciesielczyk B., *Determination of composition and structure of spongy bone tissue in human head of femur by Raman spectral mapping.* Journal of Materials Science-Materials in Medicine, 2011. **22**(7): p. 1653-1661.
6. Bilezikian J.P., Raisz L.G., and Martin T.J., eds. *Principles of Bone Biology*. 3 ed. Vol. 1. 2008, Academic Press: USA. 1900.
7. Hollinger J.O., Einhorn T.A., Doll B.A., and Sfeir C., eds. *Bone Tissue Engineering* 2005, CRC Press: USA. 336.
8. Matsuo K., *Cross-talk among bone cells.* Current Opinion in Nephrology and Hypertension, 2009. **18**(4): p. 292-297.
9. Stenbeck G., *Formation and function of the ruffled border in osteoclasts.* Seminars in Cell & Developmental Biology, 2002. **13**(4): p. 285-292.
10. Guanabens N., Garrido J., Gobbo M., Piga A.M., del Pino J., Torrijos A., Descalzo M.A., Garcia F.J., Cros J.R., Carbonell J., Perez M.R., Tornero J., and Carmona L., *Prevalence of paget's disease of bone in Spain.* Bone, 2008. **43**(6): p. 1006-1009.
11. Service P.H., *Bone Health and Osteoporosis: A Report of The Surgeon General*. 2004: USA. p. 440.
12. Ratner B.D. H.A.S., Schoen F.J., Lemons J.E., ed. *Biomaterials Science: an Introduction to Materials in Medicine*. 2nd ed. 2004, Elsevier Academic Press. 879.
13. Enderle J.D. B.S.M., BronzinoJ.D. , ed. *Introduction to Biomedical Engineering*. 2nd ed. 2005, Elsevier Academic Press. 1118.
14. Bronzino J.D., ed. *The Biomedical Engineering Handbook*. 2nd ed. Vol. 1. 2000, CRC Press LLC. 3189.
15. Dee K.C. P.D.A., Bizios R., ed. *An Introduction To Tissue-Biomaterial Interactions*. 1st ed. 2002, Wiley-Liss, Inc. 248.

16. M.M. Y., ed. *Comprehensive Biotechnology*. 1 ed. Vol. 5. 2011, Elsevier: Oxford. 752.
17. Binyamin G. S.B.M., Mery C.M., *Biomaterials: A primer for surgeons.* Seminars in Pediatric Surgery, 2006. **15**(4): p. 276-283.
18. Gutierres M. L.M.A., Hussain N.S., Cabral A.T., Almeida L., Santos J.D. , *Substitutos ósseos: conceitos gerais e estado actual.* Arquivos de Medicina 2006. **19**(4): p. 153-162.
19. Bostrom M.P.G. and Seigerman D.A., *The clinical use of allografts, demineralized bone matrices, synthetic bone graft substitutes and osteoinductive growth factors: a survey study.* HSS Journal, 2005. **1**(1): p. 9-18.
20. Zimmermann G. and Moghaddam A., *Allograft bone matrix versus synthetic bone graft substitutes.* Injury, 2011. **42**: p. 16-21.
21. Giannoudis P.V., Dinopoulos H., and Tsiridis E., *Bone substitutes: an update.* Injury, 2005. **36**(3): p. 20-27.
22. Moore W.R., Graves S.E., and Bain G.I., *Synthetic bone graft substitutes.* ANZ Journal of Surgery, 2001. **71**: p. 354-361.
23. Vaccaro A.R., *The role of the osteoconductive scaffold in synthetic bone graft.* Orthopedics, 2002. **25**: p. 571-578.
24. Bohner M., *Design of ceramic-based cements and putties for bone graft substitution.* European Cells and Materials, 2010. **20**: p. 1-12.
25. Nandi S.K., Roy S., Mukherjee P., Kundu B., De D.K., and Basu D., *Orthopaedic applications of bone graft & graft substitutes: a review.* Indian Journal of Medical Research, 2010. **132**: p. 15-30.
26. Lopes M.A., Monteiro F.J., and Santos J.D., *Glass-reinforced hydroxyapatite composites: fracture toughness and hardness dependence on microstructural characteristics.* Biomaterials, 1999. **20**(21): p. 2085-2090.
27. Ravarian R., Moztarzadeh F., Solati Hashjin M., Rabiee S.M., Khoshakhlagh P., and Tahriri M., *Synthesis, characterization and bioactivity investigation of bioglass/hydroxyapatite composite.* Ceramics International, 2010. **36**(1): p. 291-297.
28. Slaughter B.V., Khurshid S.S., Fisher O.Z., Khademhosseini A., and Peppas N.A., *Hydrogels in regenerative medicine.* Advanced Materials, 2009. **21**(32-33): p. 3307-3329.
29. Fedorovich N.E., Alblas J., Wijn J.R., Hennink W.E., Verbout A.J., and Dhert W.J.A., *Hydrogels as extracellular matrices for skeletal tissue engineering: state-of-the-art and novel application in organ printing.* Tissue Engineering, 2007. **13**(8): p. 1905-1925.
30. Ruel-Gariépy E. C.A., Chaput C., Guirguis S., Leroux J.C., *Characterization of thermosensitive chitosan gels for the sustained delivery of drugs.* International Journal of Pharmaceutics, 2000. **203**: p. 89–98.

31. Rossi F. S.M., Casalini T., Veglianese P., Masi M., Perale G., *Characterization and degradation behavior of agar–carbomer based hydrogels for drug delivery applications: solute effect.* International Journal of Molecular Sciences, 2011. **12**(6): p. 3394-3408.
32. Aguilar M.R. E.C., Gallardo A., Vázquez B., Román J.S., *Smart Polymers and Their Applications as Biomaterials.* Biomaterials, 2007. **3**: p. 1-27.
33. Rey-Rico A. S.M., Couceiro J., Concheiro A., Alvarez-Lorenzo C., *Osteogenic efficiency of in situ gelling poloxamine systems with and without bone morphogenetic protein-2.* European Cells and Materials, 2011. **21**: p. 317-340.
34. Lu L., Y. Qi, C. Zhou, and Y. Jiao, *Rapidly in situ forming biodegradable hydrogels by combining alginate and hydroxyapatite nanocrystal.* Science in China Series E: Technological Sciences, 2010. **53**(1): p. 272-277.
35. Abreu F.O.M.S. B.C., Forte M. M. C., Kist T.B.L., *Influence of the composition and preparation method on the morphology and swelling behavior of alginate–chitosan hydrogels.* Carbohydrate Polymers, 2008. **74**(2): p. 283-289.
36. B.H.A. R., ed. *Alginates: Biology and Applications.* 2009, Springer.
37. Chunga T.W., Yangb J., Akaikeb T., Choc K.Y., Nahd J.W., Kima S.I., and Cho C.S., *Preparation of alginate/galactosylated chitosan scaffold.* Biomaterials, 2001. **23**: p. 2827-2834.
38. Wang L. S.R.M., Cooper P.R., Lawson M., Triffitt J.T., Barralet J.E., *Evaluation of sodium alginate for bone marrow cell tissue engineering.* Biomaterials, 2003. **24**(20): p. 3475-3481.
39. Draget K.I. S.O., Skjak-Braek G., ed. *Polysaccharides and Polyamides in the Food Industry. Properties, Production and Patents.* 1 ed. Vol. 1. Alginates from Algae. 2005. 30.
40. Lee K.Y. and Mooney D.J., *Alginate: properties and biomedical applications. Progress in Polymer Science*, 2011. **37**(1): p. 106-126.
41. Phillips G.O. and Williams P.A., eds. *Handbook of Hydrocolloids.*2000, CRC Press: England. 450.
42. Pawar S.N. and Edgar K.J., *Alginate derivatization: a review of chemistry, properties and applications.* Biomaterials, 2012. **33**(11): p. 3279-3305.
43. Sriamornsak P., Thirawong N., and Korkerd K., *Swelling, erosion and release behavior of alginate-based matrix tablets.* European Journal of Pharmaceutics and Biopharmaceutics, 2007. **66**(3): p. 435-450.
44. Funami T., Fang Y., Noda S., Ishihara S., Nakauma M., Draget K.I., Nishinari K., and Phillips G.O., *Rheological properties of sodium alginate in an aqueous system during gelation in*

relation to supermolecular structures and Ca^{2+} binding. Food Hydrocolloids, 2009. **23**: p. 1746–1755.

45. Dakhara S.L. and Anajwala C.C., *Polyelectrolyte complex: a pharmaceutical review.* Systematic Reviews in Pharmacy, 2010. **1**(2): p. 121-127.
46. Oliveira S.M., Almeida I.F., Costa P.C., Barrias C.C., Ferreira M.R.P., Bahia M.F., and Barbosa M.A., *Characterization of polymeric solutions as injectable vehicles for hydroxyapatite microspheres.* AAPS PharmSciTech, 2010. **11**(2): p. 852-858.
47. Toneli J.T. M.F.E., Park K.J., *Estudo da reologia de polissacarídeos utilizados na indústria de alimentos.* Revista Brasileira de Produtos Agroindustriais, 2005. **7**: p. 181-204.
48. Ferreira H., *Escoamento de fluidos newtonianos e viscoelásticos em torno de um cilindro: Estudo numérico de efeitos tridimensionais*, *Faculdade de Engenharia*. 2006, Universidade do Porto: Porto. p. 178.
49. Partal P. and Franco J.M., eds. *Rheology, Chapter: Non-newtonian fluids*. Vol. 1. 2007, Encyclopedia of Life Support Systems (EOLSS): Spain. 24.
50. Barbieri D. Y.H., Groot F., Walsh W.R., Bruijn J.D., *Influence of different polymeric gels on the ectopic bone forming ability of an osteoinductive biphasic calcium phosphate ceramic.* Acta Biomaterialia, 2011. **7**(5): p. 2007-2014.
51. Orive G. P.S., Hernandez R.M., Gascon A.R., Igartua M., Pedraz J.L. , *Biocompatibility of microcapsules for cell immobilization elaborated with different type of alginates.* Biomaterials, 2002. **23**: p. 3825–3831.
52. Azevedo H.S. and Reis R.L., eds. *Biodegradable Systems in Tissue Engineering and Regenerative Medicine, Chapter: 12*. 2004, CRC Press. 25.
53. Nair L.S. and Laurencin C.T., *Biodegradable polymers as biomaterials.* Progress in Polymer Science, 2007. **32**(8-9): p. 762-798.
54. Ulery B.D., Nair L.S., and Laurencin C.T., *Biomedical applications of biodegradable polymers.* Journal of Polymer Science Part B : Polymer Physics, 2011. **49**(12): p. 832-864.
55. Lin H.R. Y.Y.J., *Porous alginate/hydroxyapatite composite scaffolds for bone tissue engineering: preparation, characterization, and in vitro studies.* Journal Biomedical Materials Research Part B, 2004. **71**: p. 52-65.
56. Oliveira S.M. B.C.C., Almeida I.F., Costa P.C., Ferreira M.R.P., Bahia M.F., Barbosa M.A., *Injectability of a bone filler system based on hydroxyapatite microspheres and a vehicle with in situ gel-forming ability.* Journal of Biomedical Materials Research Part B: Applied Biomaterials, 2007: p. 49-58.
57. Chen A., Haddad D., and Wang R., *Analysis of chitosan-alginate bone scaffolds.* Rutgers University, New Jersey Governor's School of Engineering & Technology, 2009: p. 1-8.

58. Coimbra P. F.P., Sousa H. C., Batista P., Rodrigues M. A., Correia I. J., Gil M. H., *Preparation and chemical and biological characterization of a pectin/chitosan polyelectrolyte complex scaffold for possible bone tissue engineering applications.* International Journal of Biological Macromolecules, 2011. **48**(1): p. 112-118.
59. Badawy M.E.I., Rabea E.I., *A biopolymer chitosan and its derivatives as promising antimicrobial agents against plant pathogens and their applications in crop protection.* International Journal of Carbohydrate Chemistry, 2011. **2011**: p. 1-29.
60. Coimbra P. Alves P., Valente T. A. M., Santos R., Correia I. J., Ferreira P., *Sodium hyaluronate/chitosan polyelectrolyte complex scaffolds for dental pulp regeneration: Synthesis and characterization.* International Journal of Biological Macromolecules, 2011. **49**(4): p. 573-579.
61. Aranaz I., Mengíbar M., Harris R., Paños I., Miralles B., Acosta N., Galed G., Heras A., *Functional characterization of chitin and chitosan.* Current Chemical Biology, 2009. **3**: p. 203-230.
62. Il'ina A.V. and Varlamov V.P., *Hydrolysis of chitosan in lactic acid.* Applied Biochemistry and Microbiology 2004. **40**(3): p. 300-303.
63. Patterson J., Siew R., Herring S.W., Lin A.S.P. and Guldberg R., Stayton P.S., *Hyaluronic acid hydrogels with controlled degradation properties for oriented bone regeneration.* Biomaterials, 2010. **31**(26): p. 6772-6781.
64. Prestwich G.D., *Hyaluronic acid-based clinical biomaterials derived for cell and molecule delivery in regenerative medicine.* Journal of Controlled Release, 2011. **155**(2): p. 193-199.
65. Lei Y., Gojgini S., Lam J., Segura T., *The spreading, migration and proliferation of mouse mesenchymal stem cells cultured inside hyaluronic acid hydrogels.* Biomaterials, 2011. **32**(1): p. 39-47.
66. Brown M.B. and Jones S.A., *Hyaluronic acid: a unique topical vehicle for the localized delivery of drugs to the skin.* Journal of the European Academy of Dermatology and Venereology, 2005. **19**(3): p. 308-318.
67. Martínez-Sanz E., Ossipov D.A., Hilborn J., Larsson S., Jonsson K.B., and Varghese O.P., *Bone reservoir: injectable hyaluronic acid hydrogel for minimal invasive bone augmentation.* Journal of Controlled Release, 2011. **152**(2): p. 232-240.
68. Kim J., Kim I. S., Cho T. H., Lee K.B., Hwang S.J., Tae G., Noh I., Lee S.H., Park Y., and Sun K., *Bone regeneration using hyaluronic acid-based hydrogel with bone morphogenic protein-2 and human mesenchymal stem cells.* Biomaterials, 2007. **28**(10): p. 1830-1837.
69. El-Safory N.S., Fazary A.E., Lee C., *Hyaluronidases, a group of glycosidases: current and future perspectives.* Carbohydrate Polymers, 2010. **81**(2): p. 165-181.

70. Liu H., Li H., Cheng W., Yang Y., Zhu M., and Zhou C., *Novel injectable calcium phosphate/chitosan composites for bone substitute materials.* Acta Biomaterialia, 2006. **2**(5): p. 557-565.
71. Larsson S. and Hannink G., *Injectable bone-graft substitutes: current products, their characteristics and indications, and new developments.* Injury, 2011. **42**: p. 30-34.
72. Finkemeier C.G., *Bone-grafting and bone-graft substitutes.* The Journal of Bone and Joint Surgery, 2002. **48-A**(3): p. 454-464.
73. Campoccia D., Montanaro L., and Arciola C.R., *The significance of infection related to orthopedic devices and issues of antibiotic resistance.* Biomaterials, 2006. **27**(11): p. 2331-2339.
74. Stanić V., Janaćković D., Dimitrijević S., Tanasković S.B., Mitrić M., Pavlović M.S., Krstić A., Jovanović D., and Raičević S., *Synthesis of antimicrobial monophase silver-doped hydroxyapatite nanopowders for bone tissue engineering.* Applied Surface Science, 2011. **257**(9): p. 4510-4518.
75. Peleg A.Y. and Hooper D.C., *Hospital-acquired Infections due to gram-negative bacteria reply.* New England Journal of Medicine, 2010. **363**(15): p. 1483-1484.
76. Campoccia D., Montanaro L., Speziale P., and Arciola C.R., *Antibiotic-loaded biomaterials and the risks for the spread of antibiotic resistance following their prophylactic and therapeutic clinical use.* Biomaterials, 2010. **31**(25): p. 6363-6377.
77. Jakupec M.A., Unfried P., and Keppler B.K., *Pharmacological properties of cerium compounds.* Reviews of Physiology Biochemistry and Pharmacology, 2005. **153**: p. 101-111.
78. Leonelli C., Lusvardi G., Malavasi G., Menabue L., and Tonelli M., *Synthesis and characterization of cerium-doped glasses and in vitro evaluation of bioactivity.* Journal of Non-Crystalline Solids, 2003. **316**(2-3): p. 198-216.

Chapter 2

Synthesis and physical-chemical characterization of biodegradable alginate-based hydrogels as vehicles for glass-reinforced hydroxyapatite (GR-HA) granules

Synthesis and physical-chemical characterization of biodegradable alginate-based hydrogels as vehicles for glass-reinforced hydroxyapatite (GR-HA) granules

Abstract

Bone disorders and injuries affect millions of people worldwide, thus having an enormous impact in world health and economy. In recent years several scientific efforts have been made in order to develop a bone substitute with the ideal features for bone tissue regeneration. Injectable bone substitutes are among the most promising biomedical approaches, since the application of such material requires minimally invasive surgical techniques. In this work three different hydrogels were developed to associate, as vehicles, with the synthetic bone substitute GR-HA. One based on an alginate matrix cross-linked with Ca^{2+} ions (hydrogel *Alg*); a second on a mixture of alginate and chitosan, using Ca^{2+} ions as the cross-linking agent (hydrogel *Alg/Ch*); and a third based on a mixture of alginate and hyaluronate, using the same cross-linking agent (*Alg/HA*). The hydrogels, as well as the respective injectable bone substitutes (*IBS*s), were fully characterized from the physical-chemical point of view. Weight change studies proved that all hydrogels were able to swell and degrade within 72 hours at pH 7.4 and 4.0, being *Alg/HA* the hydrogel with the highest degradation rate (80%). Rheology studies demonstrated that all hydrogels are non-Newtonian viscoelastic fluids, and injectability tests showed that *IBS*s presented low maximum extrusion forces (*Alg_IBS* - 7.33±0.19 N; *Alg/Ch_IBS* - 4.64±0.32 N; *Alg/HA_IBS*) - 4.55±0.42 N, as well as quite stable average forces. In conclusion, the studied hydrogels present the necessary features to be successfully used as vehicles of GR-HA, particularly the hydrogel *Alg/HA*.

2.1. Introduction

Every year, millions of patients, worldwide, are affected by bone defects caused by bone disorder or injury.[1-3] In the last years, synthetic bone substitutes, mainly based on hydroxyapatite (HAP) and tricalcium phosphate, have been developed as treatment for those bone defects. These substitutes present several advantages against autografts or xenografts, namely, their unlimited availability and the fact that they eliminate the risk of disease transmission.[1, 4, 5] To improve the chemical similarity between these bioceramics and bone inorganic part, glass-reinforced hydroxyapatite (GR-HA) composites have been developed.[6-8]

In order to potentiate the clinical application of the synthetic substitutes, they have also been developed in injectable form, by association with hydrogels. This approach presents some advantages, it can decrease the surgery time, allow a better fill of the bone defects and facilitate the substitute application in clinical situations with a difficult access to the defect. The hydrogel, working as a vehicle, should present a suitable viscosity to enable the bone substitute granules injectability.[9-13]

Alginate is a polysaccharide produced mainly from brown seaweeds. It is a linear binary co-polymer composed of (1-4)-linked β-D-mannuronic acid (M) and α-L-guluronic acid (G) residues as monomers, constituting M-, G-, and MG-sequential block structures.[14-16] This polymer has been widely used to produce biomedical hydrogels, mainly due to its biocompatibility, biodegradation, gel-forming ability through simple divalent cations (such as Ca^{2+}, Ba^{2+} and Sr^{2+}) addition and its very low cost.[17-19] For pH values above alginate pKa value (about 3.38 and 3.65 for M and G residues, respectively) it presents a polyanionic chemical structure, the monomers carboxylic groups are negatively charged.[20, 21] Thus, the cations bind to them, preferentially toward the G-block rather than the M-block, forming a structure named as “egg-box” and providing the cross-linking of the polymeric chains.[15, 16, 22] When G monomer proportion is higher than M monomer proportion, a strong brittle gel will be obtained. When M proportion is higher, the hydrogel will be weaker, but more flexible, because there are less junction zones between chains.[15, 16, 23] Alginate hydrogels have already been used in bone tissue engineering as vehicles of HAP, allowing to properly fill the whole bone defect. To produce biomedical alginate hydrogels, Ca^{2+} ions are the most used crosslinking agents due to the mild reaction conditions compared to the cellular toxicity of both Ba^{2+} and Sr^{2+}. Moreover, for bone application this ion is preferred since it is the main extracellular matrix (ECM) ion. However, in biomedical applications, alginates have the main disadvantage of being non-biologically active, presenting a low cell adhesion. [16, 18, 20, 24]

One way of improving the biological properties of alginate scaffolds, it is to ionically associate it to another polymer, namely a polycation as chitosan, forming a polyelectrolyte complex.[25, 26] Thus, a complex between alginate and another polyanion, such as hyaluronic acid (HA), can also be formed using cations as

intermediate agents.[27] Obviously, to ensure the complexes formation, the solution pH has to be controlled for the two polymers being charged.[28]

In the present study, we developed three different alginate-based hydrogels for being used as vehicles of the GR-HA bone substitute granules. One hydrogel was just composed by alginate cross-linked with Ca^{2+} ions, and other two hydrogels resulted from the association of chitosan and hyaluronic acid to alginate. The developed hydrogels were submitted to a physical-chemical characterization, as well as the respective injectable systems composed by each hydrogel and the GR-HA granules.

2.2. Materials and methods

2.2.1. Materials

Alginic acid sodium salt from brown algae (bioreagent grade; low viscosity; 39% (w/w) of guluronic acid and 61% (w/w) of mannuronic acid), hyaluronic acid sodium salt from *Streptococcus equi* and calcium chloride hexahydrate ($CaCl_2.6H_2O$, medical grade) were purchased from *Sigma* (USA). Chitosan HCl (medical grade) was purchased from *Heppe Medical Chitosan GmbH* (Germany). The hydroxyapatite powder was purchased from *Plasma Biotal* (UK).

2.2.2. Methods

2.2.2.1. Hydrogels preparation

a) Hydrogel *Alg*

Sodium alginate was dissolved overnight in deionized water at room temperature, in order to prepare a polymeric solution with a concentration of 7% (w/V) with pH 6. $CaCl_2.6H_2O$ was also dissolved in deionized water to a concentration of 15 mg/mL. Finally, the $CaCl_2$ solution was added to the sodium alginate solution at a proportion of 1:4 (V_{CaCl2}: $V_{sodium\ alginate}$).

b) Hydrogel *Alg/Ch*

Chitosan HCl was dissolved in deionized water to prepare a solution of 0.5% (w/V). Then, the $CaCl_2$ and sodium alginate solution were added to it, by this order, in the proportions of 1:4 (V_{CaCl2}:$V_{sodium\ alginate}$) and 1:1 ($V_{sodium\ alginate}$:$V_{chitosan\ HCl}$), respectively.

c) Hydrogel *Alg/HA*

Sodium hyaluronate was dissolved overnight in deionized water, at 4 ^{o}C, to a concentration of 0.5% (w/V). This solution was added to the sodium alginate solution in a proportion of 1:1 ($V_{sodium\ alginate}$: $V_{sodium\ hyaluronate}$). Finally, to the solution of the two polymers the $CaCl_2$ solution was added in a proportion of 1:4 (V_{CaCl2}: $V_{sodium\ alginate}$).

2.2.2.2. GR-HA and injectable bone substitutes (*IBSs*) preparation

a) GR-HA

GR-HA was obtained by adding 2.5% (w/w) of glass (with the composition $65P_2O_5$-15CaO-$10CaF_2$-$10Na_2O$, mol %) to pure phase of prepared HAP mixed with

microcrystalline cellulose. Then, discs were prepared by uniaxial pressing and heat treated at 600 ^{o}C to burn out the microcrystalline cellulose and then sintered at 1300 ^{o}C for 1 hour. Finally the discs were milled and sieved to produce granules of a 500-1000 µm size range.

b) *IBS*s

In order to optimize the preparation of the three different *IBS*s, GR-HA granules were simply mixed and aggregated with each one of the developed hydrogels until the desired consistency was achieved. For each system, the apparent ideal proportions of the bone substitute and each hydrogel are presented in table 2.1.

Table 2.1: Proportions of GR-HA and hydrogel for each *IBS*: ***Alg_IBS*:** substitute with hydrogel *Alg*; ***Alg/Ch_IBS*:** substitute with hydrogel *Alg/Ch*; ***Alg/HA_IBS*:** substitute with hydrogel *Alg/HA*.

IBS	% GR-HA (w/w)	% Hydrogel (w/w)
Alg_IBS	41	59
Alg/Ch_IBS	47	53
Alg/HA_IBS	48	52

2.2.2.3. Scanning Electron Microscopy (SEM) analysis

In order to do the SEM analysis of the three hydrogels, the samples were firstly frozen at -28 ^{o}C during 3 hours, and then freeze-dried for 48 hours.

On the case of the *IBS*s, the samples were firstly fixed with 1.5% (m/V) glutaraldehyde in 0.14 M sodium cacodylate buffer (pH 7.3). Afterwards, the samples were dehydrated using graded ethanol solutions from 50% (V/V) to 100% (V/V), followed by immersion in hexamethyldisilazanes (HMDS) solutions ranging from 50% (V/V) to 100% (V/V). The samples lasted 10 minutes in each ethanol and HMDS solution and overnight in 100% (V/V) HMDS. All the used reagents were purchased from *Sigma* (USA).

Afterwards, the hydrogels and *IBS*s samples were mounted onto an aluminum stub and coated with gold/palladium using a *SPI Sputter Coater*. Finally, the samples morphology was analyzed using the equipment *FEI Quanta 400FEG SEM* (*FEI,* USA).

2.2.2.4. Fourier transform infrared - attenuated total reflectance (FTIR-ATR) spectroscopy analysis

The FTIR-ATR spectra, over the wavelength range of 1800–800 cm^{-1}, of the sodium alginate, chitosan HCl and sodium hyaluronate polymeric solutions, and of the three developed hydrogels were obtained by the FTIR spectrometer *FT/IR-4100* (*Jasco,* USA). FTIR-ATR analysis of the sodium alginate powder before and after autoclaving was also performed over the wavelength range of 2000–750 cm^{-1}.

2.2.2.5. Hydrogels swelling profile

Swelling studies were performed according to ASTM (American Society for Testing and Materials) F2900-11. For that, the hydrogels were immersed (in quadriplicate) in two different buffer solutions, phosphate buffered saline (PBS: pH 7.4, *Sigma*, USA) and potassium hydrogen phthalate (KHP: pH 4.0, *Sigma*, USA) as follows:

A sample of each gel was weighed before immersion in any of the solutions and it was designated as W_0. Afterwards, the samples were placed inside a previously weighed standard mesh and immersed in the buffers and incubated at 37 ^{o}C. The mesh was removed every minute for 5 minutes and left to dry until no drop was formed. The gel/mesh system was weighed and the mesh weight was subtracted to the system weight and designated as W_t. The weight change (%) for each sample at time *t*, was calculated using the equation 1:

$$\boldsymbol{Weight\ change}\ (\%) = \frac{\boldsymbol{W_t - W_0}}{\boldsymbol{W_0}} \times \mathbf{100} \qquad \textbf{(1)}$$

2.2.4. Hydrogels degradation profile

Hydrogels degradation studies were performed according to ASTM F2900-11, using two different buffer solutions, PBS (pH 7.4) and KHP (pH 4.0) as follows:

Firstly, *IBS*s were prepared (in triplicate) according to 2.2.2.2.b). Both GR-HA and hydrogels weights were recorded, and the hydrogel weight was designated as W_0. All samples were enclosed in glass vessels with each of the above mentioned buffer solution and incubated at 37 ^{o}C and 1 Hz orbital agitation. *IBS*s were removed at 24 and 72 hours, carefully filtered and weighed. After subtracting GR-HA's weight, this

final weight was designated as W_t. The degradation percentage was calculated using the equation 2:

$$\boldsymbol{Degradation}\ (\%) = \frac{\boldsymbol{W_0 - W_t}}{\boldsymbol{W_0}} \times \mathbf{100} \qquad \textbf{(2)}$$

2.2.5. Rheology tests

The rheological behavior of the three hydrogels was evaluated by performing measurements with the rheometer *Physica MCR-300 (Anton Paar,* Austria*)*, employing the concentric cylinders geometry. To perform the flow measurements of each hydrogel, 1mL of the material was introduced between the cylinders, and this procedure was done in duplicate. The measurements were performed at 20 ^{o}C, between 1 and 100 s^{-1} frequencies.

2.2.6. Injectability tests

To evaluate the injectability of the three developed *IBS*s, equal volume of each one was placed in a 2 mL syringe, which was fixed vertically on the texture analyzer *TA-XT2i (Stable Mycro Systems,* UK*)*, as presented in figure 2.1. During the test, while using a load cell of 5 kg, the syringe piston was pushed at a velocity of 1 mm/s, through a distance of 10 mm. For each *IBS* the test was performed in triplicate.

Figure 2.1: Syringe with the injectable system on the texture analyzer.

2.2.9. Statistical analysis

Experimental data was presented as mean ± SD (Standard Deviation). Statistical analysis of data was performed using the one-way ANOVA and the Bonferroni post-hoc analysis, with the software *SigmaStat* 3.5. The differences were considered to be significant at a level of $p<0.05$.

2.3. Results and discussion

2.3.1. Hydrogels and *IBSs* macroscopic evaluation

Initially, to produce and optimize the hydrogel *Alg* according to the required handling features of a vehicle for the bone substitute, different sodium alginate and $CaCl_2$ concentrations were tested and the final result evaluated. It was observed that for a given alginate concentration, as the added volume of $CaCl_2$ solution increases the hydrogel becomes stiffer. This fact is caused by a stronger cross-linking due to the higher Ca^{2+} concentration, which leads to more junction zones between chains.[15, 16] Hence, it was considered that the alginate optimal concentration was of of 7% (m/V) and cross-linker optimal proportion of 1:4 (V_{CaCl2}: $V_{sodium\ alginate}$).

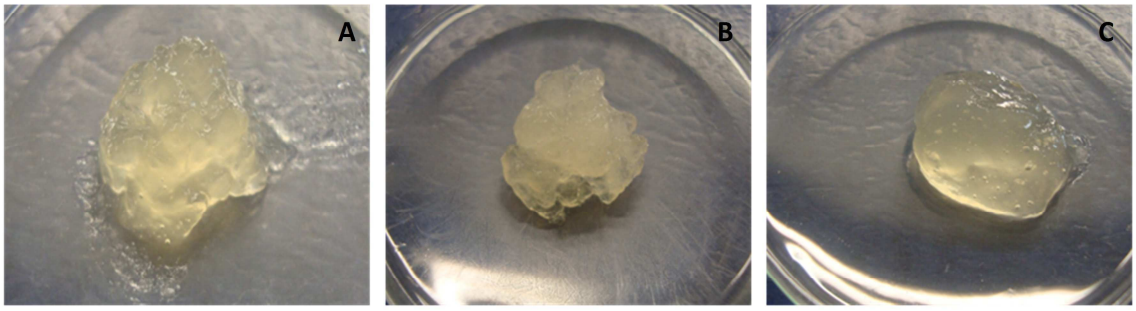

Figure 2.2: Macroscopic appearance of the three developed hydrogels: **A**-*Alg* hydrogel; **B**-*Alg/Ch* hydrogel; **C**- *Alg/HA* hydrogel.

As observed in figure 2.2, the three developed hydrogels present distinct aspects. Visually, hydrogels *Alg* and *Alg/HA* have a homogeneous aspect (figure 2.2-A and 2.2-C), while the hydrogel *Alg/Ch* has a heterogeneous aspect. It is also important to mention that hydrogel *Alg/HA* appears to be more fluid than the other ones.

Figure 2.3: Macroscopic appearance of the *Alg_IBS*.

The three different *IBSs* present similar aspect and handling; the three hydrogels can envelop and aggregate the GR-HA granules well, maintaining a whole and moldable structure, as observed in figure 2.3. These characteristics are extremely important as they allow a simple and efficient application of the material by simply injecting the bone substitute into the bone defect. However, it should be referred that hydrogel *Alg* maintains the injectable (GR-HA granules plus hydrogel) structure slightly

better as a whole, during the injection, without breaking it, which sometimes occurs with the others gels.

2.3.2. SEM analysis

The hydrogels morphology was analyzed by SEM and it is presented in figure 2.4. The hydrogels exhibit a similar morphology, namely irregular microstructures with many heterogeneous pores, which seem to be interconnected. The bone regeneration process has been shown to be dependent on the porosity and pore size of the regenerative structures used. The cell attachment and growth are enhanced by a large surface area and highly porous structures are also desirable for a good diffusion of nutrients to and waste products from the structure. These are essential requirements for the tissue regeneration.[29-31] Within the hydrogels structure pores with sizes between 40 µm and 100 µm were identified, which is in accordance with the appropriated pore size range for a good osteoid ingrowth.[30-32]

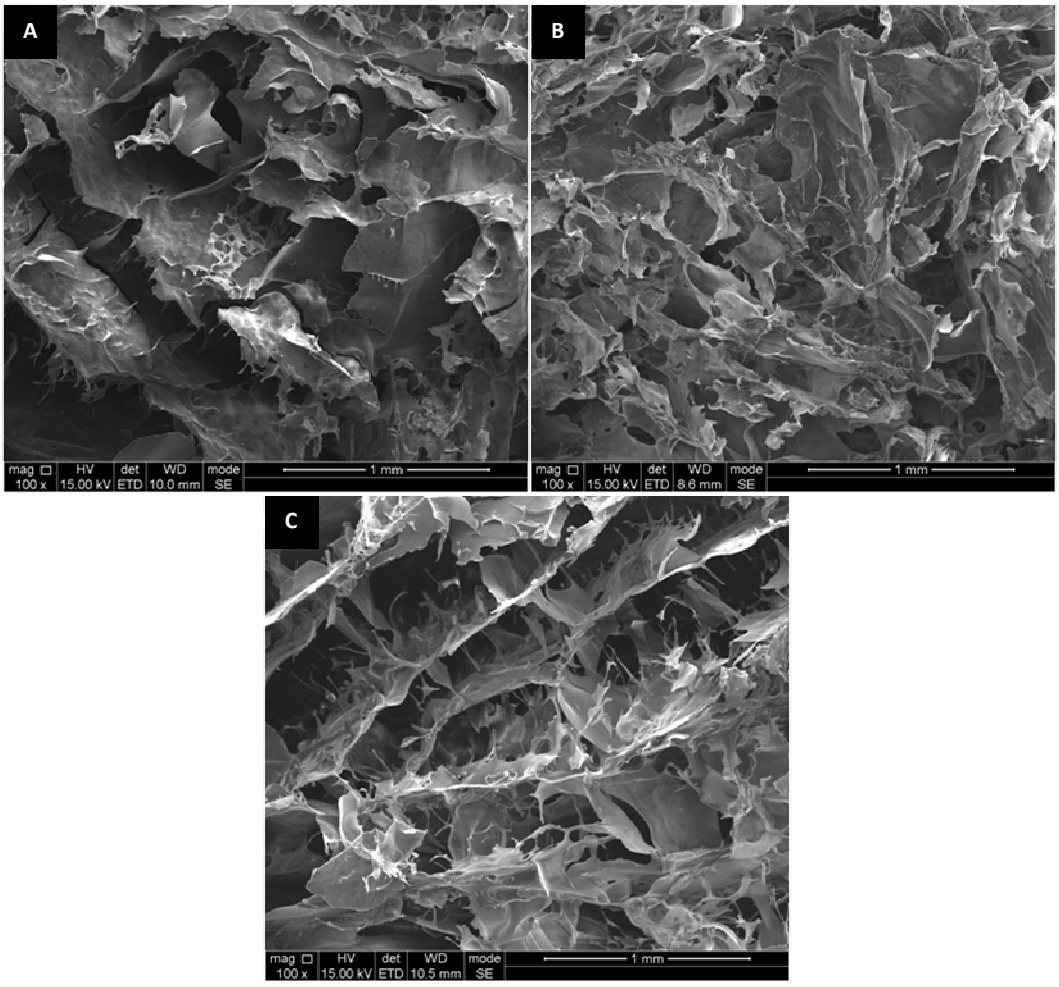

Figure 2.4: SEM images of the three hydrogels: **A**-*Alg*; **B**-*Alg/Ch*; **C**-*Alg/HA*.

The *IBS*s morphology was also analyzed by SEM and it is presented in figure 2.5. It is observed, in figure 2.5-A1, B1, C1, that the three hydrogels can involve and aggregate the GR-HA granules very well. In greater detail, it is possible to observe, in figure 2.5-A2, B2, C2, polymeric material at the granules surface enveloping them.

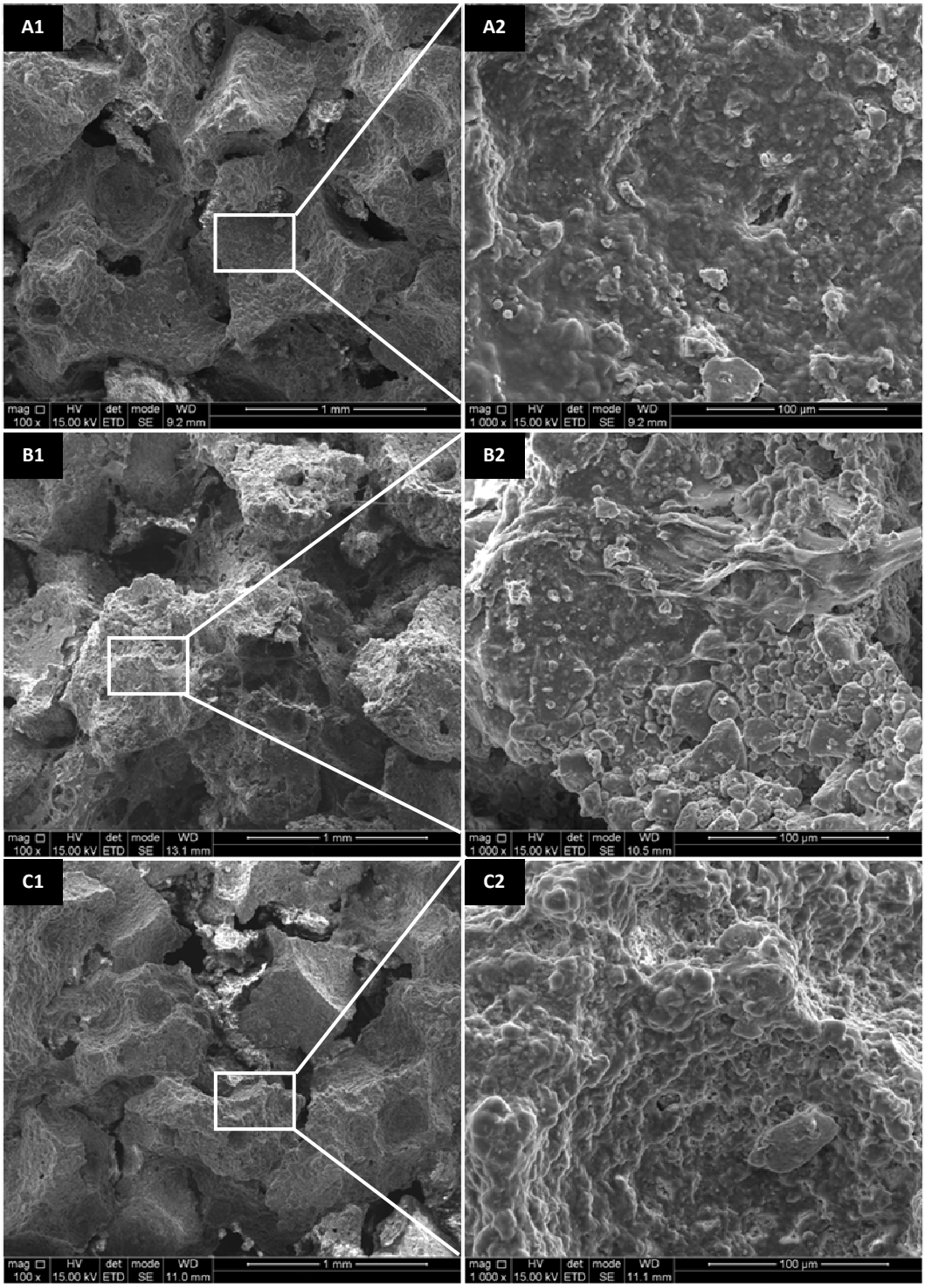

Figure 2.5: SEM images of the three injectable systems: **A1,A2**-*Alg_IBS*; **B1,B2**-*Alg/Ch_IBS*; **C1,C2**-*Alg/HA_IBS.*

2.3.3. FTIR-ATR spectroscopy analysis

Figure 2.6 shows the FTIR-ATR spectra of hydrogels *Alg*, *Alg/Ch*, *Alg/HA*, and each of the three polymeric solutions used in their preparation. In the spectra region between 1700 cm^{-1} and 1500 cm^{-1}, it is possible to observe a broad band with a peak at 1634 cm^{-1} in all solutions which represents a transmittance band typical of water O-H stretching vibration.[33] This band was expected since water is the major component (>90% w/V) of all studied solutions. This band cloaks the band expected for the asymmetric stretching vibration of C=O of carboxylic acids.[34]

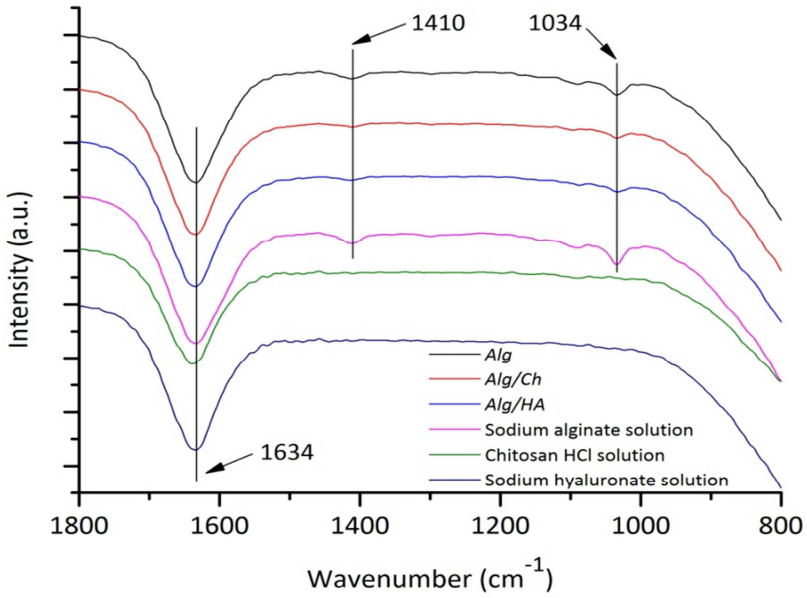

Figure 2.6: FTIR-ATR spectra of the three developed hydrogels and the polymeric solutions used to produce them.

At the three polymeric solutions and the hydrogel *Alg* it is possible to observe the typical transmittance bands exhibited by polysaccharides with peaks at 1410 cm^{-1} (assigned to the stretching vibration of C-OH of carboxylic group) and 1034 cm^{-1} (assigned to the stretching vibration of C-O of the alcohol groups).[35] Since no shifts were observed in any of the mentioned spectra, a conclusion can be drawn: the transmittance peaks obtained in the first four spectra, are all due to the presence of alginate. This finding is supported by the total absence of such peaks where alginate is not present (chitosan HCL and sodium hyaluronate solution) and by the decreasing intensity of said peaks in the same proportion as the decreasing concentration of alginate in the hydrogels (table 2.2), when compared to the sodium alginate solution concentration. Moreover, it should be referred that the last two spectra showed no

fingerprinting regions, because the solutions were of only 0.5% (w/V) of polymer, not being detectable by FTIR analysis.[35, 36]

Table 2.2: Peaks intensity reduction in hydrogels, when compared to sodium alginate solution.

Hydrogel	Peak	Intensity redution (%)
Alg	**1034**	**42**
Alg/Ch		**76**
Alg/HA		**76**
Alg	**1410**	**26**
Alg/Ch		**83**
Alg/HA		**81**

Attending to the biomedical application of the developed hydrogels it was primordial to define a sterilization method for them. The alginate solution, due to its viscosity, was impossible to filter, so its powder was sterilized by autoclaving at 121 ^{o}C for 15 minutes. However, it is reported that autoclaving and most sterilization methods involving heat can enhance polymer degradation.[15] Thus, FTIR-ATR analysis of the autoclaved and non-autoclaved powder was performed in order to investigate how the used sterilization method affected the polymer structure.

Figure 2.7 depicts FTIR-ATR results and it is possible to observe analogous spectra for both samples. In the region between 1750 cm^{-1} and 1450 cm^{-1}, a band is visible with an intense peak (band 1) at 1594 cm^{-1} for both samples, typical of the antisymmetric stretch vibration of alginate carboxylic group -COO^{-}.[37] The symmetric stretch vibration of the same group is exposed in band 2 with an intense peak at 1400 cm^{-1}.[38]

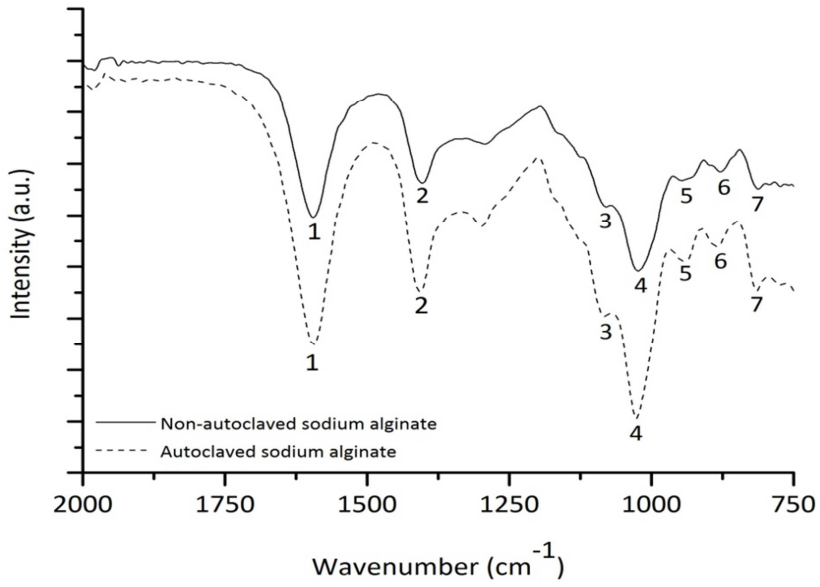

Figure 2.7: FTIR-ATR spectra of the sodium alginate powder autoclaved and non-autoclaved.

The weak bands 3 (1082 cm^{-1}) and more intense 4 (1024 cm^{-1}) may be assigned to C–O and C–C stretching vibrations of pyranose ring.[38, 39] The anomeric region of fingerprint (950–750 cm^{-1}) shows three characteristic bands in all polysaccharide standards (bands 5–7) of alginates.[38-41] The band 5 at 941 cm^{-1} is assigned to the C–O stretching vibration of uronic acid residues, the one at 879 cm^{-1} (band 6) is assigned to the C1-H deformation vibration of β-mannuronic acid residues. Finally, the band 7 at 812 cm^{-1} is characteristic of mannuronic acid residues.[38-41]

2.3.4. Hydrogels swelling profile

The hydrogels weight change behavior is illustrated in figure 2.8. This study was done using two buffer solutions in order to mimic the pH found at physiological and inflammatory conditions, pH 7.4 and 4.0 respectively. As observed, at the first minute, the three hydrogels undergo a weight increase, for both pH values, due to the swelling phenomenon. This behavior was expected, since by definition hydrogels are able to swell in aqueous solutions.[13, 42, 43] Initially, the osmotic pressure is greater than the forces of the crosslinking bonds that maintain the structure of the polymeric network stable, leading to hydrogel water uptake.[22, 44, 45] The void regions of the polymer network are filled until an equilibrium state with aqueous medium is reached,

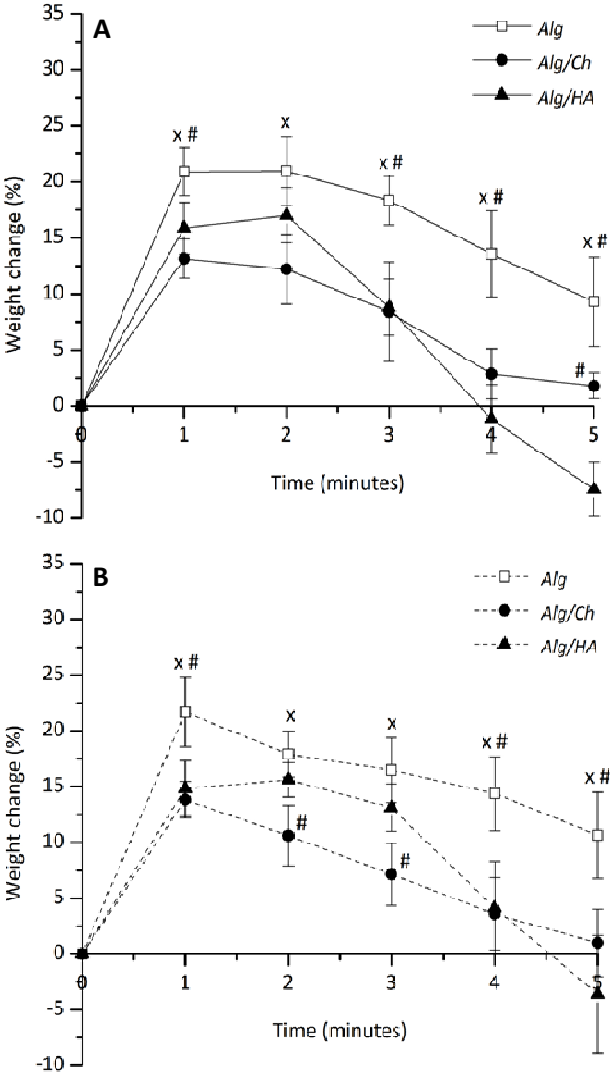

Figure 2.8: Weight change of the three hydrogels at 37 °C:
A-PBS (pH 7.4); **B**- KHP (pH 4).
Data are presented as mean ± SD.
x $p < 0.05$-significant difference compared with *Alg/Ch.*
# $p < 0.05$-significant difference compared with *Alg/HA.*

increasing the hydrogel volume.[22, 43, 46] After that time point, the hydrogels *Alg* and *Alg/Ch* experience a weight loss, as well as the hydrogel *Alg/HA* after 3 minutes and onward.

It is noticeable that regardless the pH, the weight change behavior of each hydrogel is similar (figure 2.8-A and 2.8-B). Both solutions pH are above alginate pKa, being the carboxylic groups, in both cases, in a charged state, so the cross-linked alginate structure is maintained. Therefore, since the alginate matrix is the base of the three hydrogels there is no change of the hydrogels structure for each pH value, leading to a similar swelling behavior.[20, 21]

When comparing the weight change behavior of each hydrogel, it is visible that the hydrogel *Alg* has a higher swelling ratio than hydrogels *Alg/Ch* and *Alg/HA*. This difference comes from the polymer concentration difference between hydrogels.[44] The higher the polymer concentration within a hydrogel, the lower the water present is, therefore, the osmotic pressure is greater from the medium into the hydrogel.[22, 44] Since the hydrogel *Alg* has lower water content than hydrogels *Alg/Ch* and *Alg/HA*, the water uptake will be higher, resulting in a larger weight change, as seen in figure 2.8.[45]

2.3.5. Hydrogels degradation profile

These studies were performed due to the vital importance of knowing the degradation profile of any biodegradable biomaterial intended to be implanted. Moreover, for these specific hydrogels application it was defined, as requirement, a 72 hours degradation time, being essential to assess this parameter. The tests were performed using the same buffer solutions of swelling tests.

For pH 7.4, figure 2.9-A, a degradation percentage increase is observed, for all hydrogels. Hydrogel *Alg* is only composed of cross-linked alginate, and its degradation mechanism is reported as being a result of the glycosidic bonds hydrolysis and the Na^+ ions (present in PBS) interchange with cross-linking Ca^{2+} ions, leading to a weight decrease in time.[17, 24, 47, 48]

Chitosan and HA are also degradable by hydrolysis of the glycosidic bonds.[49, 50] Thus, the weight loss of the hydrogels *Alg/Ch* and *Alg/HA* happens by the hydrolysis of the two constituent polymers of each one and also by the Na^+ ions interchange with

Ca^{2+} ions in the alginate matrix. Thereby, the higher degradation of the hydrogels *Alg/Ch* and *Alg/HA* compared to *Alg*, can be mainly explained by their lower polymeric concentration. In case of the hydrogel *Alg/Ch*, there is another possible degradation cause. For a pH 7.4, which is above the chitosan pKa (6.2-7 range), its amino groups are protonated.[51] Therefore, the possible ionic bonds between alginate carboxylate and chitosan amino groups are broken, improving weight loss.[48, 52]

The degradation by Na^+ ions interchange with Ca^{2+} ions is more pronounced for a longer exposure time to the medium with Na^+ ions.[53] As observed in figure 2.9-A, the degradation difference between the hydrogel *Alg/HA* and *Alg* or *Alg/Ch* is greater at 72 hours than at 24 hours. This phenomenon can be explained by the fact of the hydrogel *Alg/HA* polymeric matrix being supported by ionic interaction between hyaluronate and alginate, mediated by Ca^{2+} ions. Thus, the ions interchange phenomenon has a higher effect in this hydrogel, promoting a higher degradation at 72 hours.[27]

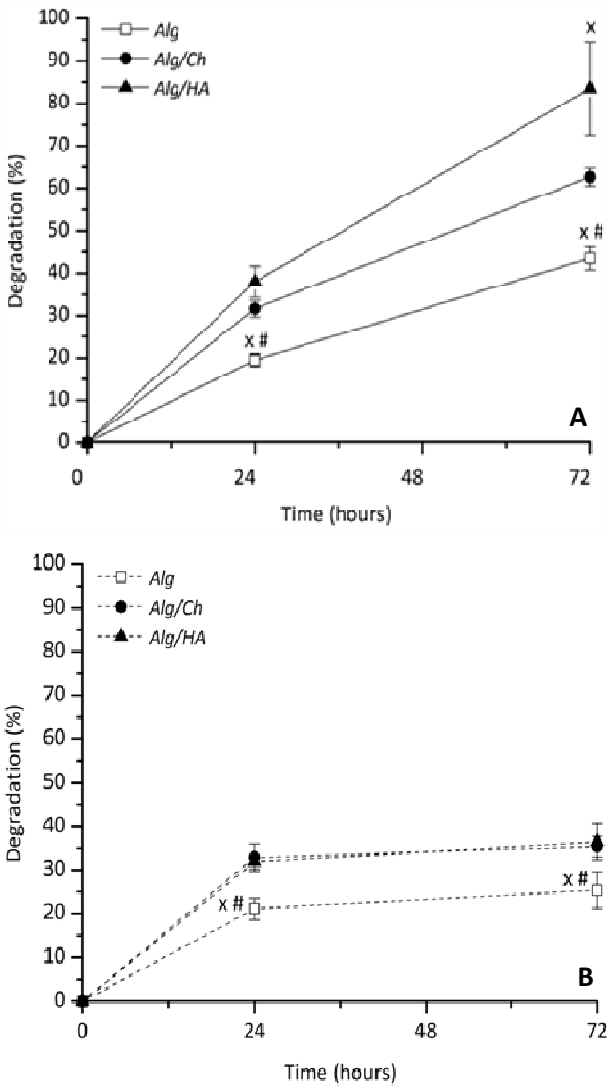

Figure 2.9: Degradation of the three hydrogels at 37 °C and 1 Hz orbital agitation: **A**-PBS (pH 7.4); **B**-KHP (pH 4). Data are presented as mean ± SD.
$^{x}p < 0.05$-significant difference compared with *Alg/Ch.*
$^{\#}p < 0.05$-significant difference compared with *Alg/HA.*

For pH 4, figure 2.9-B, the hydrogels degradation can only happen by hydrolysis of the three polymers, because there are no Na^+ ions and the solution pH is below the chitosan pKa. Thus, lower degradation values are expected for the three hydrogels at the two time points. In this pH condition, a higher degradation of the hydrogels *Alg/Ch* and *Alg/HA*, compared to the hydrogel *Alg*, is also verified due to the lower polymeric

content. Moreover, as observed in figure 2.9-B, for the three hydrogels, the difference between the degradation values at 24 and 72 hours is lower than in pH 7.4 solution. This result proves the higher Na^+ ions effect for longer time periods.

2.3.6. Rheology tests

Since the developed hydrogels are intended to be used in injectable systems it is important to study their rheological features. The rheological characterization of a material involves studies in flow and oscillatory modes.[54, 55]

In flow mode, the material viscosity change with the shear rate is evaluated.[54, 55] As presented in figure 2.10-A, the three hydrogels have a non-Newtonian behavior, because the non- linear relation between the shear rate and the shear stress results in a shear rate dependent of the viscosity, called apparent viscosity.[56, 57] More specifically, the materials have a shear-thinning behavior (pseudoplastic material), meaning that viscosity decreases with shear rate increase.[12, 27, 56, 57] This viscosity decrease can be explained by the structural change of the hydrogel polymeric network, due to the shear between the chains. With the velocity gradient increase, the chaotic organization of the hydrogels polymeric chains is converted into an alignment between them according to the flow direction, leading to a viscosity decrease.[58, 59]

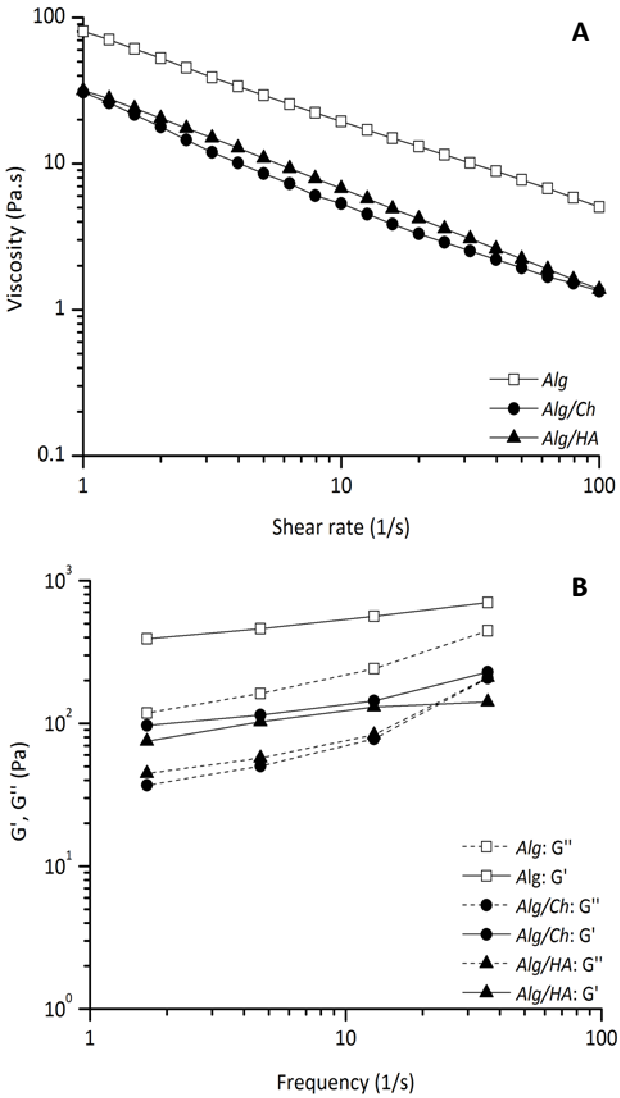

Figure 2.10: Rheological characterization of the three developed hydrogels: **A**-viscosity frequency dependence; **B**-storage modulus (G') and loss modulus (G'') frequency dependence.

Additionally, as observed in figure 2.10-A, for all shear rate values

the hydrogel *Alg* presents a higher viscosity than the other two hydrogels, which have similar viscosity values. The polymeric concentration in the hydrogel, as well as, the average molecular weight of its constituent polymers are two parameters that determine its viscosity.[27, 54] For a higher concentration, maintaining the molecular weight, a higher viscosity is verified. This phenomenon is owed to the polymer chains become closer, promoting the setting of intermolecular associations, leading to the formation of a more compact network. Maintaining the concentration, a higher molecular weight leads to a higher viscosity.[27, 54]

The two distinct constituent polymers in the hydrogels *Alg/Ch* and *Alg/HA* present very different molecular weights, chitosan HCl has a very lower molecular weight than HA, and their polymer concentrations are the same in each hydrogel. However, they present very similar values for every shear rate values. This phenomenon indicates that these hydrogels viscosity is mainly influenced by the alginate concentration in each hydrogel, which is the same. Moreover, the fact of the hydrogel Alg, which has a greater alginate concentration than those two, having higher viscosity values is in accordance with this hypothesis.[54, 60, 61]

In the oscillatory mode, two parameters can be determined: the storage modulus (G') that quantifies the stored energy, representing the elastic response of the material; the loss modulus (G''), that quantifies the dissipated energy as heat during the process, representing the viscous response of the material.[54, 57] When a material exhibits simultaneously typical behaviors of a viscous liquid and an elastic solid it is named as viscoelastic.[56, 57]

In figure 2.10-B, for the three hydrogels, it is showed the G´ and G'' values increase with the frequency increase. For all the studied frequencies, the hydrogel *Alg* presents G´>G´´, indicating a mainly elastic behavior. This was also observed for the other two hydrogels until frequencies of aproximatly 10 s^{-1}. At the higher studied frequencies, in hydrogel *Alg/Ch* and *Alg/HA,* an intersection point (*crossover point*) between G´and G'' can be observed. Posteriorly, G'' becomes higher than G' indicating that the materials behavior become more viscous than elastic, revealing that the material structure starts to breakdown.[55, 57, 62] Once again, the existence of the *crossover point* only in *Alg/Ch* and *Alg/HA,* can be explained by the lower polymeric concentration relatively to the hydrogel *Alg*.[62]

Moreover, as depicted in figure 2.10-B, for all frequencies, the G´´ value of the hydrogel *Alg* is above the other hydrogels G'' values, which are very similar among them. This fact can be related with their viscosity differences discussed previously, namely, the higher viscosity of hydrogel *Alg* may causes the observed higher G'' value.[54, 62] Moreover, once that G' and G'' can be related by the equation 3, for the same δ (phase angle shift between sine waves of stress and strain) a material with a higher G'' value has a higher G´ value than the other ones, as in figure 10-B.[54, 57, 62]

$$tan\,\delta = \frac{G''}{G'} \quad (3)$$

2.3.7. Injectability tests

In an injectable system it is essential to study the necessary extrusion force to inject the material. In figure 2.11, the injectability curves of the three developed *IBS*s can be observed, they depict the evolution of the applied force during the material movement through the syringe. In the beginning of the extrusion, maximum forces are observed for the three *IBS*s, being very low: *Alg_IBS* - 7.33±0.19 N; *Alg/Ch_IBS* - 4.64±0.32 N (p<0.05 - significant difference compared with *Alg_IBS*); *Alg/HA_IBS* - 4.55±0.42 N (p<0.05 - significant difference compared with *Alg_IBS*). Afterwards, the extrusion force decreases, for the three *IBS*s, reaching even lower values and stabilizing during the rest of the injection process, as desired.

During the extrusion process, a very thin hydrogel film is formed between the *IBS*s and the syringe wall. Thus, the higher maximum extrusion force recorded for *Alg_IBS* may be due to a higher static frictional force between the injectable and the syringe wall. Thus, it is necessary to apply a higher extrusion force, in the beginning, in order to initiate the material movement. The other two hydrogels present a lower maximum force, probably, due to a lower static frictional force, so the needed initial extrusion force is lower.[63, 64] The higher static frictional force can be explained by the higher viscosity of *Alg*, meaning an increased internal resistance to flow or shear. The viscosity of a fluid can be termed as a drag force and is a measure of the frictional fluid properties, simply put, the less viscous the fluid is, the greater its ease of movement.[63, 65, 66]

Usually, between two surfaces, the dynamic frictional force is lower than the static frictional force, which means that to maintain the movement it is necessary a

lower force than to start it, as happens in figure 2.11 at about 0.5 mm.[63, 64] Afterwards, the dynamic frictional force tends to stabilize in the three gels until the conclusion of the assay, being the medium force similar between them. However, hydrogel *Alg* is the one that presents less force variations, possibly due to previous macroscopically observation that hydrogel *Alg* can aggregate GR-HA granules slightly better, allowing a more continuous and uniform extrusion.

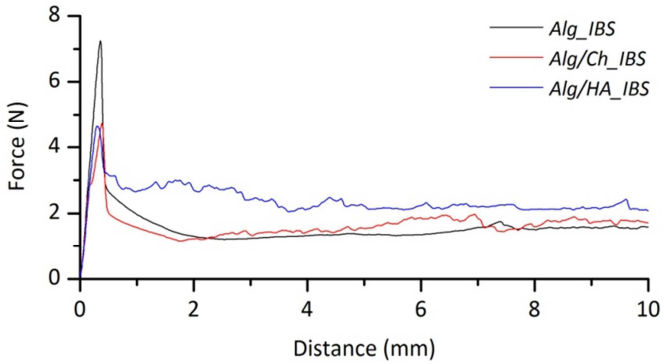

Figure 2.11: Injectability curves of the three *IBS*s, at an extrusion velocity of 1mm/s.

2.4. Conclusions

The developed materials presented a characteristic swelling behavior of any hydrogel. It was verified that the hydrogels degradation is mainly due to hydrolysis of the glycosidic bonds and by Na^+ ions interchange with Ca^{2+}. For pH 7.4 the hydrogel *Alg/HA* presented the highest degradation, about 80% of weight loss, after three days.

A shear-thinning and viscoelastic behavior was verified for the three hydrogels, being the viscosity, G' and G'' mainly influenced by the polymeric content in each hydrogel. The *IBS*s presented low but different maximum extrusion forces, due to the viscosity of the respective polymeric vehicle. By SEM analysis, it was observed a similar highly porous morphology between the hydrogels and their ability to properly envelope the GR-HA granules. In addition, the hydrogels pore size range was in accordance with the reported as ideal to the osteoid ingrowth.

According to the results, the three developed hydrogels are potential vehicles to associate with GR-HA granules, being able of well aggregate them, maintaining the injectable system entirety and allowing a good handling of the *IBS* with low and stable injectability forces.

In future, a biological follow-up study must be conducted to ascertain the biomedical application of the developed *IBS*s.

2.5. References

1. Giannoudis P.V., Dinopoulos H., and Tsiridis E., *Bone substitutes: an update.* Injury, 2005. **36**(3): p. 20-27.
2. Vaccaro A.R., *The role of the osteoconductive scaffold in synthetic bone graft.* Orthopedics, 2002. **25**: p. 571-578.
3. Bostrom M.P.G. and Seigerman D.A., *The clinical use of allografts, demineralized bone matrices, synthetic bone graft substitutes and osteoinductive growth factors: a survey study.* HSS Journal, 2005. **1**(1): p. 9-18.
4. Zimmermann G. and Moghaddam A., *Allograft bone matrix versus synthetic bone graft substitutes.* Injury, 2011. **42**: p. 16-21.
5. Moore W.R., Graves S.E., and Bain G.I., *Synthetic bone graft substitutes.* ANZ Journal of Surgery, 2001. **71**: p. 354-361.
6. Lopes M.A., Knowles J.C., Santos J.D., Monteiro F.J., and Olsen I., *Direct and indirect effects of P_2O_5 glass reinforced-hydroxyapatite composites on the growth and function of osteoblast-like cells.* Biomaterials, 1999. **21**: p. 1165-1172.
7. Lopes M.A., Knowles J.C., and Santos J.D., *Structural insights of glass-reinforced hydroxyapatite composites by Rietveld refinement.* Biomaterials, 2000. **21**: p. 1905-1910.
8. Salih V., Georgiou G., Knowles J.C., and Olsen I., *Glass reinforced hydroxyapatite for hard tissue surgery - part II: in vitro evaluation of bone cell growth and function.* Biomaterials, 2001. **22**(20): p. 2817 - 2824.
9. Liu H., Li H., Cheng W., Yang Y., Zhu M., and Zhou C., *Novel injectable calcium phosphate/chitosan composites for bone substitute materials.* Acta Biomaterialia, 2006. **2**(5): p. 557-565.
10. Larsson S. and Hannink G., *Injectable bone-graft substitutes: current products, their characteristics and indications, and new developments.* Injury, 2011. **42**: p. 30-34.
11. Couto D., Hong Z., and Mano J., *Development of bioactive and biodegradable chitosan-based injectable systems containing bioactive glass nanoparticles.* Acta Biomaterialia, 2009. **5**(1): p. 115-123.
12. Oliveira S.M., Almeida I.F., Costa P.C., Barrias C.C., Ferreira M.R.P., Bahia M.F., and Barbosa M.A., *Characterization of polymeric solutions as injectable vehicles for hydroxyapatite microspheres.* AAPS PharmSciTech, 2010. **11**(2): p. 852-858.
13. Gaharwar A.K., Dammu S.A., Canter J.M., Wu C., and Schmidt G., *Highly extensible, tough, and elastomeric nanocomposite hydrogels from poly(ethylene glycol) and hydroxyapatite nanoparticles.* Biomacromolecules, 2011. **12**(5): p. 1641-1650.

14. Stevens M.M., Qanadilo H.F., Langer R., and Prasad Shastri V.P., *A rapid-curing alginate gel system: utility in periosteum-derived cartilage tissue engineering.* Biomaterials, 2004. **25**(5): p. 887-894.
15. Pawar S.N. and Edgar K.J., *Alginate derivatization: a review of chemistry, properties and applications.* Biomaterials, 2012. **33**(11): p. 3279-3305.
16. Nunamaker E.A., Purcell E.K., and Kipke D.R., *In vivo stability and biocompatibility of implanted calcium alginate disks.* Journal of Biomedical Materials Research Part A, 2007. **83A**(4): p. 1128-1137.
17. Lee K.Y. and Mooney D.J., *Alginate: properties and biomedical applications.* Progress in Polymer Science, 2011. **37**(1): p. 106-126.
18. Ulery B.D., Nair L.S., and Laurencin C.T., *Biomedical applications of biodegradable polymers.* Journal of Polymer Science Part B : Polymer Physics, 2011. **49**(12): p. 832-864.
19. Ueng S.W., Yuan L., Lee N., Lin S., Chan E., and Weng J., *In vivo study of biodegradable alginate antibiotic beads in rabbits.* Journal of Orthopaedic Research, 2004. **22**: p. 592-599.
20. Andersen T., Strand B.L., Formo K., Alsberg E., and Christensen B.E., *Alginates as biomaterials in tissue engineering.* Carbohydrate Chemistry, 2012. **37**: p. 227-258.
21. Funami T., Fang Y., Noda S., Ishihara S., Nakauma M., Draget K.I., Nishinari K., and Phillips G.O., *Rheological properties of sodium alginate in an aqueous system during gelation in relation to supermolecular structures and Ca^{2+} binding.* Food Hydrocolloids, 2009. **23**: p. 1746–1755.
22. Davidovich-Pinhas M. and Bianco-Peled H., *A quantitative analysis of alginate swelling.* Carbohydrate Polymers, 2010. **79**(4): p. 1020-1027.
23. Sriamornsak P., Thirawong N., and Korkerd K., *Swelling, erosion and release behavior of alginate-based matrix tablets.* European Journal of Pharmaceutics and Biopharmaceutics, 2007. **66**(3): p. 435-450.
24. Nair L.S. and Laurencin C.T., *Biodegradable polymers as biomaterials.* Progress in Polymer Science, 2007. **32**(8-9): p. 762-798.
25. Chunga T.W., Yangb J., Akaikeb T., Choc K.Y., Nahd J.W., Kima S.I., and Cho C.S., *Preparation of alginate/galactosylated chitosan scaffold.* Biomaterials, 2001. **23**: p. 2827-2834.
26. Chen A., Haddad D., and Wang R., *Analysis of chitosan-alginate bone scaffolds.* Rutgers University, New Jersey Governor's School of Engineering & Technology, 2009: p. 1-8.
27. Oerther S., Maurin A., Payan E., Hubert P., Lapicque F., Presle N., Dexheimer J., Netter P., and Lapicque F., *High Interaction Alginate–Hyaluronate Associations by Hyaluronate*

Deacetylation for the Preparation of Efficient biomaterials. Biopolymers, 2000. **54**: p. 273-281.

28. Dakhara S.L. and Anajwala C.C., *Polyelectrolyte complex: a pharmaceutical review.* Systematic Reviews in Pharmacy, 2010. **1**(2): p. 121-127.
29. Salgado A.J., Gomes M.E., Chou A., Coutinho O.P., Reis R.L., and Hutmacher D.W., *Preliminary study on the adhesion and proliferation of human osteoblasts on starch-based scaffolds.* Materials Science and Engineering C, 2002. **20**: p. 27-33.
30. Yang S., Leong K., Du Z., and Chua C., *The Design of scaffolds for use in tissue engineering. part I. traditional factors.* Tissue Engineering, 2001. **7**(6): p. 679-689.
31. Mattiasson B., Kumar A., and Galaev I.Y., eds. *Macroporous Polymers*. 2009, CRC Press Sweden. 525.
32. Cerroni L., Filocamo R., Fabbri M., Piconi C., Caropreso S., and C. S.G., *Growth of osteoblast-like cells on porous hydroxyapatite ceramics: an in vitro study.* Biomolecular Engineering, 2002. **19**: p. 119-124.
33. Matrajt G., Borg J., Raynal P.I., Djouadi Z., d'Hendecourt L., Flynn G., and Deboffle D., *FTIR and Raman analyses of the tagish Lake meteorite: relationship with the aliphatic hydrocarbons observed in the diffuse interstellar mediu.* Astronomy and Astrophysics, 2003. **416**(3): p. 983-990.
34. Lasagabaster A., Abad M.J., Barral L., and Ares A., *FTIR study on the nature of water sorbed in polypropylene (PP)/ethylene alcohol vinyl (EVOH) films.* European Polymer Journal, 2006. **42**(11): p. 3121-3132.
35. Papageorgiou S.K., Kouvelos E.P., Favvas E.P., Sapalidis A.A., Romanos G.E., and Katsaros F.K., *Metal-carboxylate interactions in metal-alginate complexes studied with FTIR spectroscopy.* Carbohydrate Research, 2010. **345**(4): p. 469-473.
36. Singh J., Dutta P.K., Dutta J., Hunt A.J. , Macquarrie D.J., and Clark J.H., *Preparation and properties of highly soluble chitosan–l-glutamic acid aerogel derivative.* Carbohydrate Polymers, 2009. **76**(2): p. 188-195.
37. Thanos C.G., B.E. Bintz, W.J. Bell, H. Qian, P.A. Schneider, D.H. MacArthur, and D.F. Emerich, *Intraperitoneal stability of alginate-polyornithine microcapsules in rats: an FTIR and SEM analysis.* Biomaterials, 2006. **27**(19): p. 3570-3579.
38. Gomez-Ordonez E. and P. Ruperez, *FTIR-ATR spectroscopy as a tool for polysaccharide identification in edible brown and red seaweeds.* Food Hydrocolloids, 2011. **25**(6): p. 1514-1520.

39. Chandia N.P., B. Matsuhiro, E. Mejias, and A. Moenne, *Alginic acids in Lessonia vadosa: Partial hydrolysis and elicitor properties of the polymannuronic acid fraction.* Journal of Applied Phycology, 2004. **16**(2): p. 127-133.
40. Chandia N.P. and B. Matsuhiro, *Characterization of a fucoidan from Lessonia vadosa (Phaeophyta) and its anticoagulant and elicitor properties.* International Journal of Biological Macromolecules, 2008. **42**(3): p. 235-240.
41. Sakugawa K., A. Ikeda, A. Takemura, and H. Ono, *Simplified method for estimation of composition of alginates by FTIR.* Journal of Applied Polymer Science, 2004. **93**(3): p. 1372-1377.
42. Fedorovich N.E., Alblas J., Wijn J.R., Hennink W.E., Verbout A.J., and Dhert W.J.A., *Hydrogels as extracellular matrices for skeletal tissue engineering: state-of-the-art and novel application in organ printing.* Tissue Engineering, 2007. **13**(8): p. 1905-1925.
43. Hoffman A.S., *Hydrogels for biomedical applications.* Advanced Drug Delivery Reviews, 2002. **43**: p. 3–12.
44. Chan A.W. and Neufeld R.J., *Modeling the controllable pH-responsive swelling and pore size of networked alginate based biomaterials.* Biomaterials, 2009. **30**(30): p. 6119-6129.
45. Pasparakis G. and Bouropoulos N., *Swelling studies and in vitro release of verapamil from calcium alginate and calcium alginate–chitosan beads.* International Journal of Pharmaceutics, 2006. **323**(1-2): p. 34-42.
46. Slaughter B.V., Khurshid S.S., Fisher O.Z., Khademhosseini A., and P. N.A., *Hydrogels in Regenerative Medicine.* Advanced Materials, 2009. **21**(32-33): p. 3307-3329.
47. Dashevsky A., *Protein loss by the microencapsulation of an enzyme (lactase) in alginate beads.* International Journal of Pharmaceutics, 1998. **161**(1): p. 1-5.
48. Lertsutthiwong P., Rojsitthisak P., and Nimmannit U., *Preparation of turmeric oil-loaded chitosan-alginate biopolymeric nanocapsules.* Materials Science & Engineering C-Biomimetic and Supramolecular Systems, 2009. **29**(3): p. 856-860.
49. Kim J., Kim I. S., Cho T. H., Lee K.B., Hwang S.J., Tae G., Noh I., Lee S.H., Park Y., and Sun K., *Bone regeneration using hyaluronic acid-based hydrogel with bone morphogenic protein-2 and human mesenchymal stem cells.* Biomaterials, 2007. **28**(10): p. 1830-1837.
50. Il'ina A.V. and Varlamov V.P., *Hydrolysis of chitosan in lactic acid.* Applied Biochemistry and Microbiology, 2004. **40**(3): p. 300-303.
51. Badawy M.E.I. R.E.I., *A Biopolymer Chitosan and Its Derivatives as Promising Antimicrobial Agents against Plant Pathogens and Their Applications in Crop Protection.* International Journal of Carbohydrate Chemistry, 2011. **2011**: p. 1-29.

52. Li X. X., Xu A. H., Xie H. G., Yu W. T., Xie W. Y., and Ma X. J., *Preparation of low molecular weight alginate by hydrogen peroxide depolymerization for tissue engineering.* Carbohydrate Polymers, 2010. **79**(3): p. 660-664.
53. LeRoux M. A., Guilak F., and Setton L. A., *Compressive and shear properties of alginate gel: effects of sodium ions and alginate concentration.* Journal of Biomedical Materials Research, 1999. **47**(1): p. 46-53.
54. Pelletier S., Hubert P., Payan E., Marchal P., Choplin L., and Dellacherie E., *Amphiphilic derivatives of sodium alginate and hyaluronate for cartilage repair: rheological properties.* Journal of Biomedical Materials Research, 2000. **54**: p. 102-108.
55. Vallée F., Müller C., Durand A., Schimchowitsch S., Dellacherie E., Kelche C., Cassel J.C., and Leonard M., *Synthesis and rheological properties of hydrogels based on amphiphilic alginate-amide derivatives.* Carbohydrate Research, 2009. **344**(2): p. 223-228.
56. Partal P. and Franco J.M., eds. *Rheology, Chapter: Non-Newtonian Fluids*. Vol. 1. 2007, Encyclopedia of Life Support Systems (EOLSS): Spain. 24.
57. Tadros T.F., ed. *Rheology of Dispersions-Principles and Applications*. 2010, Wiley-VCH: Singapore. 199.
58. Cui S.T., Gupta S.A., and Cummings P.T., *Molecular dynamics simulations of the rheology of normal decane, hexadecane, and tetracosane.* Journal of Chemical Physics, 1996. **105**(3): p. 1214-1220.
59. Yucel T., Cebe P., and Kaplan D.L., *Vortex-induced injectable silk fibroin hydrogels.* Biophys Journal, 2009. **97**(7): p. 2044-2050.
60. Gargiulo V., Morando M.A., Silipo A., Nurisso A., Pérez S., Imberty A., Cañada F.J., Parrilli M., Jiménez-Barbero J., and Castro C., *Insights on the conformational properties of hyaluronic acid by using NMR residual dipolar couplings and MD simulations.* Glycobiology, 2010. **20**(10): p. 1208–1216.
61. Manojlovic V., Djonlagic J., Obradovic B., Nedovic V., and Bugarski B., *Investigations of cell immobilization in alginate: rheological and electrostatic extrusion studies.* Journal of Chemical Technology & Biotechnology, 2006. **81**(4): p. 505-510.
62. Mason T.G., Dhople A., and Wirtz D., *Linear viscoelastic moduli of concentrated DNA Solutions.* Macromolecules, 1998. **31**: p. 3600-3603.
63. Dobre A. and Ramtal D., eds. *The Essential Guide to: Physics for Flash Games, Animation, and Simulations*. 1 ed. 2011, Apress: USA. 558.
64. Kirkpatrick L.D. and Francis G.E., eds. *Physics: a World View*. 6 ed. 2007, Thomson Wadsworth: USA. 645.

65. Viswanath D.S., Ghosh T.K., Prasad D.H.L., Dutt N.V.K., and Rani K.Y., eds. *Viscosity of Liquids: Theory, Estimation, Experiment, and Data*. 2007, Springer: Netherlands. 662.
66. Murakamia T., Sawaea Y., Horimotob M., and Nodac M., *Role of surface layers of natural and artificial cartilage in thin film lubrication.* Tribology Series, 1999. **36**: p. 737–747.

Chapter 3

Biological evaluation of biocompatible alginate-based hydrogels as vehicles for glass-reinforced hydroxyapatite (GR-HA) granules

Biological evaluation of biocompatible alginate-based hydrogels as vehicles for glass-reinforced hydroxyapatite (GR-HA) granules

Abstract

Biocompatibility is the most important feature a biomaterial must have. In the present work, three previously developed alginate-based hydrogels (*Alg*, *Alg/Ch* and *Alg/HA*) associated with a bone substitute were subject to biological evaluation. As such, the effect of the injectable one substitutes (*IBS*s) on the metabolic activity of MG63 cells was evaluated. *Alg/HA_IBS* showed significantly increased cellular metabolic activity of the MG63 cells at all the time points. This higher metabolic activity may indicate a better adaptation of cells to the material, increasing their predisposition to produce extracellular matrix, allowing faster bone regeneration. SEM showed evident filopodia on human osteoblastic cells when seeded on *Alg/HA_IBS*. Thus, the hydrogel *Alg/HA* underwent subcutaneous implantation showing a slight irritating tissue response and visible tissue repairing. The next step was to confer antimicrobial properties to the *IBS* that showed the best biological behavior, *Alg/HA_IBS*. Hence, Ce(III) was incorporated into the hydrogel *Alg/HA*, and this ion significantly enhanced the hydrogel antimicrobial activity, without compromise the hydrogel cell viability.

3.1. Introduction

Bone defects remain a concern due to their high incidence in people of different ages, limiting their life quality. In the last few decades, synthetic bone substitutes have been developed in attempt of solve this medical challenge.[1, 2] For instance, glass-reinforced hydroxyapatite (GR-HA) composites are bioceramics able of chemically mimic the bone inorganic phase. They are osteoconductive, creating an ideal ambient for bone cells adhesion and proliferation, promoting bone regeneration.[3-5]

Synthetic bone substitutes have been associated with hydrogels, which are three-dimensional polymeric structures, in order to inject them, what is advantageous in some clinical applications. Moreover, the hydrogel association can improve the osteoconductive properties of the synthetic bone substitutes and even grant them osteoinductive and osteogenic properties by the incorporation of growth factors and stem cells in the gel.[6-10]

Natural polysaccharides are very promising for tissue engineering applications, since they present high biocompatibility and resemble glycosaminoglycans of the extracellular matrix (ECM). These polymers present a lower stimulation of immunological reactions than some synthetic polymers. [11, 12] Alginate is a natural biodegradable linear block co-polymer composed of two monomers, β-D-mannuronic acid (M) and α-L-guluronic acid (G), which are linked by (1-4) glycosidic bonds. This natural polysaccharide has been used to produce hydrogels by the simple addition of divalent cations, such as Ca^{2+}, which bind to monomers carboxylic groups providing the cross-linking of the polymeric chains and thus the gelation of the alginate solution.[13-15] However, alginate has the biomedical disadvantage of presenting a lower cell adhesion than other natural polymers. This polymer promotes a very low protein adsorption and cell attachment due to its negative charge and high hydrophilicity.[16-18]

Thus, in order to improve the cell adhesion on alginate, it can be easily associated with another polyelectrolyte that allows a better cell adhesion phenomenon. Chitosan is a natural biodegradable polycation composed by the monomers D-glucosamine and N-acetyl-D-glucosamine linked by β(1–4)-glycosidic bond. This polymer has been used in biomedical applications as a promoter of cell adhesion, proliferation and differentiation.[11, 19, 20] Hyaluronic acid (HA) is a natural biodegradable polyanion composed by the monomers D-glucuronic acid and *N*-acetyl-D-glucosamine, linked by β(1-3) and β(1-4) glycosidic bonds.[21, 22] This polysaccharide is the main component of ECM, being found in all body connective tissues. HA is involved in different biological processes, namely, in morphogenesis, wound repair, inflammation and metastasis, through the interaction with cellular receptors.[21, 23] This polymer has a strong potential in bone repair, it has been discovered in high concentrations in the fracture callus. Moreover, it can be involved in inhibition of osteoclasts differentiation and even participate in the migration of mesenchymal stem cells. [24-26]

In every surgical procedure there is the major risk of infection, presenting serious consequences that can compromise the recovery success. To prevent those infections, several approaches have been tried, such as, sterility protocols and the antibiotic administration or incorporation into the implanted biomaterials. However, these

methods are not always effective and the antibiotic activity can even fail due to the resistance developed to it by some pathogens.[27, 28]

Cerium (Ce), a rare earth element which belongs to the lanthanide group, has revealed antimicrobial properties against several microorganisms. Thus, it can be incorporated in different biomaterials to grant them an antimicrobial activity, contributing to a better implant performance.[29-31]

The purpose of the present study was to evaluate the biological *in vitro* and *in vivo* performance of three hydrogels previously developed, one just composed by alginate, and other two composed by the mixture of alginate with chitosan and hyaluronic acid, using the ion Ca^{2+} as cross-linking agent. Moreover, in order to enhance the antimicrobial properties of the hydrogel based on alginate and hyaluronic acid, the addition of Ce(III) ion was evaluated *in vitro*.

3.2. Materials and methods

3.2.1. Materials

Alginic acid sodium salt from brown algae (bioreagent grade; low viscosity; 39% of guluronic acid and 61% of mannuronic acid), hyaluronic acid sodium salt from *Streptococcus equi***,** calcium chloride hexahydrate ($CaCl_2.2H_2O$, medical grade) and cerium(III) nitrate hexahydrate ($Ce(NO_3)_3.6H_2O$) were purchased from *Sigma* (USA). Chitosan HCl (medical grade) was purchased from *Heppe Medical Chitosan GmbH* (Germany). The hydroxyapatite powder was purchased from *Plasma Biotal* (UK).

3.2.2. Methods

3.2.2.1. Hydrogels preparation

Three hydrogels, developed in our previous work, were prepared according to the already optimized protocol. Briefly, an alginate hydrogel (*Alg*) was prepared by adding a $CaCl_2$ solution ($15x10^3$ mg/L) to a sodium alginate solution (7% (w/V)) in a proportion of 1:4 (V_{CaCl2}:$V_{sodium\ alginate}$). An alginate/chitosan based hydrogel (*Alg/Ch*) was prepared by adding a chitosan HCl solution (0.5% (w/V)) to the $CaCl_2$ solution, and then the alginate solution, according to the proportions: 1:4 (V_{CaCl2}:$V_{sodium\ alginate}$) and 1:1 ($V_{sodium\ alginate}$: $V_{chitosan\ HCl}$). An alginate/hyaluronate based hydrogel (*Alg/HA*) was prepared by adding to the alginate solution a sodium hyaluronate solution (0.5% (w/V)), and then the $CaCl_2$ solution in the proportions: 1:1 ($V_{sodium\ alginate}$: $V_{sodium\ hyaluronate}$) and 1:4 (V_{CaCl2}: $V_{sodium\ alginate}$).

In addition, two other alginate/hyaluronate based hydrogels with Ce(III) were prepared. For that, two cross-linking solutions, with different Ce(III) concentrations were prepared. One solution with $15x10^3$ mg/L of $CaCl_2$ and $6.6x10^2$ mg/L of $Ce(NO_3)_3$. Other solution also with $15x10^3$ mg/L of $CaCl_2$, but with $13.2x10^2$ mg/L of $Ce(NO_3)_3$. Then, each solution was added, in a proportion of 1:4 ($V_{cross\text{-}linking\ solution}$: $V_{sodium\ alginate}$), to the alginate/hyaluronate mixture (1:1 ($V_{sodium\ alginate}$: $V_{sodium\ hyaluronate}$)), obtaining the hydrogel *Alg/HA1* and *Alg/HA2,* respectively.

3.2.2.2. Glass reinforced hydroxyapatite (GR-HA) and injectable bone substitutes (*IBS*s) preparation

GR-HA was obtained by adding 2.5% (w/w) of glass (with the composition $65P_2O_5$-15CaO-$10CaF_2$-$10Na_2O$, mol %) to pure phase of prepared HAP mixed with microcrystalline cellulose. Then, discs were prepared by uniaxial pressing and heat treated at 600 ^oC to burn out the microcrystalline cellulose and then sintered at 1300 ^oC for 1 hour. Finally the discs were milled and sieved to produce granules of a 500-1000 µm size range.

Five different *IBS*s were prepared by just mixing and aggregating the GR-HA granules with each one of the developed hydrogels, in the proportions presented in table 1, which have already been optimized in our previous work.

Table 3.1: Proportions of GR-HA and hydrogel for each *IBS*: ***Alg_IBS*:** substitute with hydrogel *Alg*; ***Alg/Ch_IBS*:** substitute with hydrogel *Alg/Ch*; ***Alg/HA_IBS*:** substitute with hydrogel *Alg/HA*; ***A/HA1_IBS*:** substitute with hydrogel *Alg/HA1;* ***A/HA2_IBS*:** substitute with hydrogel *Alg/HA2.*

IBS	% GR-HA (w/w)	% Hydrogel (w/w)
Alg_IBS	41	59
Alg/Ch_IBS	47	53
Alg/HA_IBS ***Alg/HA1_IBS*** ***Alg/HA2_IBS***	48	52

To perform the *in vitro* and *in vivo* behavior evaluation of the developed materials, it was obviously necessary to sterilize them. Thus, before the hydrogels preparation the raw materials were sterilized. The sodium alginate powder was autoclaved (121 ^oC for 15 minutes), after proving by FTIR-ATR (Fourier transform infrared - Attenuated total reflectance) spectroscopy analysis that this method does not degrade the polymer, and its solution was prepared under sterile conditions. All the other polymeric solutions were filtered also under sterile conditions and GR-HA granules were autoclaved (121 ^oC for 15 minutes).

3.2.2.3. Metabolic activity

a) Cell culture

MG63 human osteosarcoma cells were seeded in 75 cm^2 flasks with 10 mL of α-MEM (α-minimal essential medium, *Gibco*, USA), supplemented with 10% (V/V) of fetal

bovine serum and 1% (V/V) antibiotic-antimycotic solution (*PAA,* Germany), in a humidified atmosphere, with 5% CO_2, at 37 ^{o}C. The culture medium was changed every two days.

b) MTT assay

Firstly, 0.6 mL samples of each *IBS* were placed on 24-well plates. Then, 1 mL of MG63 cell suspension ($2x10^4$ cells/mL) was seeded on the surface of each sample and the plates were incubated, at 37 ^{o}C, in a 5% CO_2 humidified atmosphere, for different time periods (24, 48 and 72 hours). As comparative model, for the same time periods, wells with cells seeded on GR-HA granules were used. Ethanol (96% (V/V)), as null cell viability control, was added to wells with cell suspension while as cell viability control only cell suspension was used.

After each incubation period, the metabolic activity of the cells was measured using the MTT assay (3-[4,5-dimethyl-thiazol-2-yl]-2,5-diphenyltetrazolium bromide, *Sigma*, USA) according to the manufacture instructions. The absorbance was read at 565nm (with a 630nm background) using the microplate reader *STAT FAX 3200* (*Awareness Technology*, USA). The experiment was performed in triplicate for each *IBS* and GR-HA granules.

3.2.2.4. Scanning Electron Microscopy (SEM) analysis

The morphology of the osteoblastic human cells seeded on the surface of the *Alg_IBS*, *Alg/Ch_IBS* and *Alg/HA_IBS*, after a contact period of 24 hours, was analyzed by SEM. Briefly, samples with cells were firstly fixed with 1.5% (m/V) glutaraldehyde in 0.14 M sodium cacodylate buffer (pH 7.3). Afterwards, the samples were dehydrated using graded ethanol solutions from 50% (V/V) to 100% (V/V), followed by immersion in hexamethyldisilazanes (HMDS) solutions ranging from 50% (V/V) to 100% (V/V). The samples lasted 10 minutes in each ethanol and HMDS solution and overnight in 100% (V/V) HMDS. All the used reagents were purchased from *Sigma* (USA).

Finally, the samples were placed onto an aluminum stub and coated with gold/palladium using a sputter coater (*SPI*, USA). Then, the samples were analyzed using a *Quanta 400FEG SEM* (*FEI*, USA).

3.2.2.5. Hydrogels and *IBS*s interaction with blood

The hydrogels *Alg*, *Alg/Ch* and *Alg/HA*, and the corresponding *IBS*s were placed in contact with sheep blood. Briefly, in a glass petri dish, 4 mL of fresh blood were added to 2 mL of each sample, completely covering the samples, and left in contact for 5 minutes.

3.2.2.6. Subcutaneous implantation

All the surgical procedures were performed with the approval of the Veterinary Authorities of Portugal in accordance with the European Communities Council Directive of November 1986 (86/609/EEC).

The hydrogel *Alg/HA* was implanted in three adult male Sprague Dawley® rats. Under general anesthesia, three longitudinal 3 cm-long dorsal incisions were made and 1 mL of hydrogel was implanted in each one, being then sutured (figure 3.1). Moreover, as control, three sutured incisions were done. After two weeks the animals were euthanized. From the implantation sites, samples of subcutaneous tissue were collected, and the cross-sections were stained with hematoxylin/eosin to perform histological analysis according to the standard ISO 10993-6.

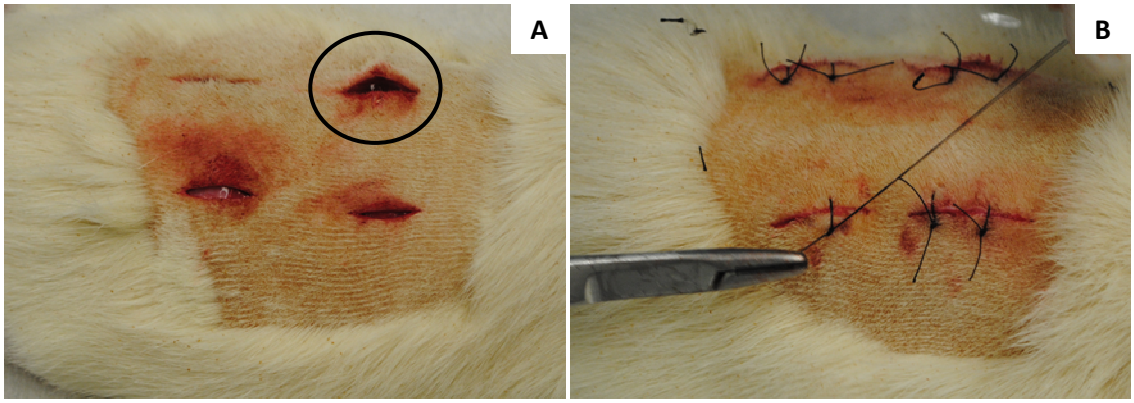

Figure 3.1: Subcutaneous implantation of the hydrogel *Alg/HA*: **A-** the dorsal incisions made on the dorsal area of the Sprague Dawley® rats; **B**-incisions suture after implantation.

3.2.2.7. Antimicrobial profile of the sodium hyaluronate-based hydrogels

To evaluate the antimicrobial activity of the hydrogels *Alg/HA*, *Alg/HA1* and *Alg/HA2,* four different microorganisms and two different techniques were used. The antimicrobial activity of the hydrogel *Alg* was used as control of null microbial inhibition.

a) Colony-forming units (CFU) count technique

The CFU count technique was used for *Staphylococcus aureus*, *Staphylococcus epidermidis* and *Candida albicans* in the presence of the hydrogels *Alg/HA*, *Alg/HA1* and *Alg/HA2.* Firstly, 50 µL of the microbial suspension ($1.5x10^4$ CFU/mL) were spread onto a plate with solid growth medium (*Liofilchem,* Italy)**.** Then, 2 mL of hydrogel were spread over it and the plates were incubated in aerobic conditions, at 37 ^oC with 5% CO_2, for 24 hours. After incubation, standard CFU count of each plate was done. This procedure was performed in quadruplicate for each microorganism and each hydrogel.

b) Inhibitory zone diameters technique

This technique was used for *Pseudomonas aeruginosa* bacteria. For that, 50 µL of the bacterial suspension ($1.5x10^8$ CFU/mL) were spread onto the plates with solid medium. Then, sterilized stainless-steel tubes with an external diameter of 1 mm (inner diameter, 7 mm) were placed over it and filled with 1 mL of sterilized hydrogel. The plates were incubated in aerobic conditions, at 37 ^oC with 5% CO_2, for 24 hours. After this incubation period, the shortest distance between the outer border of the cylinder and the first point of bacterial growth was measured. This procedure was performed in triplicate for each hydrogel.

3.2.2.8. Statistical analysis

Experimental data was presented as mean ± SD (Standard Deviation). Statistical analysis of data was performed using the one-way ANOVA and the Bonferroni post-hoc analysis, with the software *SigmaStat* 3.5. The differences were considered to be significant at a level of $p<0.05$.

3.3. Results

3.3.1. Metabolic activity

The MG63 cells metabolic activity seeded on the *Alg_IBS*, *Alg/Ch_IBS*, Alg/HA_*IBS* and GR-HA granules was evaluated and compared by the MTT assay. Ethanol represents null cell viability. MTT reduction can be generally attributed to mitochondrial succinate dehydrogenase redox activity, as such, the results presented in figure 3.2, are proportional to cell metabolism and therefore cell viability.[32]

As observed in figure 3.2, all the tested samples present a metabolic activity increase with time and always much higher values than the null cell viability control. Moreover, at 24 hours, the association of the hydrogels *Alg/Ch* and *Alg/HA* to GR-HA granules significantly increase the cell metabolic activity on the substitute. At 48 and 72 hours only the hydrogel *Alg/HA* significantly improves the cell viability. A higher metabolic activity can reveal a better cell adaptation to the material, leading to a higher cell production of ECM components and proliferation.

Cell growth and function are influenced by the biomaterial surface characteristics, such as, morphology and/or chemical composition.[33, 34] GR-HA is reported as presenting a better osteoblastic growth and function than hydroxyapatite (HAP), due to its triphasic composition: HAP, α- and β-tricalcium phosphate (TCP). These two TCP crystal phases are less stable than HAP, improving the osteoblasts performance because of ions release to the extra-cellular environment.[4, 5, 33] Moreover, the released ions react with physiologic ions, leading to the formation of a new apatite layer between the implant and bone, promoting the osteointegration.[35]

The association of the hydrogels *Alg/Ch* and *Alg/HA* to GR-HA can improve the cell viability due to their morphology or their chemical composition. Moreover, as observed, the association of chitosan and HA to alginate enhance the bioactive ability of the polymeric vehicle, as expected. Chitosan and HA are natural polysaccharides, having the advantage of mimic ECM biological macromolecules, which cells are naturally prepared to recognize and deal with metabolically.[11, 12, 36]

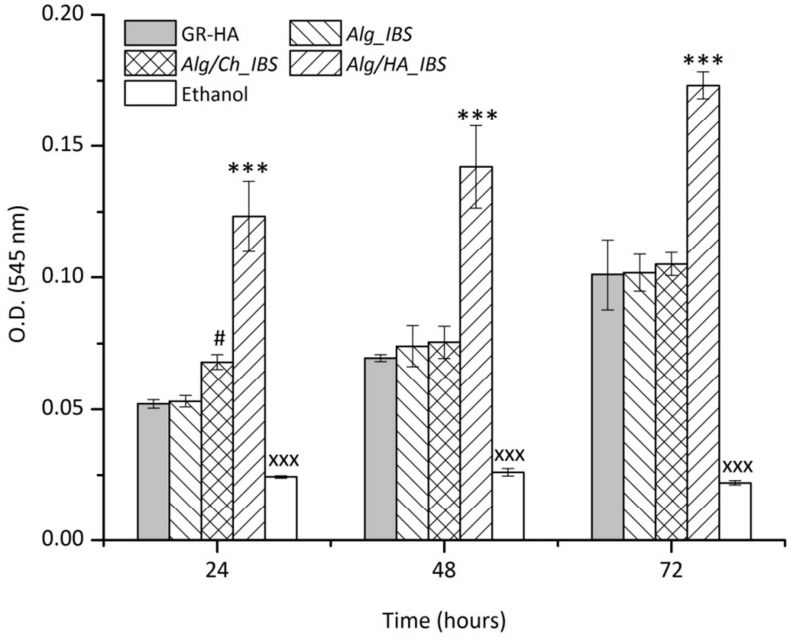

Figure 3.2: Metabolic activity of the MG63 cells seeded on the three developed *IBS*s, after 24, 48 and 72 hours of incubation. Data are presented as mean ± SD.

*** $p < 0.001$: significant difference between *Alg/HA_IBS* and each one of the other samples.

xxx $p < 0.001$: significant difference between Ethanol and each one of the other samples.

# $p < 0.05$: significant difference of *Alg/Ch_IBS* compared with GR-HA and *Alg_IBS* .

3.3.2. SEM analysis

Cells attachment, adhesion and spreading are very important steps for a good cells/material interaction. The way these phenomena occur influences the cell's ability to proliferate and to differentiate, which is essential for the formation of an implant/bone functional interface and the subsequent biomaterial osteointegration.[34, 37, 38] Therefore, this assay was performed in order to observe the cell adhesion to the different injectable systems, as well as, their morphology.

After 24 hours of incubation, it is possible to observe that MG63 cells adhered to the *Alg_IBS, Alg/Ch_IBS* and *Alg/HA_IBS* surface, although, the cells have different morphologies, as observed in figure 3.3-A2, B2, C2. The cells seeded on the *Alg_IBS* surface have a spherical shape with some visible lamellipodia. Two different cell adhesion stages can be distinguished on the *Alg/Ch_IBS* surface. Cells with a spherical morphology and lamellipodia can be observed, which indicate an initial stage of adhesion, and a more advanced stage where the osteoblastic-like cells have a spread morphology and some filopodia. On the *Alg/HA_IBS* surface, after just one day of incubation, cells have a spreader shape with more developed filopodia.

The distinct cell morphology on the three *IBS*s can be explained by the different cells/material interaction, which is influenced by the implant surface properties.[5, 38] What mainly distinguishes the *IBS*s surfaces it is the polymeric vehicle that is associated with the GR-HA. Thus, the objective of improving the cell adhesion phenomenon on the bone substitute by associating a bioactive polymer to an alginate vehicle was successfully achieved, as expected according to the literature.[19, 39]

Chitosan structure resembles the glycosaminoglycans of the extracellular matrix, and it has been reported that it can act as a promoter of cell adhesion, mainly, due to its positively charged surface, which will attract the negatively charged cell surface.[19, 20] Hyaluronic acid is the main component of the living tissues extracellular matrix (ECM), namely in the connective tissue, being involved in cell signaling and matrix organization.[40, 41] Its incorporation in the *IBS* allows it to mimic the organic part of the bone ECM, while GR-HA mimics the inorganic part of bone. This synergy can lead to a better cell adhesion and spreading. This polymer is able to interact with different cell surface receptors, establishing several sites of adhesion between cells and the material surface.[40, 42] In a cell adhesion process, during the establishment of those sites, there is an organization and/or production of the cytoskeleton filamentous proteins, namely actin filaments, which tend to assemble in long bundles leading to a spreader shape with protrusions (filopodia) of the plasma membrane.[34, 38, 43, 44] The cytoskeleton organization controls the cell morphology, and, once its proteins are involved in signal transduction, the cell shape can also be related with cell growth and function.[44, 45] Interestingly, the *IBS* which presents cells with the spreader and organized structure have also presented the highest metabolic activity, as discussed in point 3.3.1.. If a cell does not spread on the material surface it cannot migrate, which, in some cases, can influence the cell growth and proliferation, what can explain the higher metabolic activity on the *Alg/HA_IBS*.[34, 44]

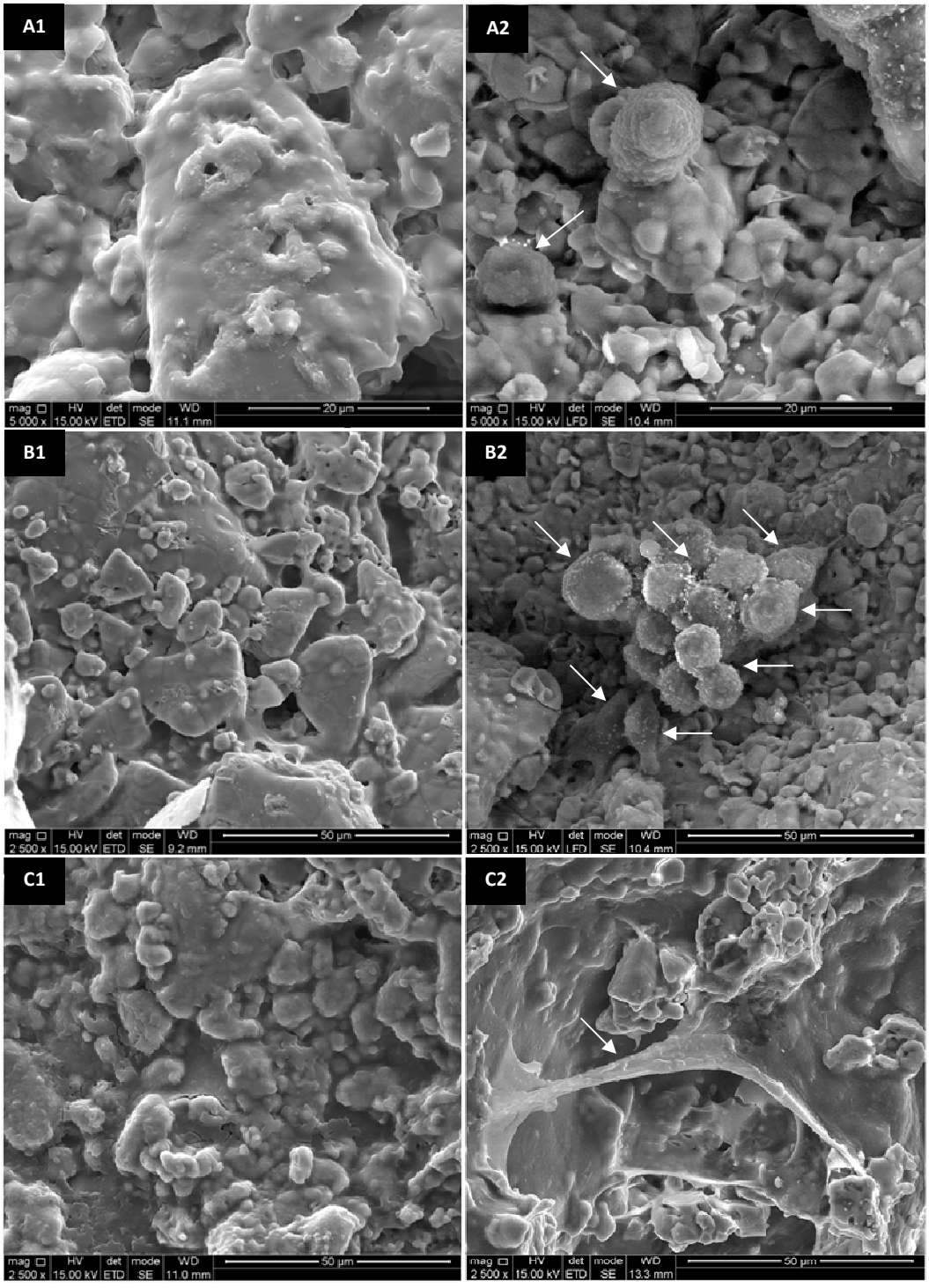

Figure 3.3: SEM appearance of the MG63 cells adhered on the three developed *IBS*s after 24 hours of incubation: **A1**-*Alg_IBS* non-cell seeded**; A2**-*Alg_IBS* cell seeded; **B1**-*Alg/Ch_IBS* non-cell seeded**; B2**-*Alg/Ch_IBS* cell seeded; **C1**-*Alg/HA_IBS* non-cell-seeded; **C2**-*Alg/HA_IBS* cell seeded.
The arrows indicate cells adhered on the materials.

3.3.3. Hydrogels and *IBS*s interaction with blood

As is can be seen from the previous results the develop *IBS*s have a positive effect on cell adhesion, morphology and activity, which is a good indicator that these materials are suitable for usage as bone substitutes.

It is known that several hydrogels, some of them available in the market, that have been tested as a vehicle for GR-HA, had immediately lost its consistency upon contact with blood. Thus, during the surgical process the GR-HA granules disaggregate, being extremely difficult to implant the bone substitute material, which limits its applicability.

Therefore, a simple preliminary experiment was performed in order do understand the behavior of the new materials when placed in contact with blood, namely, the materials apparent consistency change. As observed in figure 3.4 (A,B,C), the three hydrogels did not lose their consistency when in contact with blood. Only after few minutes (about 2-3), it was verified a slight loss, mainly for the hydrogels *Alg/Ch* and *Alg/HA*. Nevertheless, the observed consistency loss did not influence the hydrogels performance as granules aggregation agents, since the *IBS*s maintained their integrity and moldability (figure 3.4-C).

The slight higher consistency loss of the hydrogels *Alg/Ch* and *Alg/HA* can be owed to the lower polymeric content, which leads to a faster destruction of the polymeric network by hydrolysis of the polymeric chains.[16, 23, 46, 47] Besides that, chitosan and hyaluronate can also undergo enzymatic-hydrolysis, namely by lysozyme and hyaluronidase, respectively, present in mammals blood.[23, 48-50] Thus, this is another factor that can accelerate the polymeric chains degradation, resulting in a consistency loss.

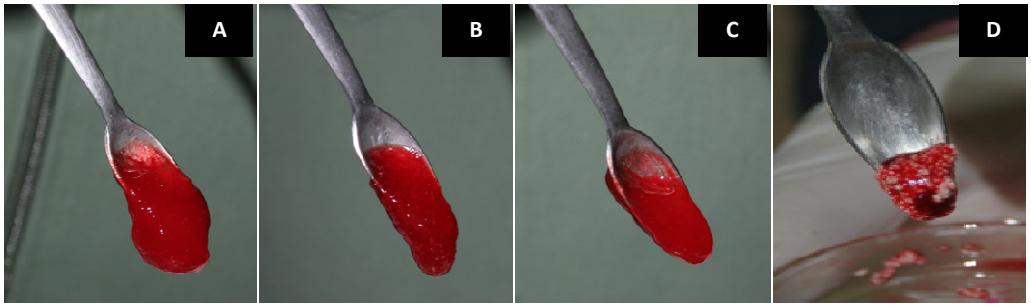

Figure 3.4: Interaction of the hydrogels and *IBS*s with sheep blood:
A-hydrogel *Alg*; **B**-hydrogel *Alg/Ch*; **C**-hydrogel *Alg/HA*; **D**-*Alg/HA_IBS*.

3.3.4. Subcutaneous implantation

After *in vitro* characterization, *Alg/AH* as the hydrogel with the best performance was evaluated by histological analysis, after 14 days of subcutaneous implantation in Sprague Dawley® rat, to assess the tissue local biological response to this hydrogel. Throughout this two-weeks follow-up time, all animals remained healthy and none developed local or systemic signs of infection and/or inflammation were observed. Using a descriptive analysis and a scoring system according to Standard ISO 10993-6, the following criteria were considered for semi-quantitative histological study of the tissue around the implanted material: collagen fiber formation, inflammatory infiltrate, the presence of necrosis and other tissue alterations such as vascularization, lipid infiltration.[51, 52]

Table 3.2: Semi-quantitative scoring of the biological response to the implanted material, according to ISO 10993-6.

Cell type/response	Average number
Neutrophils	0.33
Lymphocytes	2.89
Plasma cells	2.33
Macrophages	3.89
Giant cells	0.11
Necrosis	0.00
Sub-total (x2)	**19.11**
Neovascularization	2.78
Fibrosis	1.33
Lipid infiltration	0.00
Sub-total	**4.11**
Total	**23.22**

In figure 3.5 various lymphocytes and plasma cells are visible. Such histological findings are in agreement with an attempt at healing by connective tissue replacement of damaged tissue, strengthened by the presence of macrophages since these cells play a critical role in the initiation, maintenance, and resolution of inflammation.[51-53] Quantitatively, table 3.2 indicates the very low number of neutrophils and giant cells (not seen in figure 3.5), and even the absence of necrosis and lipid infiltration. Neovascularization and fibrosis are clearly visible in figure 3.5, two typical phenomena of tissue regeneration process.[51, 52]

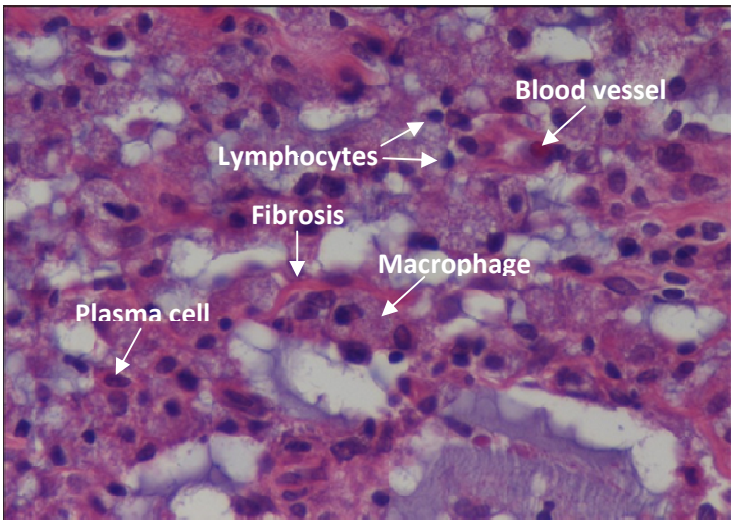

Figure 3.5: Histological image (magnification x 400) of a subcutaneous tissue sample, after 2 weeks of the hydrogel *Alg/HA* implantation.

According to ISO 10993-6, the sample biological response must be evaluated by subtracting the control quantitative analysis (16.29) to the sample's

(23.22). After this operation the quantitative result is 6.93. By ISO 10993-6, this result corresponds to a slight irritating response, thus making this material biocompatible.

3.5. Antimicrobial profile of the sodium hyaluronate-based hydrogels

Every surgical procedure, even the less invasive ones, presents susceptibility to infections, which can compromise the success of the implanted material. Thus, the use of a vehicle with the ability to decrease or inhibit the growth of several microorganisms could significantly improve the clinical outcomes of the bone substitute.[27, 54]

Therefore, to enhance the applicability of the hydrogel which revealed the better biological performance *in vitro* and a good response *in vivo*, it was modified in an attempt to obtain a bioactive vehicle also with potential antimicrobial properties. In order to achieve this purpose, Ce(III) ions, which have revealed antimicrobial properties, were incorporated in hydrogel *Alg/HA* in two different concentrations: *Alg/HA1* and *Alg/HA2.*

Thus, to perform a more complete analysis, the hyaluronic acid and Ce(III) antimicrobial properties were evaluated against the main bacteria responsible for infections in hospital environment, namely in orthopedic surgical procedures, and even against the most prevalent fungus.[27, 54-56] In order to determine the growth of such microbes in the presence of each tested hydrogel, two different techniques were used. *S.aureus*, *S.epidermidis* and *C.albicans* grow in form of individual colonies, which are countable.[57] *P.aeruginosa* form irregular spots, which sometimes are overlapping, thus making the inhibitory zone diameters technique more appropriate to use.[58]

As presented in figure 3.6, the hydrogel *Alg/HA* shows antimicrobial activity against all the tested microorganisms, when compared with the hydrogel *Alg* (considered as null antimicrobial activity control). These results indicate that hyaluronic acid has an antimicrobial effect, what is in accordance with the literature, including the lower effect against *P.aeruginosa*.[54, 59]

Hyaluronic acid has previously shown to have a wide bacteriostatic effect, namely, against microbes commonly found in orthopaedic practice and oral cavity.[54] *In vivo*, its activity can be even more efficient since it acts like a cell shield, avoiding the microbes penetration.[60] Moreover this polymer can induce the expression of some

innate immunity antibiotic peptides, such as β-defensin 2 produced by epithelial cells, which exhibits antimicrobial activity.[61, 62]

Regarding to Ce(III) antimicrobial ability, it is observed in figure 3.6 that the addition of this ion enhanced the antimicrobial activity of the hydrogel *Alg/HA.* For *S.aureus*, *S.epidermidis* and *C.albicans*, hydrogel *Alg/HA1* presents a significant antimicrobial activity increase compared to the hydrogel *Alg/HA*. A higher Ce(III) concentration in the hydrogel *Alg/HA2*, for these microorganisms, leads to an even stronger activity. Concerning to *P.aeruginosa*, it is necessary to add to the hydrogel *Alg/HA* the highest tested Ce(III) concentration to verify a significant antibacterial effect increase. This bacterium higher resistance to the ion, relatively to others microorganisms, has already been verified.[30, 63]

Cerium is reported as having bacteriostatic and bactericidal activity against several bacteria and also antimicrobial effect against fungi.[64] Regarding to its way of action, some possible mechanisms have been postulated: the uptake of cerium into the cytoplasm can inhibit the cellular respiration, oxygen uptake and glucose metabolism, or eventually it can disrupt the cell membrane.[29, 30] *P.aeruginosa*, being a gram-negative bacterium, has a more complex cell wall than the gram-positive bacteria (*S.aureus* and *S.epidermidis*). Its cell wall is composed by a peptidoglycan layer and a lipidic external membrane, being less permeable and susceptible to biocides than the gram-positive bacteria.[65] Thus, the weaker effect of Ce(III) in this microbe can be explained by the more difficulty of ion to enter and interfere in the cellular events.

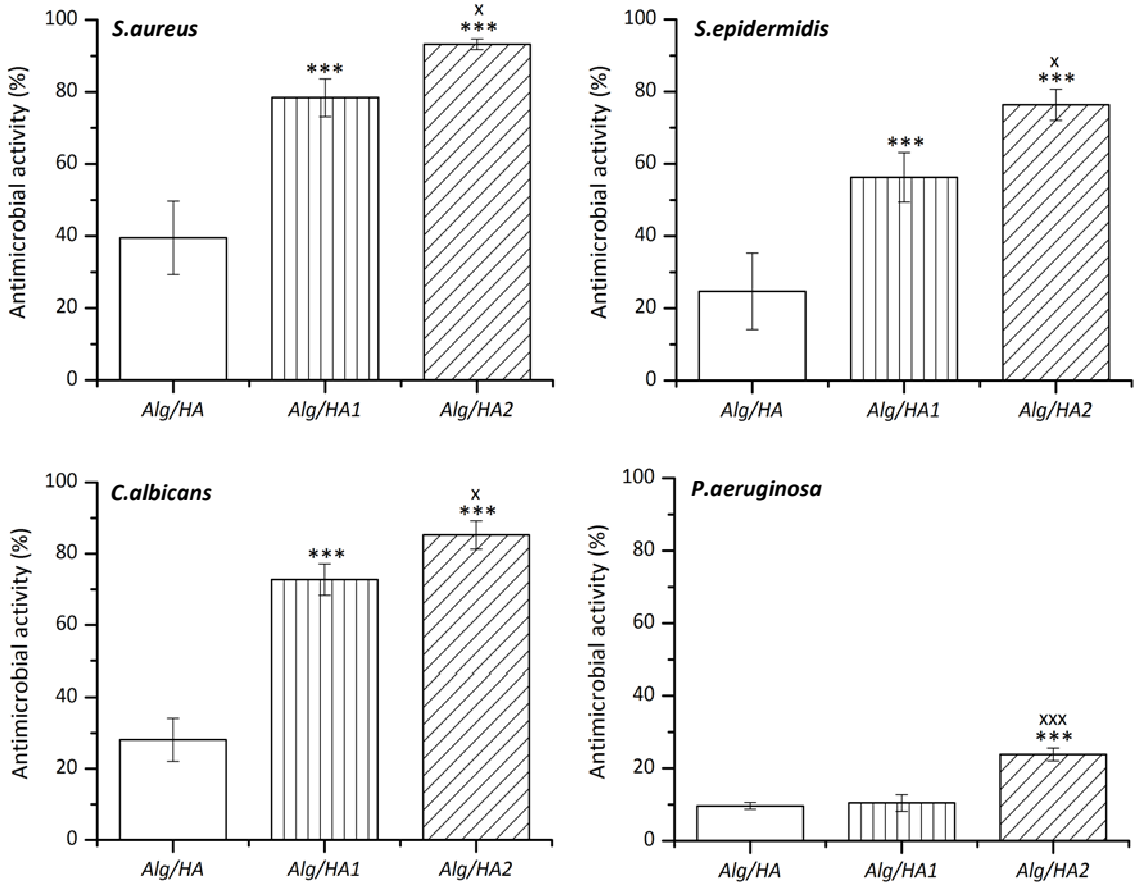

Figure 3.6: Antimicrobial activity of the hydrogels *Alg/HA*, *Alg/HA1* and *Alg/HA2* after 24 hours of incubation. Values were obtained using the hydrogel *Alg* as model of null inhibition.
Data are presented as mean ± SD.
*** $p < 0.001$: significant difference compared with *Alg/HA.*
^{x} $p < 0.05$, ^{xxx} $p < 0.001$: significant difference compared with *Alg/HA1*.

3.6. Metabolic activity on the *Alg/HA2_IBS*

The MTT assay was performed in order to evaluate if Ce(III) incorporation in the hydrogel *Alg/HA* influences the metabolic activity of MG63 cells in contact with the *IBS*. Thus, the metabolic activity on *Alg/HA_IBS* was compared with activity on *Alg/HA2_IBS*, which is composed by the highest tested Ce(III) concentration, because in point 3.5. this hydrogel presented the highest antimicrobial activity for all tested microorganisms.

It is observed, in figure 3.7, that the metabolic activity promoted by the *Alg/HA_IBS* and *Alg/HA2_IBS* increases with time. Nevertheless, the *Alg/HA2_IBS* presents a slightly lower metabolic activity than the *Alg/HA_IBS* at 24 and 72 hours. Despite this reduction, about 5.42%±0.28 at 24 hours and 5.14%±0.25 at 72 hours, the

cell metabolic activity on *Alg/HA2_IBS* is still much higher than the one verified on GR-HA granules in point 3.3.1..

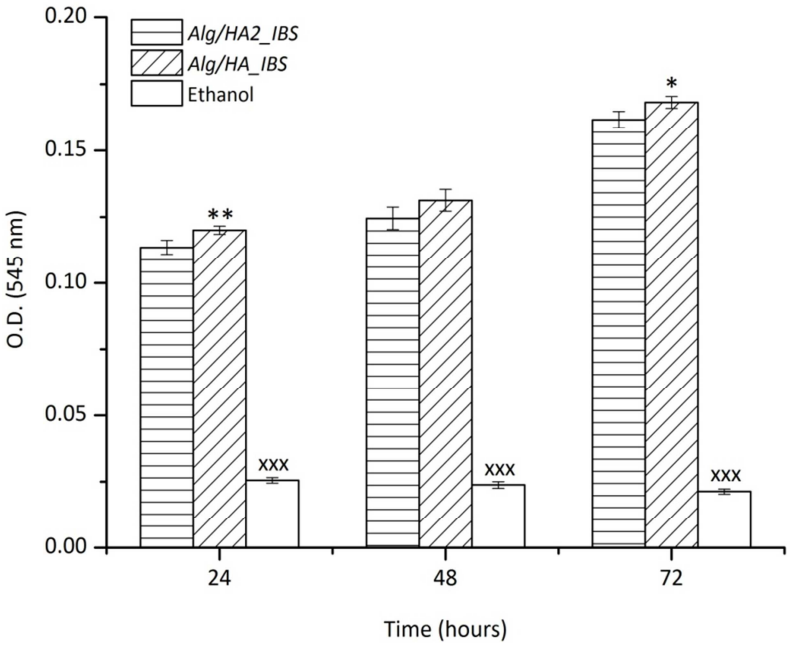

Figure 3.7: Metabolic activity of the MG63 cells seeded on *Alg/HA2_IBS* and *Alg/HA_IBS*, after 24, 48 and 72 hours of incubation. Data are presented as mean ± SD.

* $p < 0.05$, ** $p < 0.002$: significant difference compared with *Alg/HA2_IBS*.

xxx $p < 0.001$: significant difference between Ethanol and each one of the other samples.

It has been reported that Lanthanides do not penetrate living mammalian cell membranes as it happens with bacteria. Nevertheless, the Ce(III) ionic radius is very similar to the Ca^{2+} one, therefore, Ce(III) is able to interact with calcium-dependent transmembrane signaling channels, which can interfere with intracellular events and cause a decrease in the metabolic activity of osteoblasts. However, this Ce(III) competition with Ca^{2+} can also have advantages, namely, inhibitory effect on mast cells degranulation and histamine release from both these cells and basophils, by interference with a cell membrane ATPase pump. [30, 66]

3.4. Conclusions

Firstly, it was verified that the hydrogel association to the GR-HA granules can enhance the osteoblasts metabolic activity on the bone substitute, mainly the hydrogel *Alg/HA*. Besides that, the cell adhesion and morphology on the *IBS*s was influenced by the polymeric composition of the associated hydrogel.

When the hydrogels and *IBS*s were placed in contact with blood, their consistency was slight affected, but without influence their use as vehicles. The differences observed during this test may be due to the vulnerability of each hydrogel to degrade by enzymatic or non-enzymatic hydrolysis. *In vivo,* the hydrogel *Alg/HA* revealed a slightly irritating response, according to ISO 10993-6, indicating its biocompatibility to be used in biomedical applications.

The association of hyaluronic acid with alginate increased the antimicrobial effect against the tested microorganisms. Moreover, Ce(III) addition to the hydrogel *Alg/HA* significantly enhances its antimicrobial activity, without compromise the hydrogel cell viability.

Overall, these results show that the hydrogel *Alg/HA2* is a potential vehicle to associate with the synthetic bone substitute. This hydrogel, besides allowing the granules injection, it also enhances the cellular metabolic activity on the substitute and even grant it an antimicrobial activity, improving its regenerative performance.

3.5. References

1. Giannoudis P.V., Dinopoulos H., and Tsiridis E., *Bone substitutes: an update.* Injury, 2005. **36**(3): p. 20-27.
2. Bostrom M.P.G. and Seigerman D.A., *The clinical use of allografts, demineralized bone matrices, synthetic bone graft substitutes and osteoinductive growth factors: a survey study.* HSS Journal, 2005. **1**(1): p. 9-18.
3. Lopes M.A., Knowles J.C., and Santos J.D., *Structural insights of glass-reinforced hydroxyapatite composites by Rietveld refinement.* Biomaterials, 2000. **21**: p. 1905-1910.
4. Gutierres M., Lopes M.A., Sooraj Hussain N., Lemos A.F., Ferreira J.M.F., Afonso A., Cabral A.T., Almeida L., and Santos J. D., *Bone ingrowth in macroporous Bonelike® for orthopaedic applications.* Acta Biomaterialia, 2008. **4**(2): p. 370-377.
5. Lopes M.A., Knowles J.C., Santos J.D., Monteiro F.J., and Olsen I., *Direct and indirect effects of P_2O_5 glass reinforced-hydroxyapatite composites on the growth and function of osteoblast-like cells.* Biomaterials, 2000. **21**: p. 1165-1172.
6. Larsson S. and Hannink G., *Injectable bone-graft substitutes: current products, their characteristics and indications, and new developments.* Injury, 2011. **42**: p. 30-34.
7. Gaharwar A.K., Dammu S.A., Canter J.M., Wu C., and Schmidt G., *Highly extensible, tough, and elastomeric nanocomposite hydrogels from poly(ethylene glycol) and hydroxyapatite nanoparticles.* Biomacromolecules, 2011. **12**(5): p. 1641-1650.
8. Oliveira S.M., Almeida I.F., Costa P.C., Barrias C.C., Ferreira M.R.P., Bahia M.F., and Barbosa M.A., *Characterization of polymeric solutions as injectable vehicles for hydroxyapatite microspheres.* AAPS PharmSciTech, 2010. **11**(2): p. 852-858.
9. Couto D., Hong Z., and Mano J., *Development of bioactive and biodegradable chitosan-based injectable systems containing bioactive glass nanoparticles.* Acta Biomaterialia, 2009. **5**(1): p. 115-123.
10. Vaccaro A.R., *The role of the osteoconductive scaffold in synthetic bone graft.* Orthopedics, 2002. **25**: p. 571-578.
11. Mano J.F., Silva G.A., Azevedo H.S., Malafaya P.B., Sousa R.A., Silva S.S., Boesel L.F., Oliveira J.M., Santos T.C., Marques A.P., Neves N.M., and Reis R.L., *Natural origin biodegradable systems in tissue engineering and regenerative medicine: present status and some moving trends.* Journal of the Royal Society Interface, 2007. **4**(17): p. 999-1030.
12. Slaughter B.V., Khurshid S.S., Fisher O.Z., Khademhosseini A., and Peppas N.A., *Hydrogels in regenerative medicine.* Advanced Materials, 2009. **21**(32-33): p. 3307-3329.

13. Wang L., Shelton R.M., Cooper P.R., Lawson M., Triffitt J.T., and Barralet J.E., *Evaluation of sodium alginate for bone marrow cell tissue engineering.* Biomaterials, 2003. **24**(20): p. 3475-3481.
14. West E., M. Xu, T. Woodruff, and L. Shea, *Physical properties of alginate hydrogels and their effects on in vitro follicle development.* Biomaterials, 2007. **28**(30): p. 4439-4448.
15. Sriamornsak P., Thirawong N., and Korkerd K., *Swelling, erosion and release behavior of alginate-based matrix tablets.* European Journal of Pharmaceutics and Biopharmaceutics, 2007. **66**(3): p. 435-450.
16. Ulery B.D., Nair L.S., and Laurencin C.T., *Biomedical applications of biodegradable polymers.* Journal of Polymer Science Part B : Polymer Physics, 2011. **49**(12): p. 832-864.
17. Andersen T., Strand B.L., Formo K., Alsberg E., and Christensen B.E., *Alginates as biomaterials in tissue engineering.* Carbohydrate Chemistry, 2012. **37**: p. 227-258.
18. Nair L.S. and Laurencin C.T., *Biodegradable polymers as biomaterials.* Progress in Polymer Science, 2007. **32**(8-9): p. 762-798.
19. Chen A., Haddad D., and Wang R., *Analysis of chitosan-alginate bone scaffolds.* Rutgers University, New Jersey Governor's School of Engineering & Technology, 2009: p. 1-8.
20. Aranaz I., Mengíbar M., Harris R., Paños I., Miralles B., Acosta N., Galed G., and Heras A., *Functional characterization of chitin and chitosan.* Current Chemical Biology, 2009. **3**: p. 203-230.
21. Brown M.B. and Jones S.A., *Hyaluronic acid: a unique topical vehicle for the localized delivery of drugs to the skin.* Journal of the European Academy of Dermatology and Venereology, 2005. **19**(3): p. 308-318.
22. Prestwich G.D., *Hyaluronic acid-based clinical biomaterials derived for cell and molecule delivery in regenerative medicine.* Journal of Controlled Release, 2011. **155**(2): p. 193-199.
23. Kim J., Kim I. S., Cho T. H., Lee K.B., Hwang S.J., Tae G., Noh I., Lee S.H., Park Y., and Sun K., *Bone regeneration using hyaluronic acid-based hydrogel with bone morphogenic protein-2 and human mesenchymal stem cells.* Biomaterials, 2007. **28**(10): p. 1830-1837.
24. Patterson J., Siew R., Herring S.W., Lin A.S.P., Guldberg R., and Stayton P.S., *Hyaluronic acid hydrogels with controlled degradation properties for oriented bone regeneration.* Biomaterials, 2010. **31**(26): p. 6772-6781.
25. Martínez-Sanz E., Ossipov D.A., Hilborn J., Larsson S., Jonsson K.B., and Varghese O.P., *Bone reservoir: Injectable hyaluronic acid hydrogel for minimal invasive bone augmentation.* Journal of Controlled Release, 2011. **152**(2): p. 232-240.
26. Nagaoka I., Igarashi M., and Sakamoto K., *Biological activities of glucosamine and its related substances.* Advances in Food and Nutrition Research, 2012. **65**: p. 337-352.

27. Campoccia D., Montanaro L., and Arciola C.R., *The significance of infection related to orthopedic devices and issues of antibiotic resistance.* Biomaterials, 2006. **27**(11): p. 2331-2339.
28. Campoccia D., Montanaro L., Speziale P., and Arciola C.R., *Antibiotic-loaded biomaterials and the risks for the spread of antibiotic resistance following their prophylactic and therapeutic clinical use.* Biomaterials, 2010. **31**(25): p. 6363-6377.
29. Cobrado L., Azevedo M.M., Silva-Dias A., Ramos J.P., Pina-Vaz C., and Rodrigues A.G., *Cerium, chitosan and hamamelitannin as novel biofilm inhibitors?* Journal of Antimicrobial Chemotherapy, 2012. **67** (5): p. 1159-1162
30. Garner J.P. and Heppell P.S.J., *Cerium nitrate in the management of burns.* Burns, 2005. **31**: p. 539–547.
31. Zhang H., Feng J., Zhu W., Liu C., and Gu J., *Bacteriostatic effects of cerium–humic acid complex.* Biological Trace Element Research, 1999. **73**: p. 29-36.
32. Takahashi S., Abe T., Gotoh J., and Fukuuchi Y., *Substrate-dependence of reduction of MTT: a tetrazolium dye differs in cultured astroglia and neurons.* Neurochemistry International, 2002. **40**(5): p. 441-448.
33. Ferraz M.P., Fernandes M.H., Santos J.D., and Monteiro F.J., *HA and double-layer HA-P2O5/CaO glass coatings: influence of chemical composition on human bone marrow cells osteoblastic behavior.* Journal of Materials Science-Materials in Medicine, 2001. **12**(7): p. 629-638.
34. Anselme K., *Osteoblast adhesion on biomaterials.* Biomaterials, 2000. **21**(7): p. 667-681.
35. Dee K.C., Puleo D.A., and Bizios R., eds. *An Introduction To Tissue-Biomaterial Interactions*. 1st ed. 2002, Wiley-Liss, Inc. 248.
36. Fedorovich N.E., Alblas J., Wijn J.R., Hennink W.E., Verbout A.J., and Dhert W.J.A., *Hydrogels as extracellular matrices for skeletal tissue engineering: state-of-the-art and novel application in organ printing.* Tissue Engineering, 2007. **13**(8): p. 1905-1925.
37. Botelho C.M., Brooks R.A., Best S.M., Lopes M.A., Santos J.D., Rushton N., and Bonfield W., *Human osteoblast response to silicon-substituted hydroxyapatite.* Journal of Biomedical Materials Research: Part A, 2006. **79**(3): p. 723-730.
38. Hempel U., Hefti T., D. P., and Schlottig F., *Response of human bone marrow stromal cells, MG-63, and SaOS-2 to titanium-based dental implant surfaces with different topography and surface energy.* Clinical Oral Implants Research, 2011: p. 1-9.
39. Oerther S., Maurin A., Payan E., Hubert P., Lapicque F., Presle N., Dexheimer J., Netter P., and Lapicque F., *High Interaction Alginate–Hyaluronate Associations by Hyaluronate*

Deacetylation for the Preparation of Efficient biomaterials. Biopolymers, 2000. **54**: p. 273-281.

40. Lei Y., Gojgini S., Lam J., and Segura T., *The spreading, migration and proliferation of mouse mesenchymal stem cells cultured inside hyaluronic acid hydrogels.* Biomaterials, 2011. **32**(1): p. 39-47.
41. Kim I.L., Mauck R.L., and Burdick J.A., *Hydrogel design for cartilage tissue engineering: A case study with hyaluronic acid.* Biomaterials, 2011. **32**(34): p. 8771-8782.
42. Zaleski K.J., Kolodka T., Cywes-Bentley C., McLoughlin R.M., Delaney M. L., Charlton B.T., Johnson W., and Tzianabos A.O., *Hyaluronic acid binding peptides prevent experimental staphylococcal wound infection.* Antimicrobial Agents and Chemotherapy, 2006. **50**(11): p. 3856-3860.
43. Wutticharoenmongkol P., Pavasant P., and Supaphol P., *Osteoblastic Phenotype Expression of MC3T3-E1 Cultured on Electrospun Polycaprolactone Fiber Mats Filled with Hydroxyapatite Nanoparticles.* Biomacromolecules, 2007. **8**: p. 2602-2610.
44. Gwynn I.A., *Cell biology at interfaces.* Journal of Materials Science Materials in Medicine, 1994. **5**: p. 357-360.
45. Amaral M., Costa M.A., Lopes M.A., Silva R.F., Santos J.D., and Fernandes M.H., *Si_3N_4-bioglass composites stimulate the proliferation of MG63 osteoblast-like cells and support the osteogenic differentiation of human bone marrow cells.* Biomaterials, 2002. **23**(24): p. 4897-4906.
46. Il'ina A.V. and Varlamov V.P., *Hydrolysis of chitosan in lactic acid.* Applied Biochemistry and Microbiology, 2004. **40**(3): p. 300-303.
47. Rehm B.H.A., ed. *Alginates: Biology and Applications.* 2009, Springer. 266.
48. Ruel-Gariépy E., Chenite A., Chaput C., Guirguis S., and Leroux J.C., *Characterization of thermosensitive chitosan gels for the sustained delivery of drugs.* International Journal of Pharmaceutics, 2000. **203**: p. 89–98.
49. Irwin D.M., Biegel J.M., and Stewart C.B., *Evolution of the mammalian lysozyme gene family.* Bmc Evolutionary Biology, 2011. **11**.
50. Rahmanian M. and Heldin P., *Testicular hyaluronidase induces tubular structures of endothelial cells grown in three-dimensional colagen gel through a CD44-mediated mechanism.* International Journal of Cancer, 2002. **97**(5): p. 601-607.
51. Ribeiro P.D., Sanches M.G., and Okamoto T., *Comparative analysis of tissue reactions to anesthetic solutions: histological analysis in subcutaneous tissue of rats.* Anesth Prog, 2003. **50**(4): p. 169-180.

52. Oak M. and Singh J., *Chitosan-zinc-insulin complex incorporated thermosensitive polymer for controlled delivery of basal insulin in vivo.* Journal Control Release, 2012: p. 1-10.
53. Fujiwara N. and Kobayashi K., *Macrophages in inflammation.* Curr Drug Targets Inflamm Allergy, 2005. **4**(3): p. 281-286.
54. Carlson G.A., Dragoo J.L., Samimi B., Bruckner D.A., Bernard G.W., Hedrick M., and Benhaim P., *Bacteriostatic properties of biomatrices against common orthopaedic pathogens.* Biochemical and Biophysical Research Communications, 2004. **321**(2): p. 472-478.
55. Peleg A.Y. and Hooper D.C., *Hospital-acquired Infections due to gram-negative bacteria reply.* New England Journal of Medicine, 2010. **363**(15): p. 1483-1484.
56. Diba K., Rhaimirad M., Makhdoomi K., and Khorshidvand Z., *Identification of Candida species isolated from hospital acquired infections cases and hospital indoor environments.* African Journal of Microbiology Research, 2012. **6**(19): p. 4164-4168.
57. Harriott M.M. and Noverr M.C., *Candida albicans and Staphylococcus aureus form polymicrobial biofilms: effects on antimicrobial resistance.* Antimicrobial Agents and Chemotherapy, 2009. **53**(9): p. 3914-3922.
58. Ji Q.X., Zhao Q.S., Deng J., and Lu R., *A novel injectable chlorhexidine thermosensitive hydrogel for periodontal application: preparation, antibacterial activity and toxicity evaluation.* Journal of Materials Science-Materials in Medicine, 2010. **21**(8): p. 2435-2442.
59. Pirnazar P., Wolinsky L., Nachnani S., Haake S., Pilloni A., and Bernard G.W., *Bacteriostatic effects of hyaluronic acid.* Journal of Periodontology, 1999. **70**(4): p. 370-374.
60. Castleman M., ed. *The New Healing Herbs: The Classic Guide to Nature's Best Medicines*. 2001, Rodale Inc.: USA. 467.
61. Palffy R., Gardlik R., Behuliak M., Kadasi L., Turna J., and Celec P., *On the physiology and pathophysiology of antimicrobial peptides.* Molecular Medicine, 2009. **15**(1-2): p. 51-59.
62. Gariboldi S., Palazzo M., Zanobbio L., Selleri S., Sommariva M., Sfondrini L., Cavicchini S., Balsari A., and Rumio C., *Low molecular weight hyaluronic acid increases the self-defense of skin epithelium by induction of beta-defensin 2 via TLR2 and TLR4.* Journal of Immunology, 2008. **181**(3): p. 2103-2110.
63. Gracia C.G., *An open study comparing topical silver sulfadiazine and topical silver sulfadiazine–cerium nitrate in the treatment of moderate and severe burns.* Burns, 2001. **27**: p. 67-74.
64. Amara S.G., Gudermann Th., Jahn R., Lill R., Nilius B., Offermanns S., and Petersen O.H., eds. *Reviews of Physiology, Biochemistry and Pharmacology* 2005, Springer: Netherlands. 153.

65. Liaqat I. and Sabri A., *Analysis of cell wall constituents of biocide-resistant isolates from dental-unit water line biofilms.* Current Microbiology, 2008. **57**: p. 340–347.
66. Jakupec M.A., Unfried P., and Keppler B.K., *Pharmacological properties of cerium compounds.* Reviews of Physiology Biochemistry and Pharmacology, 2005. **153**: p. 101-111.

Chapter 4

Implantation of one developed injectable bone substitute

4.1. Surgical procedure

In *Chapter 3*, the injectable system (*Alg/HA_IBS*) composed by glass-reinforced hydroxyapatite (GR-HA) granules and the hydrogel composed by alginate and hyaluronate (*Alg/HA*) presented the better cell performance out of the three *IBSs* developed in *Chapter 2*. Moreover, despite the slightly irritant response to the subcutaneous implantation of the hydrogel *Alg/HA*, its *in vivo* biocompatibility was demonstrated. Thus, this *IBS* was implanted in a bone defect in order to evaluate its ability to promote bone regeneration.

To perform the intraosseous implantation of the *Alg/HA_IBS* a healthy skeletally mature Merino breed sheep (082435) was used as experimental model, presenting an average weight of 50 kg.

The sheep was housed for two weeks before the surgery, being properly fed. All procedures were performed with the approval of the Veterinary Authorities of Portugal in accordance with the European Communities Council Directive 86/609/EEC. Before the surgery the sheep leg was properly shaved and scrubbed with antiseptic solution. Then, under general anesthesia, in the lateral diaphysis of each sheep femur, a row of five holes with a diameter of 5.0 mm was drilled through the cortex and into the medulla, using a microburr continuously flushed with a sterile normal saline solution to minimize thermal damage and to remove any residual bone (figure 4.2 and 4.3). A minimal distance of 1 cm was kept between drill holes to reduce the risk of fracture. In order to ensure a complete filling of the defects, adequate volumes of *Alg/HA_IBS* were applied in three holes (figure 4.4-B). Besides that, a hole was filled with just GR-HA granules (figure 4.4-A), premixed with peripheral blood, and another was left unfilled to be used as controls in the histological analysis.

The sheep was then transferred to individual cages and allowed to move without restriction. Three weeks after the surgeries, the animals were transferred to straw yards, remaining there until the end of the implantation periods. The healing process was followed through X-ray imaging immediately after surgery and repeatedly at 2 weeks intervals until sacrifice. The sheep tolerated the surgical procedure very well and passed the follow-up period without complications.

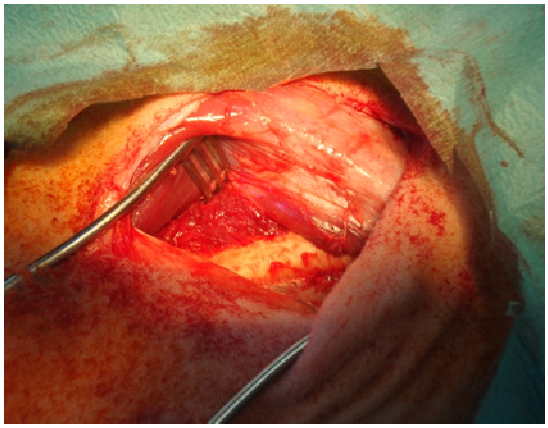

Figure 4.1: Exposed femur before the performance of the bone defects.

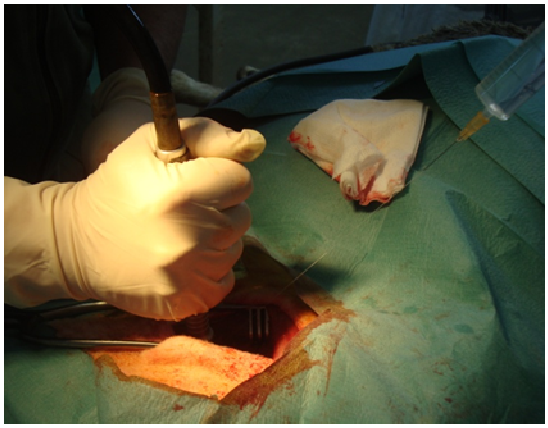

Figure 4.2: Performance of the bone defects.

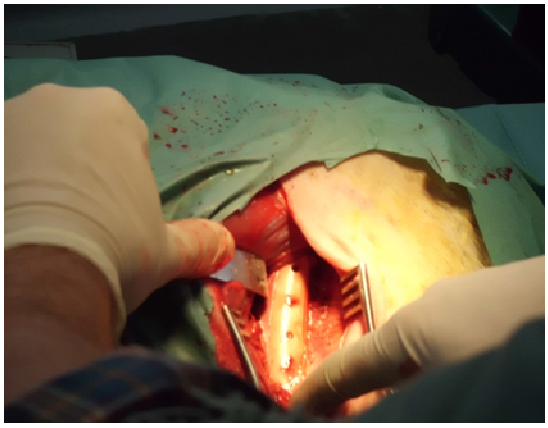

Figure 4.3: Bone defects before the biomaterials implantation.

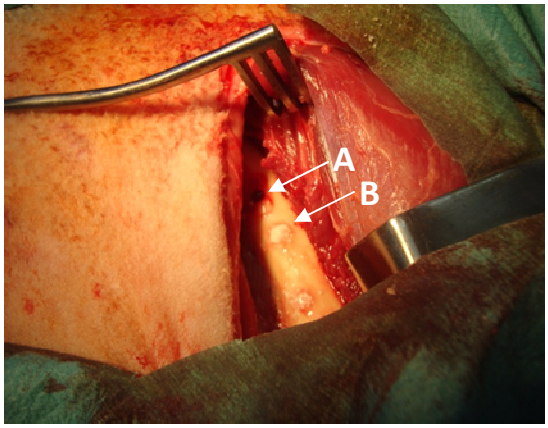

Figure 4.4: Bone defects filled with the biomaterials: **A**-GR-HA granules; **B**-*Alg/HA_IBS*.

During the surgical procedure, it was evident that the association of the hydrogel to the GR-HA granules allowed an easier and faster application of the bone substitute. Moreover, using the injectable system it was possible to better limit the GR-HA granules application just to the defect and better immobilize them on it, as can be observed in figure 4.4, comparing A and B.

4.2. Samples preparation for histological analysis

An intravenous injection of a 20% pentobarbital sodium solution was used to sacrifice the sheep one month after the surgery. Subsequently, femurs were dissected and all soft tissue was stripped from the bones. Segments of the femurs containing the implants were sawed out.

Then, those samples were immediately placed in a neutral formaldehyde fixative solution (10%) for seven days and after dehydrated in 100% acetone for 60 minutes at 4 ^{o}C and then embedded in resin (figure 4.5), using the Histo-Technik 8100 kit (*Heraeus Kulzer*, Germany).

Afterwards, thin sections of 150 µm were cut perpendicularly to the femur axis with a diamond blade microtome and hand-ground to approximately 70–80 µm. Then, the sections were stained with Solochrome cyanine R for a future histological examination with the light microscope Eclipse E600 (*Nikon*, Japan), equipped with the calibrated digital camera DS-5M-L1 Digital Sight Camera System (*Nikon*, Japan).

Figure 4.5: A sample of a bone defect filled with the *Alg/HA_IBS* embedded in resin.

In this moment, histological analysis is being performed in order to determine if osteointegration of *Alg/HA_IBS* was achieved without local or systemic signs of a foreign body response, as well as if healthy new bone was formed around the biomaterial. Furthermore, the results of *Alg/HA_IBS* will be compared with the results obtained using only the GR-HA granules. This comparison will demonstrate if the association of the hydrogel to the synthetic bone substitute can further enhance the bone regeneration.

Chapter 5

General discussion, conclusions and future work

5.1. General discussion and conclusions

In *Chapter 2* of this research work, it is described the development of three different hydrogels to associate, as vehicles, with the synthetic bone substitute glass-reinforced hydroxyapatite (GR-HA). One vehicle is based on an alginate matrix cross-linked with Ca^{2+} ions (hydrogel *Alg*); a second one is based on a mixture of alginate and chitosan, using also Ca^{2+} ions as the cross-linking agent (hydrogel *Alg/Ch*); the third one is based on a mixture of alginate and hyaluronate, using the same cross-linking agent. The hydrogels, as well as the respective injectable bone substitutes (GR-HA granules aggregated with the hydrogel-*IBS*s), were fully characterized from the physical-chemical point of view.

Additionally, in *Chapter 3*, a biological characterization of these materials and of other two developed hydrogels with antimicrobial properties, and respective *IBS*s, was performed. The two additional hydrogels developed in this chapter resulted from the incorporation of Ce(III) into the hydrogel *Alg/HA*, in two different concentrations (hydrogels *Alg/HA1* and *Alg/HA2*).

In *Chapter 2*, using scanning electron microscopy (SEM) analysis (figure 2.4) a very similar morphology for the hydrogels *Alg*, *Alg/Ch* and *Alg/HA* was observed. They all exhibited irregular structures with interconnected dissimilar pores, which seem to have the ideal size for a good osteoid ingrowth.[1, 2] Regarding to *IBS*s (figure 2.5), it was observed a good envelopment and aggregation of the GR-HA granules by each hydrogel.

The Fourier transform infrared - attenuated total reflectance (FTIR-ATR) spectra of the three hydrogels and the polymeric solutions used to produce them are presented in figure 2.6. In all spectra, the typical transmittance band of water O-H stretching vibration at 1634 cm^{-1} it is clear. This band can be attributed to the high water content in all the samples.[3] Besides this band, the sodium alginate solution spectrum presented two characteristic bands of polysaccharides, 1410 cm^{-1} (assigned to the stretching vibration of C-OH of carboxylic group) and 1034 cm^{-1} (assigned to the stretching vibration of C-O of the alcohol groups).[4] The spectra of chitosan HCl and sodium hyaluronate solutions did not present any fingerprinting region, due to the very low polymeric concentration.[4, 5] Therefore, regarding to the hydrogels, which

result from the mixture of alginate solution with chitosan HCl or sodium hyaluronate solution, only the bands verified for the alginate solution were observed. These bands presented different intensities in each hydrogel attending to the different alginate concentration.

Figure 2.7 presents the FTIR-ATR analysis of sodium alginate powder before and after autoclaving, in order to ascertain the effects of this sterilization method on the polymer chemical structure. The spectra of both samples are similar, the characteristic alginate bands can be detected in both, indicating that this method did not alter the polymeric structure. Band 1 (1594 cm^{-1}) and band 2 (1400 cm^{-1}) represent the antisymmetric and symmetric stretch vibration of alginate carboxylic group, respectively.[6, 7] Bands 5, and 7 (941 cm^{-1}, 879 cm^{-1} and 812 cm^{-1}) in the anomeric region of fingerprint, are characteristic of all polysaccharide standards of alginate.[7-10]

Since swelling is a specific characteristic of any hydrogel, the swelling profile of the three developed hydrogels was evaluated, as presented in figure 2.8. The hydrogels showed, in phosphate buffered saline (PBS, pH 7.4) and potassium hydrogen phthalate (KHP, pH 4), a weight increase, mainly during the first minute of immersion. This behavior was expected, since, as already referred, a hydrogel has the ability to swell by water retention in order to reach the equilibrium with the external medium.[11-13] However, in both solutions, the hydrogel *Alg* presented a higher weight increase than the other two. This phenomenon can be explained by the higher polymer content, which gives rise to a greater osmotic pressure from the medium into the hydrogel, providing a higher water uptake into the polymeric structure.[14]

A requirement of the developed hydrogel was its degradation time. Thus, degradation tests were performed to evaluate the degradation profile of each hydrogel. The results, exposed in figure 2.9, revealed a weight loss of the hydrogels in both used solutions (PBS and KHP), after 24 and 72 hours. At pH 7.4, the hydrogel *Alg/HA* presented the highest degradation rate, being its final weight loss of about 80% (figure 2.9-A). In both solutions, in the two time points, the hydrogels *Alg/Ch* and *Alg/HA* presented a higher weight loss than the hydrogel *Alg*. The three used polymers are degradable by hydrolysis of the glycosidic bonds.[15-17] Thus, the lower polymer content of the hydrogels *Alg/Ch* and *Alg/HA* is the main reason to a faster degradation of their structure. Moreover, after 72 hours, for pH 7.4, the three hydrogels presented

a higher weight loss than for pH 4 (figure 2.9-B). This phenomenon can be explained by the alginate cross-linked structure degradation by exchange of Ca^{2+} ions for Na^{+} ions when exposed to them for long times, what happens in the PBS solution for 72 hours.[15, 18]

The rheology studies showed that the hydrogels *Alg*, *Alg/Ch* and *Alg/HA* have a non-Newtonian behavior, more specifically, a shear-thinning behavior, the viscosity decreases with the shear rate increase (figure 2.10-A).[19, 20] Owing to the applied shear, the hydrogel polymeric structure is altered, therefore an alignment between the polymeric chains in the same direction of the flow occurs, what causes a viscosity decrease.[21, 22] Besides that, for all shear rate values, the hydrogel *Alg* presented a higher viscosity than the other two. This fact can be mainly explained by the higher polymer concentration in the hydrogel *Alg*.[23, 24]

Moreover, the studied hydrogels are considered viscoelastics, they presented simultaneously G' values, which represent the elastic response of the materials and G'' values, which represent the viscous response of the materials (figure 2.10-B).[23, 25] When G'>G'', it is considered that the material has a mainly elastic behavior, when G'<G'' the behavior is more viscous than elastic.[25-27] The higher G'' value of hydrogel *Alg* relatively to the other two, for all frequencies, can be explained by its higher viscosity.[27]

Considering the main purpose of this work, to inject the bone substitute, injectability tests of the *IBS*s are extremely important, as they will allow the evaluation of their handling easiness. As observed in figure 2.11, in the beginning of the injection process, the three *IBS*s presented a maximum extrusion force (*Alg_IBS* - 7.33±0.19 N; *Alg/Ch_IBS* - 4.64±0.32 N; *Alg/HA_IBS* - 4.55±0.42 N), and then the required force to inject them decreased and stabilized. Overall, the maximum extrusion forces for all *IBS*s were very low, being the highest one verified for the *Alg_IBS*. This higher force can be explained by the higher viscosity of the vehicle, leading to a higher static frictional force.[28-30]

After a complete physical-chemical characterization the biological behavior of the developed materials was assessed. As described in *Chapter 3*, the effect of the *IBS*s on the metabolic activity of MG63 cells was evaluated. As observed in figure 3.2, the association of the hydrogel *Alg/HA* to the GR-HA granules significantly increased the

cellular metabolic activity of the MG63 cells at all the time points. This higher metabolic activity may indicate a better adaptation of cells to the material, increasing their predisposition to produce extracellular matrix, allowing faster bone regeneration.

The morphology of the MG63 cells adhered on the *Alg_IBS, Alg/Ch_IBS and Alg/HA_IBS* was observed by SEM (figure 3.3). This analysis revealed that the different interaction of the hydrogels with cells leads not only to a distinct metabolic activity but also to a different morphology. On the *Alg/HA_IBS*, which presented a highest metabolic activity, cells had a spreader shape with more developed and evident filopodia comparing to the cells adhered on the hydrogels *Alg* and *Alg/Ch*, proving a better cell adaptation.

As described earlier (*Chapter 2*) the three hydrogels have similar morphology, thus the different cell behavior on each *IBS* should not be attributed to this parameter, but probably to the chemical structure of the used polymers.[31, 32] The improved cell adhesion on the *Alg/HA_IBS* can be explained by the hyaluronic acid (HA) ability to establish more adhesion sites between the material surface and each cell, due to its interaction with several cell surface receptors.[33, 34] During the establishment of those adhesion sites, the cytoskeleton filamentous proteins are produced and/or reorganized resulting in cell stretching.[31, 35, 36] The cytoskeleton organization, besides controlling the shape, can also be related with cell growth and function.[36, 37] In fact, the material that presented cells with a spreader shape (*Alg/HA_IBS*), also presented a higher cell metabolic activity, which can be explained, in this case, by the cytoskeleton proteins production and organization.

As a next step on the biological evaluation of the hydrogels *Alg, Alg/Ch* and *Alg/HA*, their consistency change when interact with blood was evaluated, figure 3.4. The three hydrogels presented a very slight consistency loss only after some minutes of contact (about 2-3 minutes), mainly the hydrogels *Alg/Ch* and *Alg/HA*, however their successful function as vehicles was maintained. The higher consistency loss of these two compared to the hydrogel *Alg* was expected attending to the degradation tests. In those tests, they presented a higher degradation rate, mainly caused by non-enzymatic hydrolysis due to the lower polymeric concentration. Besides this, in contact with blood, chitosan and HA are exposed to enzymatic degradation, increasing even more the degradation of the hydrogels *Alg/Ch* and *Alg/HA*.[16, 38-40]

After the *in vitro* studies, which showed a higher metabolic activity and a spreader cell shape on the *Alg/HA_IBS*, the respective vehicle was subcutaneously implanted into Sprague Dawley® rats to evaluate its *in vivo* biocompatibility. The histological analysis (figure 3.5) revealed several lymphocytes, plasma cells and macrophages, which is a normal outlook in a tissue healing phenomenon.[41-43] Neutrophils and giant cells were almost absent in the tissue samples that were analyzed (table 3.2). Thus, the material was considered as slight irritating, according to ISO 10993-6, being proved its successful real application as a biomedical hydrogel.

Due to the good *in vitro* and *in vivo* results obtained for the hydrogel *Alg/HA,* it was even tried to give it an additional property, antimicrobial activity, by incorporation of Ce(III) ions, acting as cross-linking agents besides the Ca^{2+} ions. In figure 3.6, it is possible to observe the improvement of the hydrogel *Alg/HA* antimicrobial properties against *S.aureus, S.epidermidis, C.albicans* and *P.aeruginosa* by the Ce(III) addition. For *S.aureus*, *S.epidermidis* and *C.albicans*, the two tested Ce(III) concentrations promoted a significant antimicrobial activity, for *P.aeruginosa,* that was only observed for the highest tested Ce(III) concentration. The antimicrobial properties of Ce(III) have already been reported, and it has been hypothesized that it can enter into the cytoplasm and inhibit some cellular mechanisms or disrupt the cell membrane.[44, 45] *P.aeruginosa*, is a gram-negative bacterium, therefore has a more complex cell wall, which is less permeable to biocides, complicating the ion entry and action, which can explain the higher resistance to the lowest concentration of Ce(III).[46]

In the presence of the highest studied Ce(III) concentration (hydrogel *Alg/HA2*), the metabolic activity of MG63 cells, at 72 hours, was slightly lower than using the hydrogel *Alg/HA* (figure 3.7). However, this decrease (5.14%±0.25) does not compromise the metabolic activity improvement by the hydrogel association to the GR-HA granules. The verified decrease can be due to the competition of Ce(III) ions with Ca^{2+} ions, interacting with the calcium-dependent transmembrane signaling channels and thus interfering with intracellular events.[45, 47]

According to the aims of this research work, the developed vehicle should be mostly degraded in about three days and it should allow a good injectability of the bone substitute. Thus, regarding the physical-chemical characterization, the main parameters that should be considered to choose the best vehicle are the hydrogel

degradation time and the required injectability forces. As already discussed, the three *IBS*s, developed in *Chapter 2*, presented very low extrusion forces, therefore they are easy to handle and apply in several bone defects. However, the hydrogel *Alg/Ch* and *Alg/HA* presented a lower maximum extrusion force than the hydrogel Alg. Attending to the degradation time at pH 7.4, the hydrogel *Alg/HA* has an advantage in comparison to the hydrogels *Alg* and *Alg/Ch*, as it presents the highest degradation rate after three days.

Another important objective of this work was to develop a hydrogel that not only acts as a vehicle, but also that would enhance cell adhesion on the bone substitute. The hydrogel *Alg/HA* was the one that promoted the best cellular performance and revealed a very good *in vivo* response when subcutaneously implanted.

Therefore, there is no doubt that between the three developed hydrogels, considering the physical-chemical and biological performance, the hydrogel *Alg/HA* is the best choice as a bioactive vehicle for GR-HA granules. This material will, simultaneously, allow an easy injection of the synthetic substitute and improve the osteoblasts adhesion and activity, promoting a better implant osteointegration and bone defect regeneration.

Furthermore, the hydrogel *Alg/HA2* will additionally prevent infections by several microorganisms without compromise osteoblasts activity, improving the implant success.

5.2. Future work

As future work, some other studies should be done in order to better understand the mechanism behind the enhanced bioactivity and antimicrobial properties of the developed materials, and even to improve their functional performance in bone tissue regeneration:

- Perform degradation tests using enzymes responsible for the used polymers degradation *in vivo*, namely the lysozyme and hyaluronidase, to better foresee the degradation time of the developed hydrogels when implanted in body;
- Keep on the *in vivo* tests:

  - Finish the histological analysis of the bone samples prepared in *Chapter 4* to compare the bone regeneration promoted by the *Alg/HA_IBS* against the GR-HA granules alone;
  - Perform the subcutaneous implantation of the hydrogel *Alg/HA2* to evaluate its *in vivo* biocompatibility and then the intraosseous implantation of the *Alg/HA2_IBS* to compare with *Alg/HA_IBS*;
- Evaluate the osteoclasts differentiation on the *Alg/HA_IBS*, to study the HA influence in inhibition of these cells differentiation, as has been reported, what could even improve this IBS performance;[48]
- Incorporate stem cells and growth factors in the hydrogels, in order to obtain a bone substitute with osteogenic and osteoinductive properties, besides the osteoconductive ability;[49]
- Incorporate anti-inflammatory agents in the hydrogels to modulate the body inflammatory response against the inserted biomaterial, leading to a better acceptance of the biomaterial by the organism and a more successful recovery process;[50]
- Develop custom made substitutes: attending to the cross-linking mechanism of an alginate solution and the possibility to produce a very rigid hydrogel, it would be possible to incorporate the GR-HA granules in alginate solid blocks with adaptable sizes and shapes, which can be beneficial in large defects.[51]

5.3. References

1. Yang S., Leong K., Du Z., and Chua C., *The Design of scaffolds for use in tissue engineering. part I. traditional factors.* Tissue Engineering, 2001. **7**(6): p. 679-689.
2. Cerroni L., Filocamo R., Fabbri M., Piconi C., Caropreso S., and C. S.G., *Growth of osteoblast-like cells on porous hydroxyapatite ceramics: an in vitro study.* Biomolecular Engineering, 2002. **19**: p. 119-124.
3. Matrajt G., Borg J., Raynal P.I., Djouadi Z., d'Hendecourt L., Flynn G., and Deboffle D., *FTIR and Raman analyses of the tagish Lake meteorite: relationship with the aliphatic hydrocarbons observed in the diffuse interstellar medium.* Astronomy and Astrophysics, 2003. **416**(3): p. 983-990.
4. Papageorgiou S.K., Kouvelos E.P., Favvas E.P., Sapalidis A.A., Romanos G.E., and Katsaros F.K., *Metal-carboxylate interactions in metal-alginate complexes studied with FTIR spectroscopy.* Carbohydrate Research, 2010. **345**(4): p. 469-473.
5. Singh J., Dutta P.K., Dutta J., Hunt A.J. , Macquarrie D.J., and Clark J.H., *Preparation and properties of highly soluble chitosan–l-glutamic acid aerogel derivative.* Carbohydrate Polymers, 2009. **76**(2): p. 188-195.
6. Thanos C.G., B.E. Bintz, W.J. Bell, H. Qian, P.A. Schneider, D.H. MacArthur, and D.F. Emerich, *Intraperitoneal stability of alginate-polyornithine microcapsules in rats: an FTIR and SEM analysis.* Biomaterials, 2006. **27**(19): p. 3570-3579.
7. Gomez-Ordonez E. and P. Ruperez, *FTIR-ATR spectroscopy as a tool for polysaccharide identification in edible brown and red seaweeds.* Food Hydrocolloids, 2011. **25**(6): p. 1514-1520.
8. Chandia N.P., B. Matsuhiro, E. Mejias, and A. Moenne, *Alginic acids in Lessonia vadosa: Partial hydrolysis and elicitor properties of the polymannuronic acid fraction.* Journal of Applied Phycology, 2004. **16**(2): p. 127-133.
9. Chandia N.P. and B. Matsuhiro, *Characterization of a fucoidan from Lessonia vadosa (Phaeophyta) and its anticoagulant and elicitor properties.* International Journal of Biological Macromolecules, 2008. **42**(3): p. 235-240.
10. Sakugawa K., A. Ikeda, A. Takemura, and H. Ono, *Simplified method for estimation of composition of alginates by FTIR.* Journal of Applied Polymer Science, 2004. **93**(3): p. 1372-1377.
11. Gaharwar A.K., Dammu S.A., Canter J.M., Wu C., and Schmidt G., *Highly extensible, iough, and elastomeric nanocomposite hydrogels from poly(ethylene glycol) and hydroxyapatite nanoparticles.* Biomacromolecules, 2011. **12**(5): p. 1641-1650.

12. Fedorovich N.E., Alblas J., Wijn J.R., Hennink W.E., Verbout A.J., and Dhert W.J.A., *Hydrogels as extracellular matrices for skeletal tissue engineering: state-of-the-art and novel application in organ printing.* Tissue Engineering, 2007. **13**(8): p. 1905-1925.
13. Hoffman A.S., *Hydrogels for biomedical applications.* Advanced Drug Delivery Reviews, 2002. **43**: p. 3–12.
14. Chan A.W. and Neufeld R.J., *Modeling the controllable pH-responsive swelling and pore size of networked alginate based biomaterials.* Biomaterials, 2009. **30**(30): p. 6119-6129.
15. Lee K.Y. and Mooney D.J., *Alginate: properties and biomedical applications.* Progress in Polymer Science, 2011. **37**(1): p. 106-126.
16. Kim J., Kim I. S., Cho T. H., Lee K.B., Hwang S.J., Tae G., Noh I., Lee S.H., Park Y., and Sun K., *Bone regeneration using hyaluronic acid-based hydrogel with bone morphogenic protein-2 and human mesenchymal stem cells.* Biomaterials, 2007. **28**(10): p. 1830-1837.
17. Il'ina A.V. and Varlamov V.P., *Hydrolysis of chitosan in lactic acid.* Applied Biochemistry and Microbiology, 2004. **40**(3): p. 300-303.
18. LeRoux M. A., Guilak F., and Setton L. A., *Compressive and shear properties of alginate gel: effects of sodium ions and alginate concentration.* Journal of Biomedical Materials Research, 1999. **47**(1): p. 46-53.
19. Oliveira S.M., Almeida I.F., Costa P.C., Barrias C.C., Ferreira M.R.P., Bahia M.F., and Barbosa M.A., *Characterization of polymeric solutions as injectable vehicles for hydroxyapatite microspheres.* AAPS PharmSciTech, 2010. **11**(2): p. 852-858.
20. Partal P. and Franco J.M., eds. *Rheology, Chapter: Non-Newtonian Fluids*. Vol. 1. 2007, Encyclopedia of Life Support Systems (EOLSS): Spain. 24.
21. Cui S.T., Gupta S.A., and C. P.T., *Molecular dynamics simulations of the rheology of normal decane, hexadecane, and tetracosane.* Journal of Chemical Physics, 1996. **105**(3): p. 1214-1220.
22. Yucel T., Cebe P., and Kaplan D.L., *Vortex-induced injectable silk fibroin hydrogels.* Biophys Journal, 2009. **97**(7): p. 2044-2050.
23. Pelletier S., Hubert P., Payan E., Marchal P., Choplin L., and Dellacherie E., *Amphiphilic derivatives of sodium alginate and hyaluronate for cartilage repair: rheological properties.* Journal of Biomedical Materials Research, 2000. **54**: p. 102-108.
24. Manojlovic V., Djonlagic J., Obradovic B., Nedovic V., and Bugarski B., *Investigations of cell immobilization in alginate: rheological and electrostatic extrusion studies.* Journal of Chemical Technology & Biotechnology, 2006. **81**(4): p. 505-510.
25. Tadros T.F., ed. *Rheology of Dispersions-Principles and Applications*. 2010, Wiley-VCH: Singapore. 199.

26. Vallée F., Müller C., Durand A., Schimchowitsch S., Dellacherie E., Kelche C., Cassel J.C., and Leonard M., *Synthesis and rheological properties of hydrogels based on amphiphilic alginate-amide derivatives.* Carbohydrate Research, 2009. **344**(2): p. 223-228.
27. Mason T.G., Dhople A., and W. D., *Linear Viscoelastic Moduli of Concentrated DNA Solutions.* Macromolecules, 1998. **31**: p. 3600-3603.
28. Dobre A. and Ramtal D., eds. *The Essential Guide to: Physics for Flash Games, Animation, and Simulations*. 1 ed. 2011, Apress: USA. 558.
29. Kirkpatrick L.D. and Francis G.E., eds. *Physics: a World View*. 6 ed. 2007, Thomson Wadsworth: USA. 645.
30. Viswanath D.S., Ghosh T.K., Prasad D.H.L., Dutt N.V.K., and Rani K.Y., eds. *Viscosity of Liquids: Theory, Estimation, Experiment, and Data*. 2007, Springer: Netherlands. 662.
31. Anselme K., *Osteoblast adhesion on biomaterials.* Biomaterials, 2000. **21**(7): p. 667-681.
32. Ferraz M.P., Fernandes M.H., Santos J.D., and Monteiro F.J., *HA and double-layer HA-P2O5/CaO glass coatings: influence of chemical composition on human bone marrow cells osteoblastic behavior.* Journal of Materials Science-Materials in Medicine, 2001. **12**(7): p. 629-638.
33. Lei Y. G.S., Lam J., Segura T., *The spreading, migration and proliferation of mouse mesenchymal stem cells cultured inside hyaluronic acid hydrogels.* Biomaterials, 2011. **32**(1): p. 39-47.
34. Zaleski K.J., Kolodka T., Cywes-Bentley C., McLoughlin R.M., Delaney M. L., Charlton B.T., Johnson W., and Tzianabos A.O., *Hyaluronic acid binding peptides prevent experimental staphylococcal wound infection.* Antimicrobial Agents and Chemotherapy, 2006. **50**(11): p. 3856-3860.
35. Hempel U., Hefti T., D. P., and Schlottig F., *Response of human bone marrow stromal cells, MG-63, and SaOS-2 to titanium-based dental implant surfaces with different topography and surface energy.* Clinical Oral Implants Research, 2011: p. 1-9.
36. Gwynn I.A., *Cell biology at interfaces.* Journal of Materials Science Materials in Medicine, 1994. **5**: p. 357-360.
37. Amaral M., Costa M.A., Lopes M.A., Silva R.F., Santos J.D., and Fernandes M.H., *Si_3N_4-bioglass composites stimulate the proliferation of MG63 osteoblast-like cells and support the osteogenic differentiation of human bone marrow cells.* Biomaterials, 2002. **23**(24): p. 4897-4906.
38. Ruel-Gariépy E. C.A., Chaput C., Guirguis S., Leroux J.C., *Characterization of thermosensitive chitosan gels for the sustained delivery of drugs.* International Journal of Pharmaceutics, 2000. **203**: p. 89–98.

39. Irwin D.M., Biegel J.M., and Stewart C.B., *Evolution of the mammalian lysozyme gene family.* Bmc Evolutionary Biology, 2011. **11**.
40. Rahmanian M. and Heldin P., *Testicular hyaluronidase induces tubular structures of endothelial cells grown in three-dimensional colagen gel through a CD44-mediated mechanism.* International Journal of Cancer, 2002. **97**(5): p. 601-607.
41. Fujiwara N. and Kobayashi K., *Macrophages in inflammation.* Curr Drug Targets Inflamm Allergy, 2005. **4**(3): p. 281-286.
42. Ribeiro P.D., Sanches M.G., and Okamoto T., *Comparative analysis of tissue reactions to anesthetic solutions: histological analysis in subcutaneous tissue of rats.* Anesth Prog, 2003. **50**(4): p. 169-180.
43. Oak M. and Singh J., *Chitosan-zinc-insulin complex incorporated thermosensitive polymer for controlled delivery of basal insulin in vivo.* Journal Control Release, 2012: p. 1-10.
44. Cobrado L., Azevedo M.M., Silva-Dias A., Ramos J.P., Pina-Vaz C., and Rodrigues A.G., *Cerium, chitosan and hamamelitannin as novel biofilm inhibitors?* Journal of Antimicrobial Chemotherapy, 2012. **67** (5): p. 1159-1162
45. Garner J.P. and Heppell P.S.J., *Cerium nitrate in the management of burns.* Burns, 2005. **31**: p. 539–547.
46. Liaqat I. and Sabri A., *Analysis of cell wall constituents of biocide-resistant isolates from dental-unit water line biofilms.* Current Microbiology, 2008. **57**: p. 340–347.
47. Jakupec M.A., Unfried P., and Keppler B.K., *Pharmacological properties of cerium compounds.* Reviews of Physiology Biochemistry and Pharmacology, 2005. **153**: p. 101-111.
48. Nagaoka I., Igarashi M., and Sakamoto K., *Biological activities of glucosamine and its related substances.* Advances in Food and Nutrition Research, 2012. **65**: p. 337-352.
49. Giannoudis P.V., Dinopoulos H., and Tsiridis E., *Bone substitutes: an update.* Injury, 2005. **36**(3): p. 20-27.
50. Larsson S. and Hannink G., *Injectable bone-graft substitutes: current products, their characteristics and indications, and new developments.* Injury, 2011. **42**: p. 30-34.
51. Mattiasson B., Kumar A., and Galaev I.Y., eds. *Macroporous Polymers*. 2009, CRC Press Sweden. 525.